

Kinematics and Convergent Tectonics of the Northwestern South American Plate during the Cenozoic.

Román González Afanador¹, Onno Oncken¹, Claudio Faccenna², Eline Le Breton³, Maximiliano J Bezada⁴, and Andres Mora⁵

¹GFZ Potsdam

²Univ. Roma TRE

³Freie Universität Berlin

⁴University of Minnesota

⁵Ecopetrol

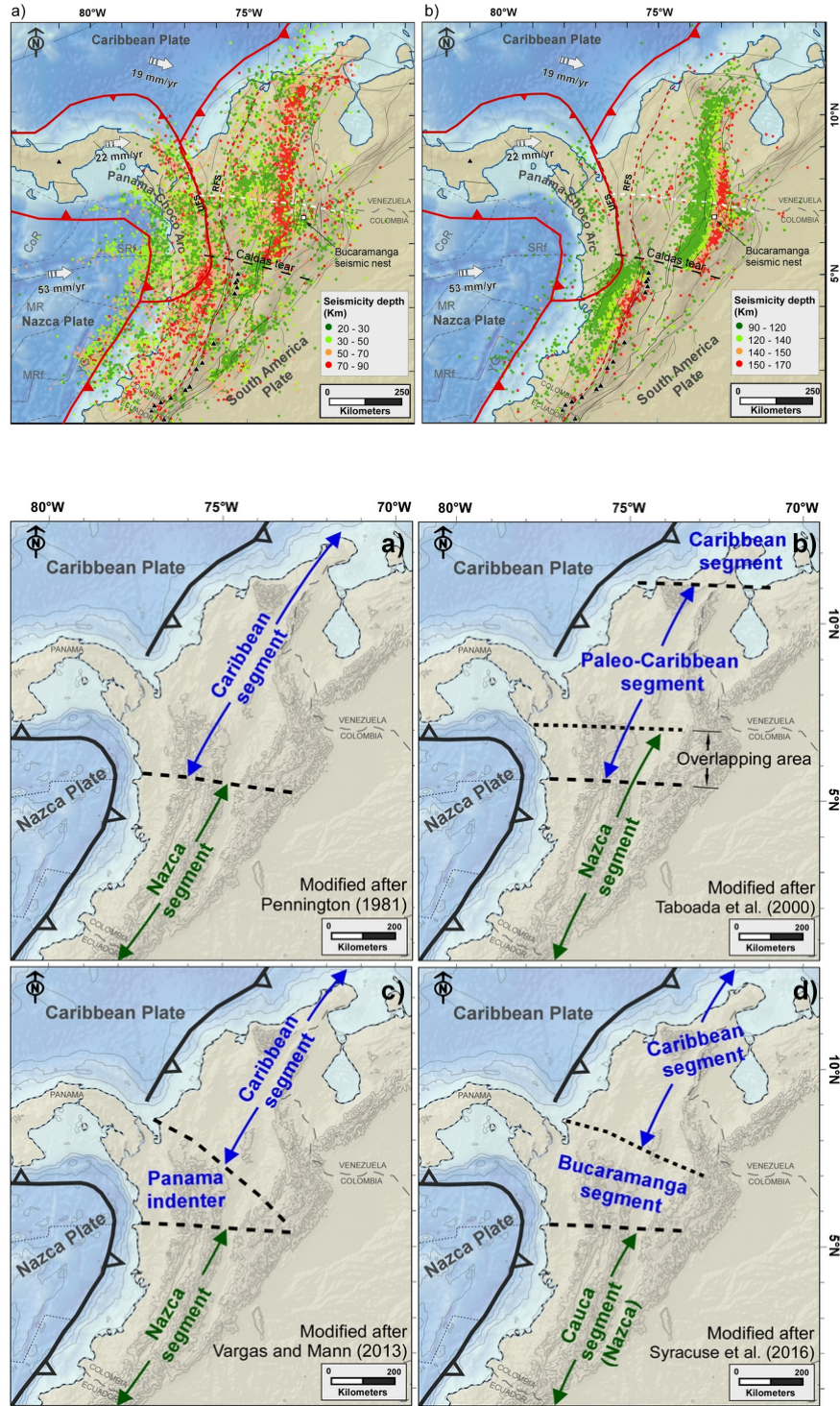
December 13, 2022

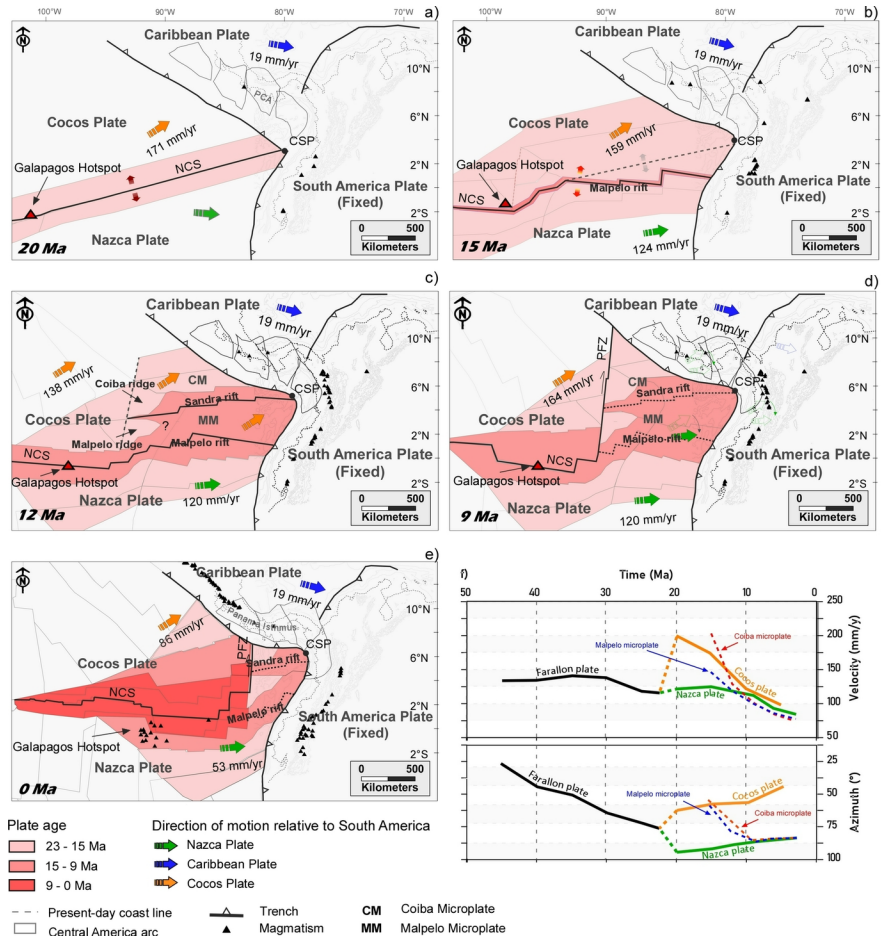
Abstract

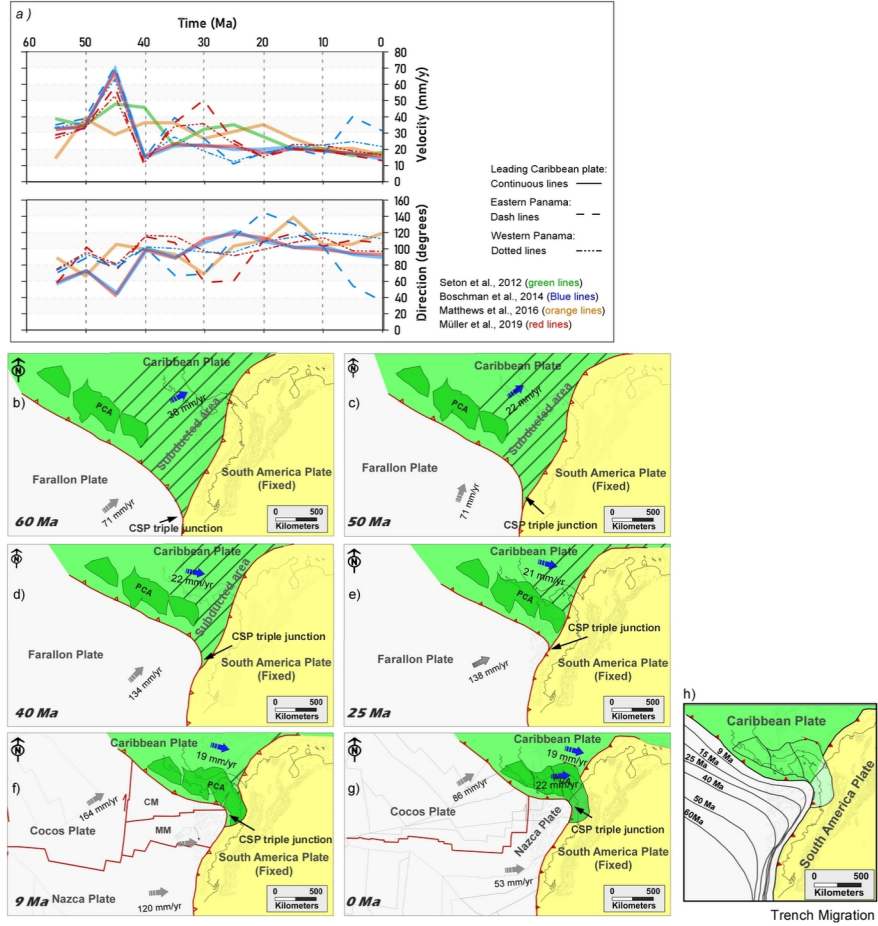
The interaction of the northern Nazca and southwestern Caribbean oceanic plates with South America, and the collision of the Panama-Choco arc have significant implications on the evolution of the northern Andes. We integrate an alternative interpretation of the Nazca and Caribbean kinematics with the magmatic and deformation history in the region. The northeastward migration of the Caribbean plate caused a progressive change in the geometry of the subducting Farallon plate, causing flat-slab subduction throughout the late Eocene-late Oligocene, inhibition of magmatism and eastward migration of the Andean deformation. Meanwhile, the Paleocene-Eocene highly oblique convergence of the Caribbean plate against South America changed by the mid-Eocene, when the Caribbean plate began to migrate in an easterly direction. These events and the late Oligocene breakup of the Farallon plate, prompted a Miocene plate reorganization, with further plate fragmentation, changes in convergence obliquity, steepening of the subducting slabs and renewal of magmatism. This tectonics was complicated by the accretion of the Panama-Choco arc to South America, which was characterized by early Miocene subduction erosion of the forearc and trench advance, followed by breakoff of the subducting slab east of Panama and collisional tectonics from the middle Miocene. By 9 Ma the Coiba and Malpelo microplates were attached to the Nazca plate, resulting in an abrupt change in convergence directions, that correlates with the main pulse of Andean orogeny. During the late Pliocene, the Nazca slab broke, triggering the modern volcanism south of 5.5° N. Seismicity data and tomography support the proposed reconstruction.

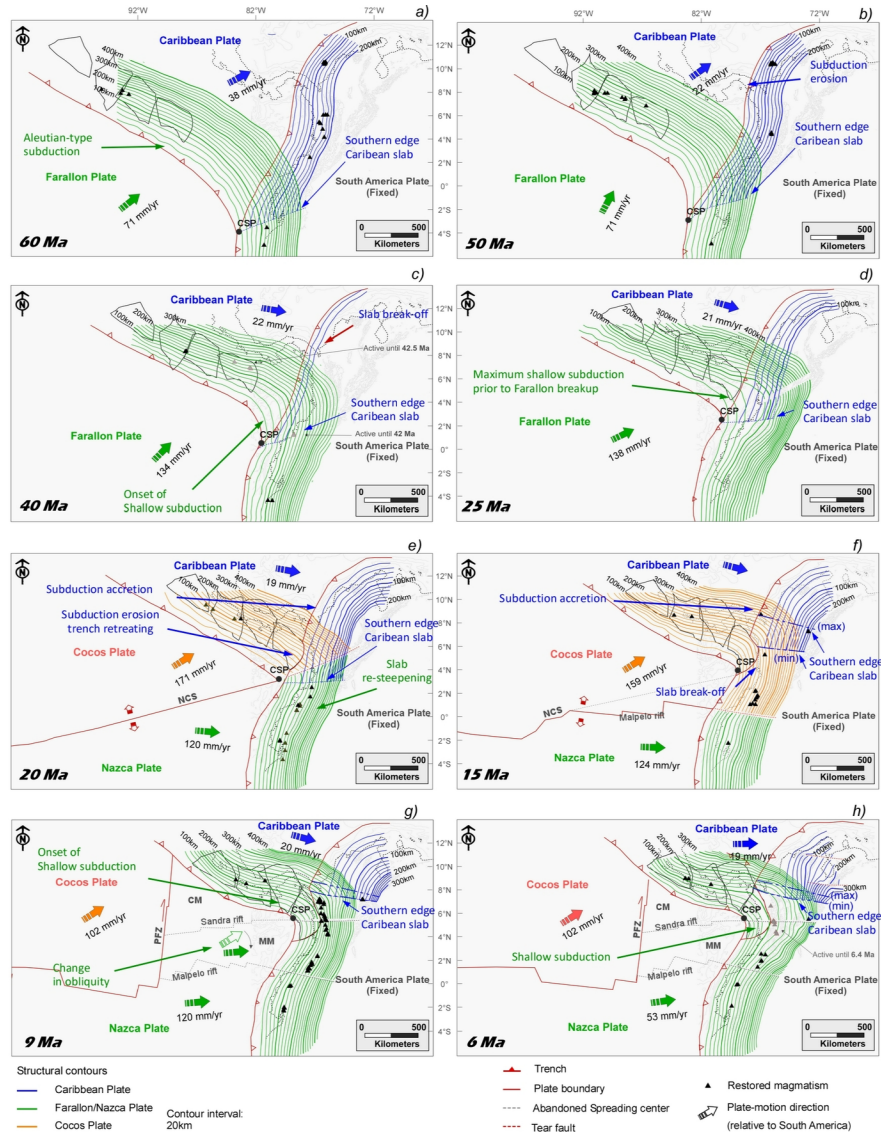
Hosted file

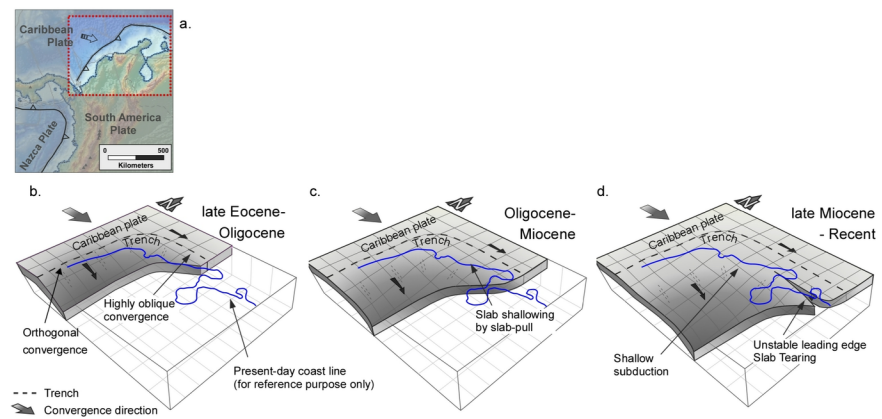
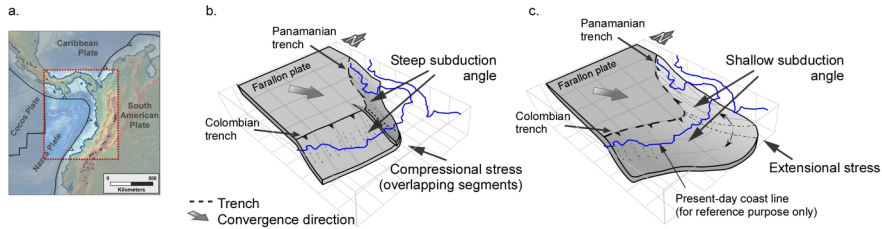
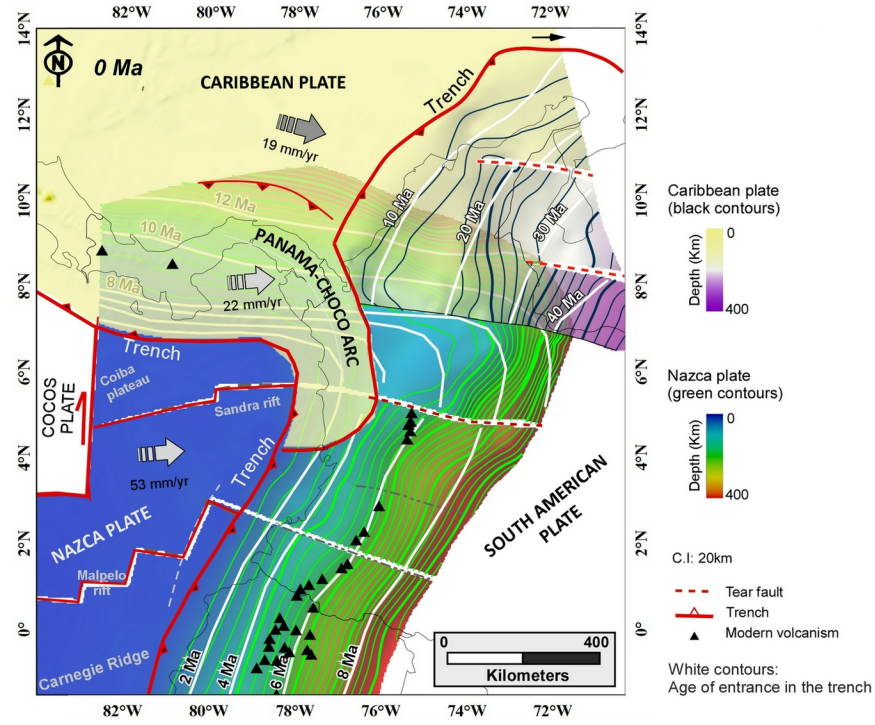
951865_0_art_file_10526484_rmqmf0.docx available at <https://authorea.com/users/565873/articles/612730-kinematics-and-convergent-tectonics-of-the-northwestern-south-american-plate-during-the-cenozoic>

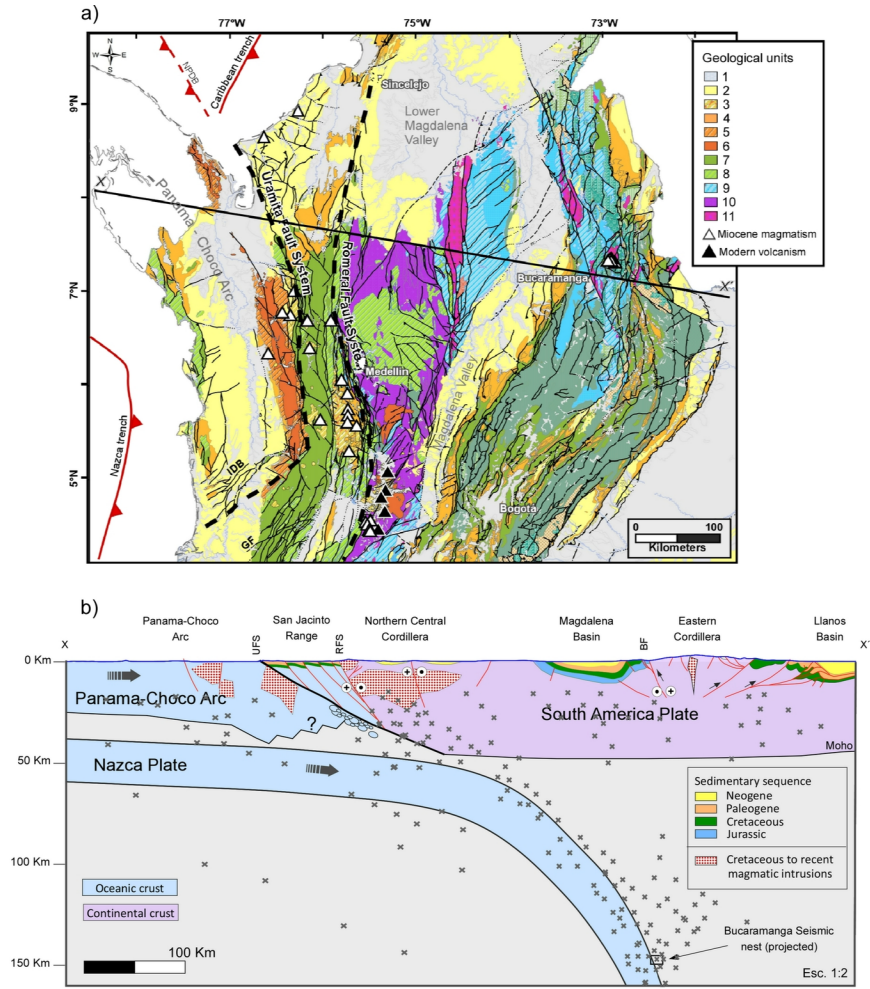


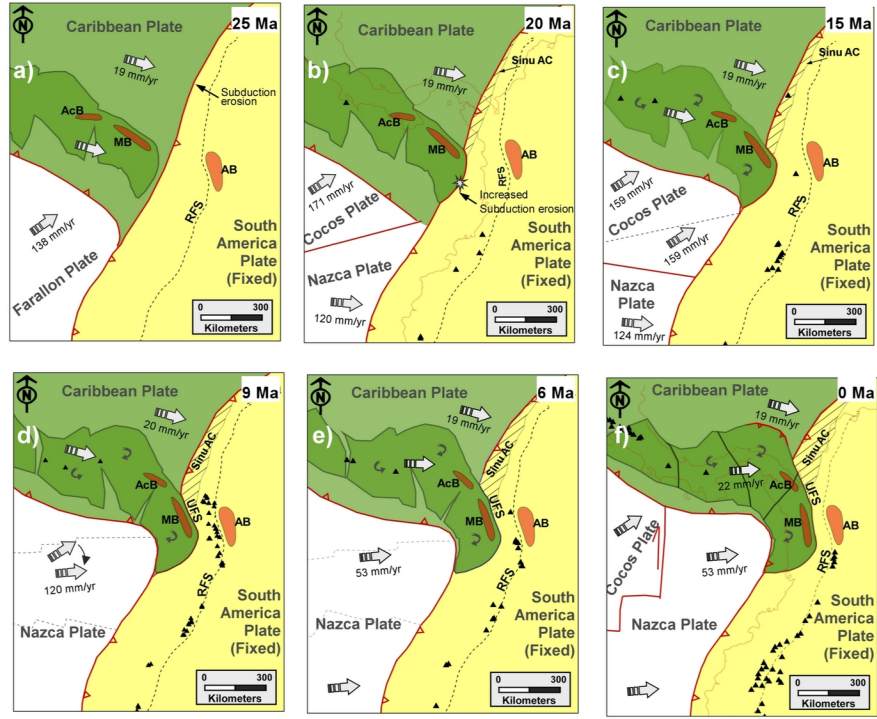


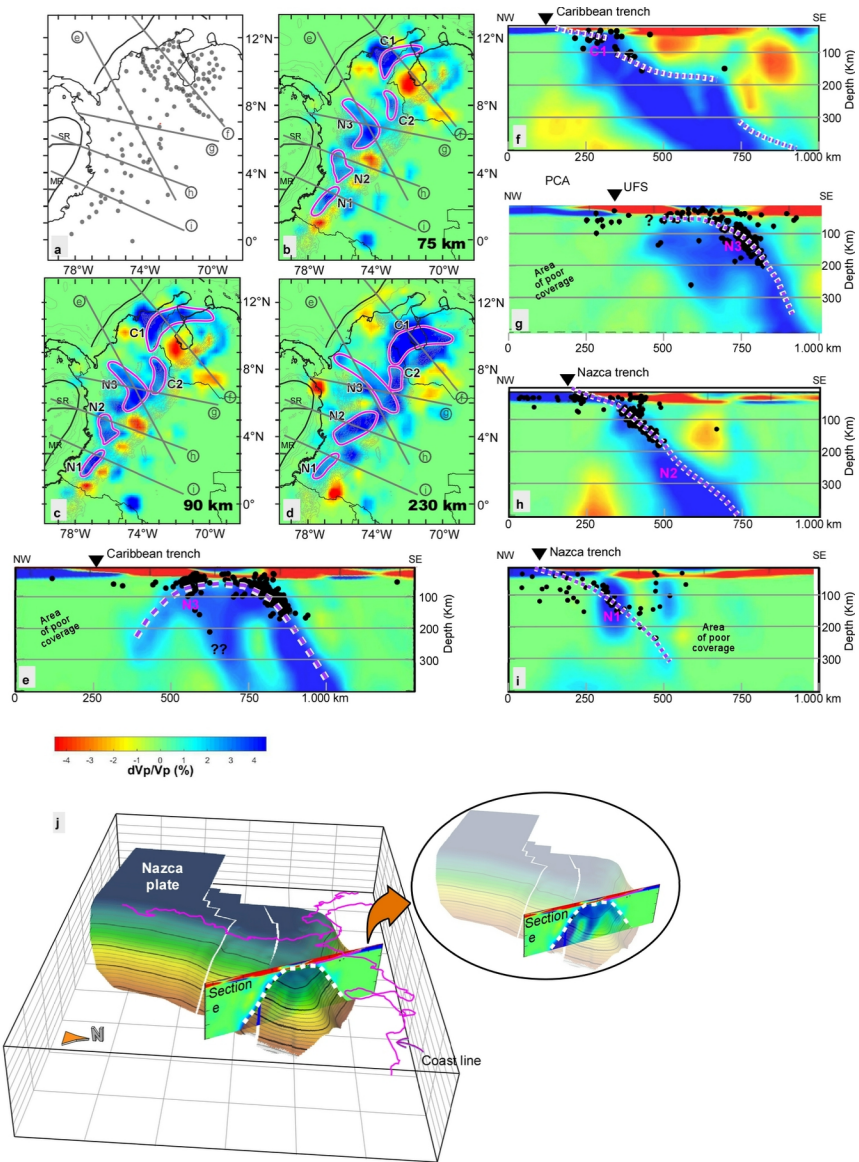


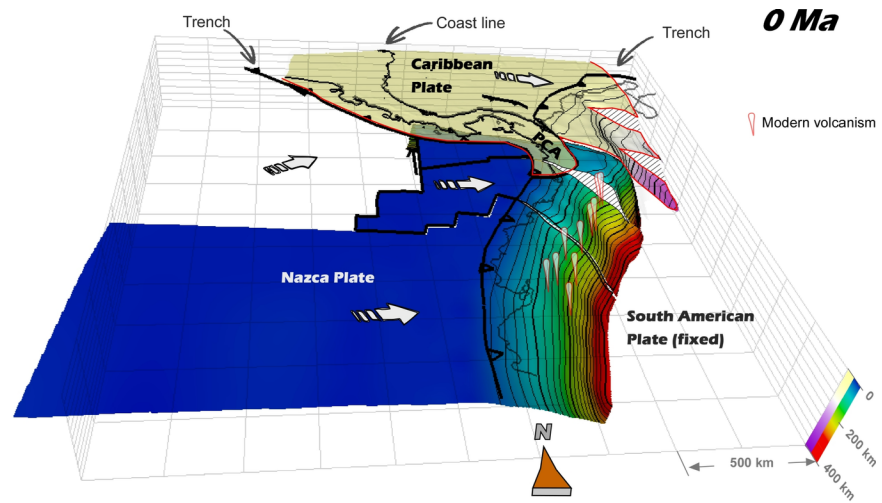






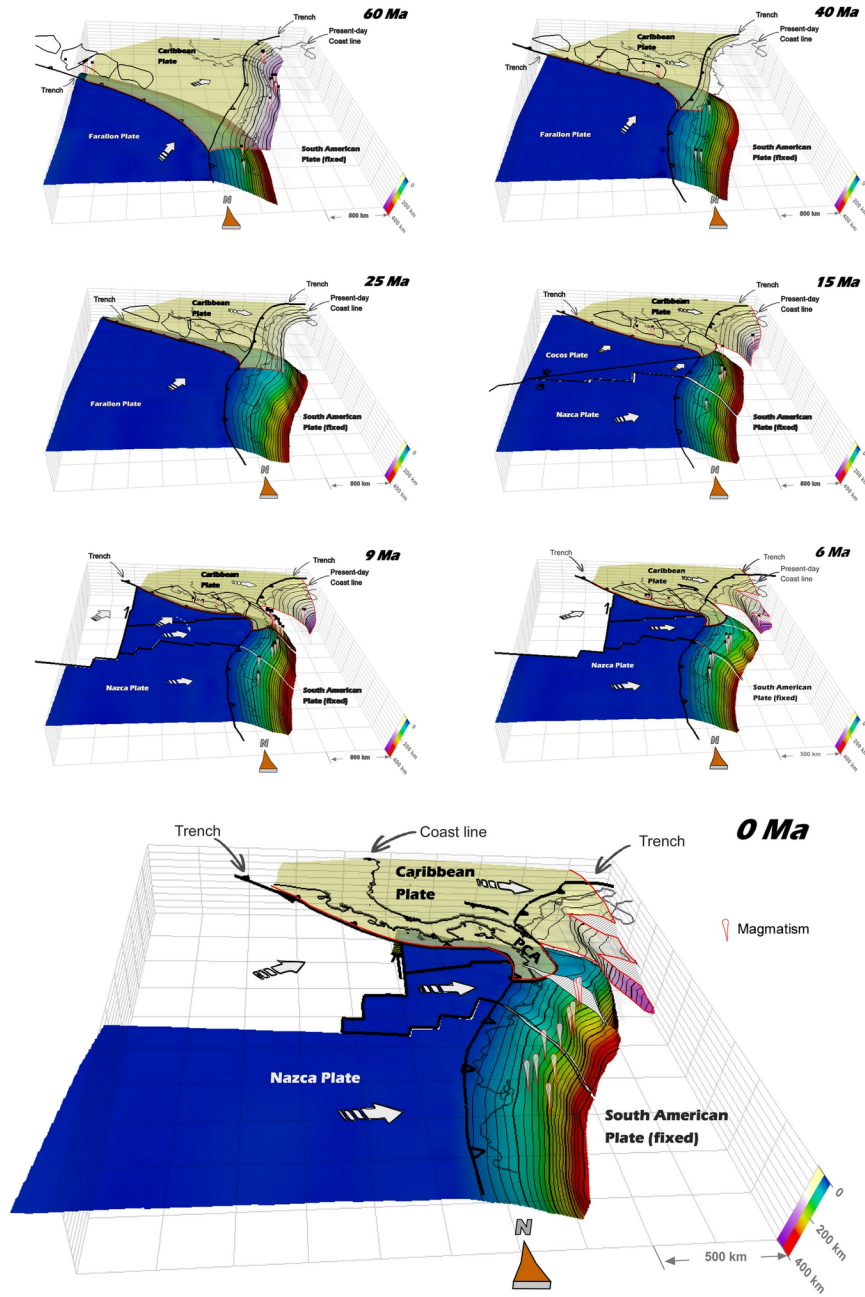


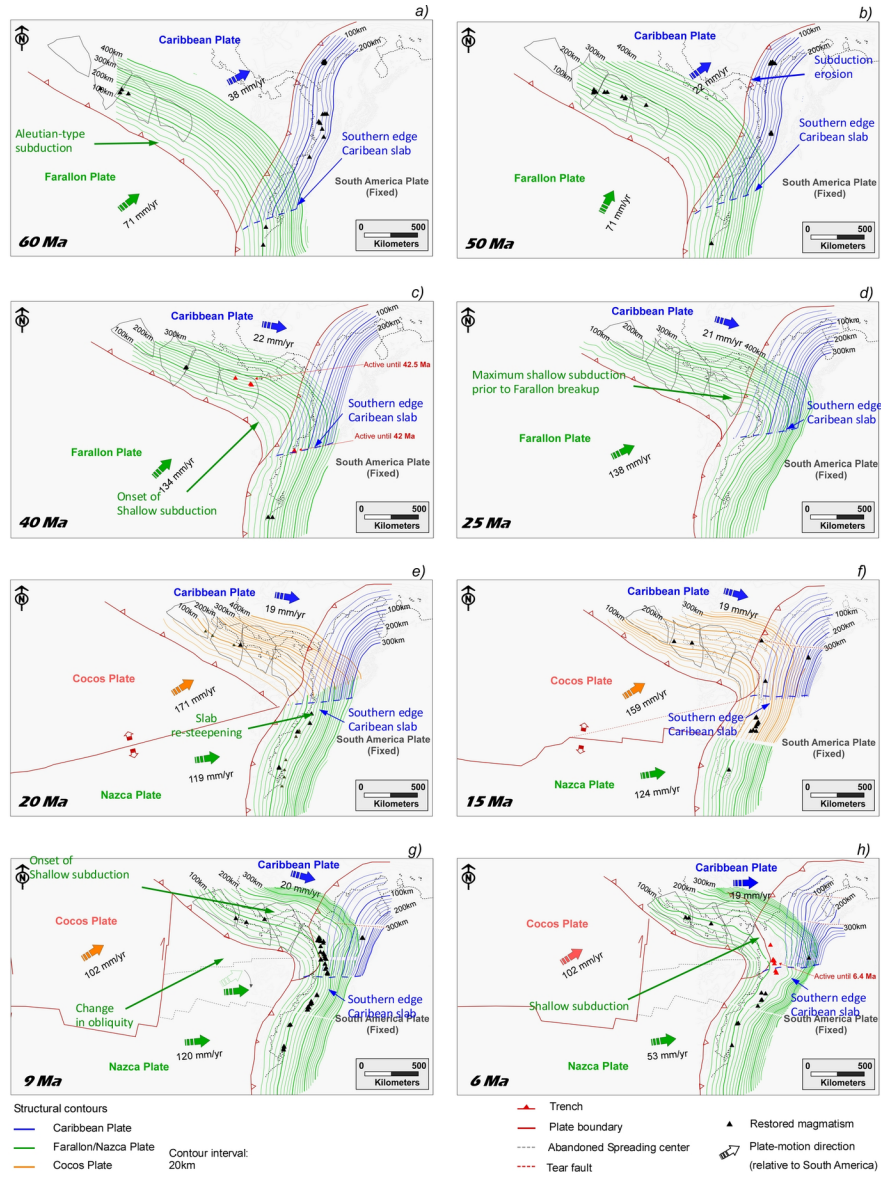


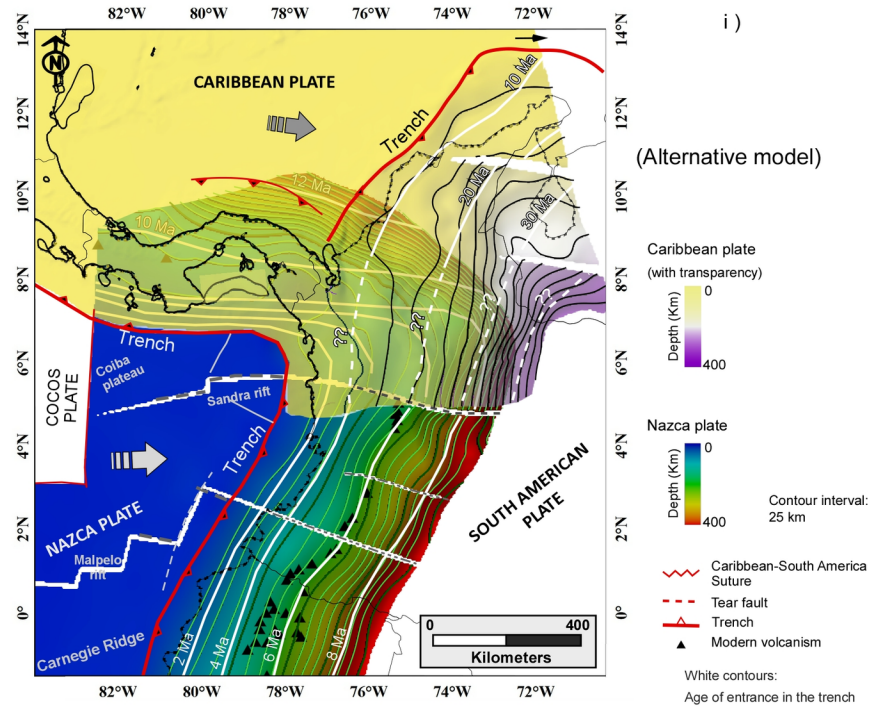


Hosted file

951865_0_supp_10526501_rmqqdd.gif available at <https://authorea.com/users/565873/articles/612730-kinematics-and-convergent-tectonics-of-the-northwestern-south-american-plate-during-the-cenozoic>







Kinematics and convergent tectonics of the Northwestern South American plate during the Cenozoic

González R.^{1,2,5,*}, O. Oncken^{1,2}, C. Faccenna^{1,3}, M. Bezada⁴, E. Le Breton², A. Mora⁶

1. GFZ German Research Centre for Geosciences, Dynamics of the lithosphere Section, Potsdam, Germany,

2. Freie Universität Berlin, Department of Earth Sciences, Berlin, Germany.

3. Roma Tre University, Department of Sciences, Roma, Italy.

4. University of Minnesota, Earth & Environmental Sciences, Minneapolis, USA.

5. Ecopetrol, Bogotá, Colombia.

6. Ecopetrol, Rio de Janeiro, Brazil.

* Corresponding author: rgonzal@gfz-potsdam.de

Key points

The tectonics of convergent triple junctions is complicated by the relative plate motion and interaction of the involved plates.

We propose a model for the kinematic and geometric evolution of the Farallon/Nazca and Caribbean plates throughout the Cenozoic.

The interaction between the Caribbean, Nazca and South American plates is closely related to the deformation history in the Northern Andes.

Abstract

The interaction of the northern Nazca and southwestern Caribbean oceanic plates with South America, and the collision of the Panama-Choco arc have significant implications on the evolution of the northern Andes. We integrate an alternative interpretation of the Nazca and Caribbean kinematics with the magmatic and deformation history in the region. The northeastward migration of the Caribbean plate caused a progressive change in the geometry of the subducting Farallon plate, causing flat-slab subduction throughout the late Eocene-late Oligocene, inhibition of magmatism and eastward migration of the Andean deformation. Meanwhile, the Paleocene-Eocene highly oblique convergence of the Caribbean plate against South America changed by the mid-Eocene, when the Caribbean plate began to migrate in an easterly direction. These events and the late Oligocene breakup of the Farallon plate, prompted a Miocene plate reorganization, with further plate fragmentation, changes in convergence obliquity, steepening of the subducting slabs and renewal of magmatism. This tectonics was complicated by the accretion of the Panama-Choco arc to South America, which was characterized by early Miocene subduction erosion of the forearc and trench advance, followed by breakoff of the subducting slab east of Panama and collisional tectonics from the middle Miocene. By 9 Ma the Coiba and Malpelo microplates were attached to the Nazca plate, resulting in an abrupt change in convergence directions, that correlates with the main pulse of Andean orogeny. During the late Pliocene, the Nazca slab broke, triggering the modern volcanism south of 5.5° N. Seismicity data and tomography support the proposed reconstruction.

Plain language summary

The tectonic reconstruction in convergent triple junctions is a particularly challenging task, as the relative motion between plates could define highly changing boundaries. Indeed, the resulting interaction between

40 these convergent plates may induce important changes in the disposition of the trenches, and in turn in
41 the three-dimensional geometry of the subducting plates. Therefore, these highly dynamic conditions
42 throughout geological time may be accommodated by different phases of plate fragmentation and
43 reorganization. These factors could explain the complex spatial-temporal distribution of subduction-
44 related magmatism and the different episodes of deformation in the upper plates. This reasoning is
45 validated in the northwestern corner of South America, where the continent has been converging with the
46 northern Nazca and southwestern Caribbean oceanic plates since Cretaceous time. Additionally, we
47 study the effects of the collision and accretion of the Panama-Choco arc with South America. To
48 accomplish that, we review the kinematic history of the Farallon/Nazca and Caribbean kinematics relative
49 to stable South America, and we integrate these results with the magmatic and deformation evolution of
50 the northern Andes, which allow us to propose a model of the geometrical evolution of the subducting
51 slabs. The obtained model is additionally constrained by seismological data and published velocity
52 anomalies.

53 **Index terms and keywords**

54 Plate Kinematics, Convergent Margins, Slab Geometry, Northern Andean Deformation Episodes.

55 **1. Introduction**

56 Lateral variations of the convergence parameters between the Farallon/Nazca and South America plates
57 have led to along strike differences along the Andean range (Fig.1) (e.g. Gansser, 1973; Cediél et al.,
58 2003; Oncken et al., 2006; Trumbull et al., 2006; Ramos, 2010). The most important element that charac-
59 terizes the tectonic evolution of the northern Andes is that the Nazca subduction is complicated by its
60 interaction with the Caribbean plate since Cretaceous time (Fig.2) (e.g. Burke, 1988; Pindell and Barrett,
61 1990; Mann, 1999), conforming a triple junction with South America. Furthermore, the tectonic setting in
62 this region is conditioned by the collision of the Panama-Choco arc (PCA) since the late Oligocene (Farris
63 et al., 2011; Montes et al., 2012). Within this context, the subduction geodynamics of the Nazca and Car-
64ibbean plate should not be simplified as the independent subduction of two oceanic slabs beneath the
65 continent, but as a triple junction that should be addressed in a three-dimensional framework. Indeed,
66 several authors (e.g. Toda et al., 2008; Faccenna et al., 2018) have demonstrated that the interaction
67 between subducting slabs in similar convergent triple junctions, has major tectonic implications on the
68 tectonic evolution of the upper plate.

69 A fundamental question to understand the tectonics of Northwestern South America (NWSA) is the pre-
70 sent-day configuration of the subducting plates. Several studies on the distribution of seismic events in
71 the northern Andes (Fig.3) (e.g. Taboada et al., 2000; Chiarabba et al., 2015; Sun et al., 2022) have led
72 to several competing models on the geometric configuration of the transition between the Nazca and Car-
73ibbean plates at depth (Fig.4) (e.g. Pennington, 1981; Vargas and Mann, 2013; Syracuse et al., 2016;
74 Kellogg et al., 2019; Sun et al., 2022). While some models support a shear zone between the Caribbean
75 and Nazca slabs at 5.5°N (Figs.3 and 4) (Pennington, 1981), implying the abrupt termination of both plates
76 at this position, other models favor an overlapping region between these slabs (e.g. Taboada et al., 2000;
77 Cortes and Angelier., 2005; Vargas, 2019; Sun et al., 2022).

78 As convergent triple junctions are not static elements in time, the understanding of the kinematic history
79 of the interacting plates is crucial for reconstructing the tectonic evolution of these margins (Faccenna et
80 al., 2018). On the one hand, the Nazca kinematics is well known between 10°S and 21°S (Fig.1) (e.g.

81 Pardo-Casas & Molnar, 1987; Somoza and Ghidela, 2012). This pattern of motion, however, is signifi-
82 cantly different from the one in the northern Nazca plate, as the kinematics in this region was complicated
83 by an intricate crustal spreading history in the Nazca/Cocos plate boundary after the breakup of the Faral-
84 lon plate (e.g. Handschumacher, 1976; Sallarès et al., 2003; MacMillan et al., 2004; Lonsdale, 2005;
85 Geldmacher et al., 2013). On the other hand, the regional Caribbean kinematics are well understood fol-
86 lowing several recent studies (Pindell and Kennan, 2009; Escalona and Mann, 2011; Farris et al., 2011;
87 Montes et al., 2012; Boschman et al., 2014). These findings allowed these authors to define a northeast-
88 ward migration of the Caribbean plate since the late Cretaceous (relative to South America) and the time
89 of initial collision of the PCA against South America by the late Oligocene (Fig.2). Although the influence
90 of this collisional event has been identified on both Central and South America (e.g. Montes et al., 2012;
91 Bayona et al., 2013, 2020; Silva et al., 2013; León et al., 2018; Mora-Bohórquez et al., 2018; Mora et al.,
92 2013a), the contribution of additional drivers in the northern Andes orogeny is not well understood.

93 We review the kinematic reconstruction of the subducting Farallon/Nazca and Caribbean plates relative to
94 South America throughout the Cenozoic. The analysis of the three-dimensional evolution of these plates
95 allowed us to identify positive correlations between different phases of subduction and the spatial and
96 temporal patterns of magmatism and first order deformation episodes in the northern Andes. An important
97 aspect of our analysis is the influence of the migration of the triple junction on the geometry of both the
98 Farallon/Nazca and Caribbean plates, and in turn on the tectonics of Northwestern South America
99 (NWSA). Finally, our kinematic reconstruction is integrated with a new interpretation of the present-day
100 tectonic configuration of NWSA.

101 **2. Tectonic Setting**

102 **2.1 The southwestern Caribbean Plate and the Panama-Choco Arc (PCA)**

103 Global and regional kinematic reconstructions agree that the Caribbean plate is a thick and buoyant oce-
104 anic plateau (e.g. Pindell et al., 2005) formed during the Late Cretaceous in the eastern Pacific region,
105 that subsequently migrated eastwards between the North and South American plates (Burke, 1988;
106 Mann, 1999; Pindell and Kennan, 2009). During its migration, the Caribbean plate underwent a major
107 collision event against South America during the Late Cretaceous, accreting the oceanic terrain that ex-
108 tends along the Ecuadorian and Colombian western margin known as the Caribbean Large Igneous Prov-
109 ince (CLIP; Fig.2) (Etayo-Serna, 1983; Cedié et al., 2003). This collision was followed by highly oblique
110 subduction below the South American plate that prevailed until the Eocene (Pindell and Kennan, 2009).
111 This early Caribbean subduction is associated with arc-related plutonism along the northern Central Cor-
112 dillera, the lower Magdalena valley, and the Santa Marta Massif (e.g. Bayona et al., 2012; Cardona et al.,
113 2014; Jaramillo et al., 2017; Leal-Mejía et al., 2019;) (Fig.2). By the Eocene, a kinematic change of the
114 Caribbean plate (Muller et al., 1999; Seton et al., 2012; Boschman et al., 2014), represented a more or-
115 thogonal convergence and the onset of shallow subduction beneath the northern South American plate
116 (e.g. Mora-Bohórquez et al., 2017b). This change in subduction dynamics has been regarded by previous
117 studies as the causal factor of the cessation of magmatism in northern Colombia between 56 and 45 Ma
118 (Cardona et al., 2014) and the middle Eocene exhumation pulse in the northern central Cordillera, San
119 Jacinto range and Santa Marta Massif (Restrepo et al., 2009; Villagómez et al., 2011; Mora-Bohórquez et
120 al., 2018) (Fig.2). Additionally, the Eocene to recent eastward displacement of the Caribbean plate
121 prompted the collision of the PCA against northern South America during the late Oligocene-early Mio-
122 cene (Farris et al., 2011; Montes et al., 2012). Oceanic rocks accreted to South America indicate that
123 initial collision of the PCA was located at 3°N (Duque-Caro, 1990) and then the accretion migrated north-

ward, currently reaching as far as 8°N (Fig.2). Based on seismological and tomography interpretations, several authors have proposed that the current geometry of the Caribbean slab is characterized by shallow subduction beneath northern Colombia and Venezuela (e.g. Taboada et al., 2000; Bezada et al., 2010; Syracuse et al., 2016; Cornthwaite et al., 2021; Sun et al., 2022).

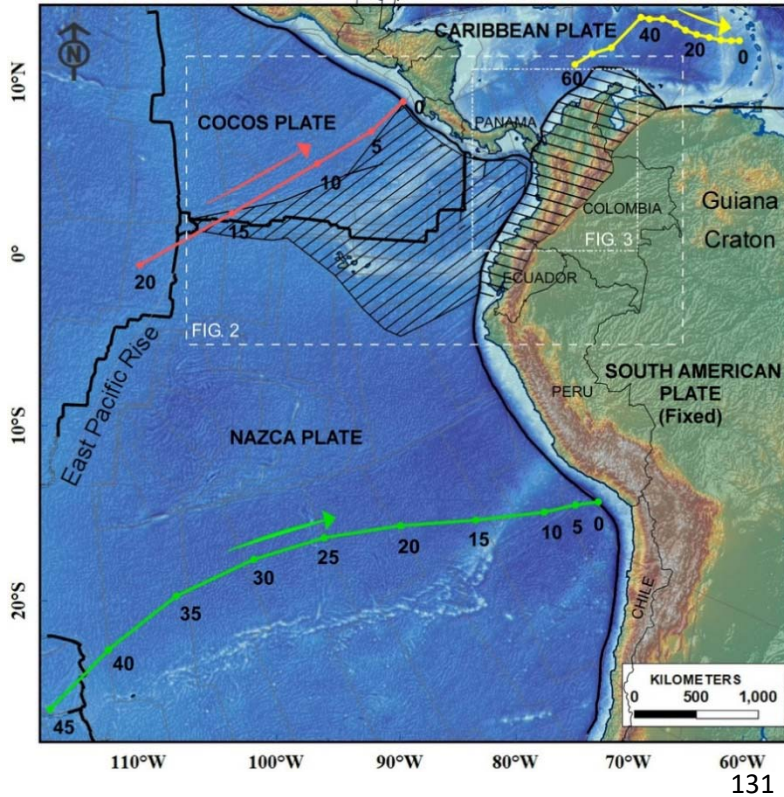
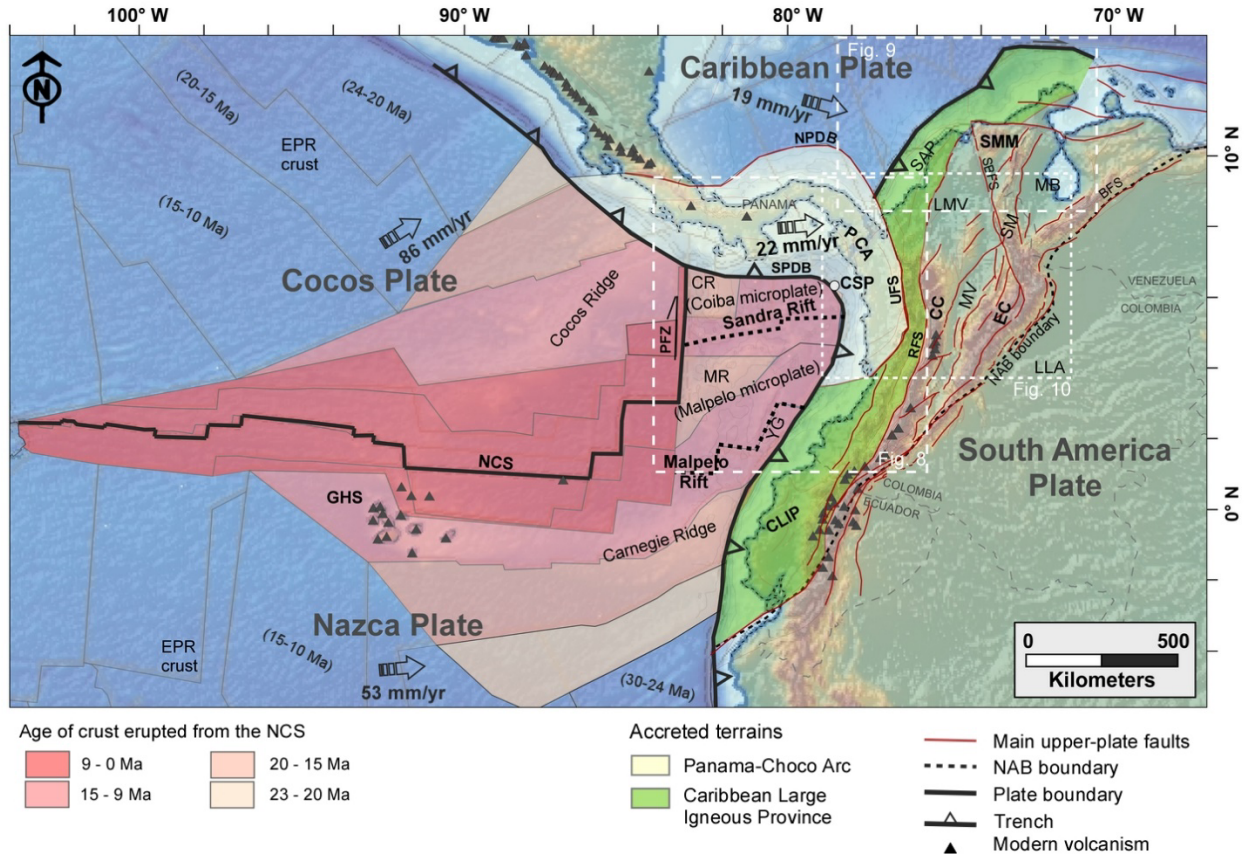


Fig. 1. Regional tectonic map of the South and Central American subduction zones showing the plate boundaries. Color lines show Cenozoic displacement vectors according to existing paleotectonic models for the Farallon/Nazca (green; Müller et al., 2019), Cocos (red; Müller et al., 2019), and Caribbean (yellow; Boschman et al., 2014) plates. Numbers refer to the reconstructed positions throughout the Cenozoic (Ma) relative to stable South America. The dashed area within the Nazca-Cocos plates shows the Miocene to Recent crust erupted from the Nazca-Cocos spreading center. The dashed area within the South American plate highlights the Northern Andean Block. Digital elevation model from Amante and Eakins (2009).

2.2 The Northern Nazca Plate

The present-day Nazca plate south of 3°S is significantly different from

the part further north (Fig.1). Age dating and paleo magnetic anomalies indicate that south of 3°S, the oceanic crust was originated at the East Pacific Rise (Figs.1 and 2), while the Nazca and Cocos plates subducting in the Ecuadorian, Colombian, Panamanian and Costa Rican margins correspond to oceanic crust entirely formed at the combined Galapagos hotspot track and the Nazca-Cocos spreading center (NCS, also known as the Galapagos spreading center; Fig.2) (e.g. Wilson and Hey, 1995; Werner et al., 2003; Sallarès et al., 2003; MacMillan et al., 2004; Lonsdale, 2005). A complicated spreading history along this plate boundary determined a particular kinematics in the region (Barckhausen et al., 2001; Lonsdale, 2005). Fig.2 shows a simplified compilation of estimated ages of the ocean floor originated in the Nazca- Cocos spreading Center (NCS) (Barckhausen et al., 2001; Werner et al., 2003; Sallarès et al., 2003; MacMillan et al., 2004; Lonsdale, 2005).



142

Fig. 2. Tectonic setting of the Northwestern South American subduction zones. Main faults in the Northern Andes modified after Veloza et al. (2012); distribution of modern Volcanoes (black triangles) taken from Siebert et al. (2002); and age of the crust originated in the Nazca-Cocos spreading center (NCS) modified after Barckhausen et al. (2001), Werner et al. (2003) and Lonsdale (2005). Motion vectors relative to stable South America (Mora-Paez et al, 2019). BFS= Bocono Fault System, CC= Central Cordillera, CLIP= Caribbean Large Igneous Province, CR= Coiba ridge, CSP= Caribbean-South America-Pacific plates triple Junction, EC= Eastern Cordillera, EPR crust= East Pacific Ridge crust, GHS= Galapagos Hotspot, LLA= Llanos basin, LMV= Lower Magdalena Valley, MB= Maracaibo Basin, MR= Malpelo Ridge, MV= Magdalena Valley, NAB= Northern Andean Block, NPDB= North Panama Deformed Belt, NCS= Nazca-Cocos Spreading center, PCA= Panama-Choco arc, PFZ= Panama Fracture Zone, RFS= Romeral Fault System, SAP= Sinu Accretionary Prism, SBFS= Santa Marta Bucaramanga Fault Zone, SM= Santander Massif, SMM= Santa Marta Massif, UFS= Uramita Fault System, YG= Yaquina graben.

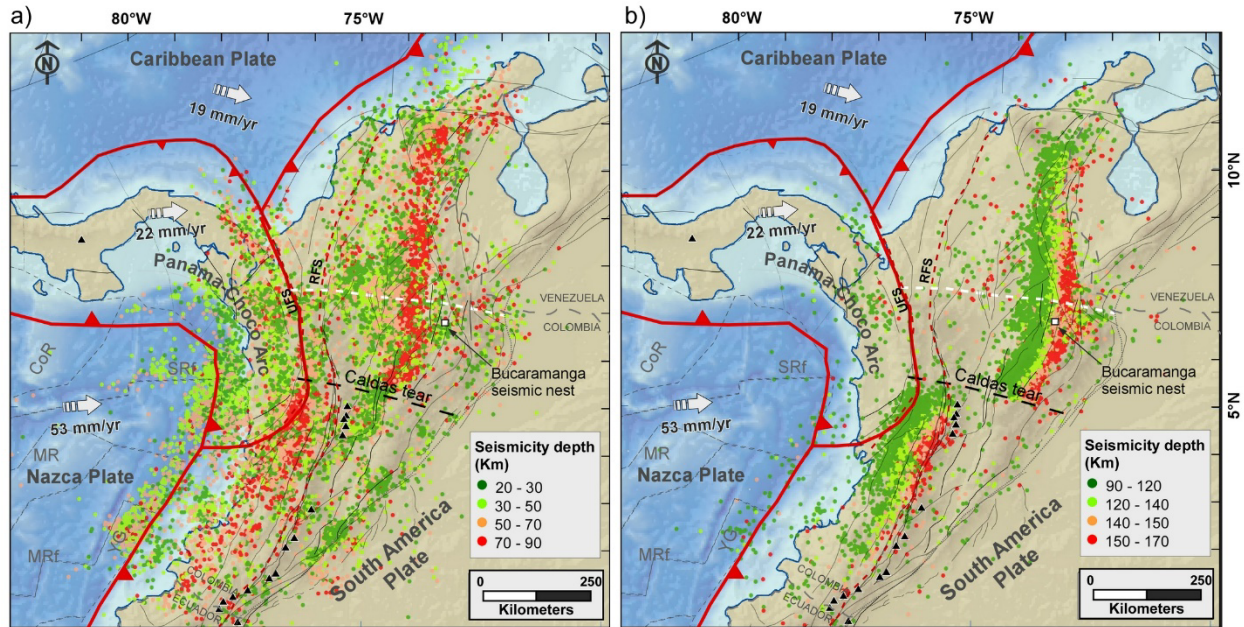


Fig. 3. Seismicity map and modern volcanism in NWSA. For visualization purposes, seismic events are shown according to their depth in shallower than 90 km (a) and deeper than 90 km (b). Earthquake data are downloaded from the catalog of the RSNC website for the period between 1993 and 2018 (<https://www2.sgc.gov.co/Paginas/aplicaciones-sismos.aspx>). Black triangles represent modern volcanoes taken from Siebert et al. (2002). Arrows indicate the current directions of tectonic motion according to Mora-Paez et al. (2019). Continuous grey lines correspond to main faults in the northern Andes (Modified after Veloza et al., 2012). Caldas tear lineament taken from Vargas and Mann, (2013). Bucaramanga seismic nest location taken from Prieto et al. (2012). CR= Coiba Ridge, MR= Malpelo Ridge, MRf= Malpelo Rift, RFS= Romeral Fault System, UFS= Uramita Fault System, SRf= Sandra Rift, YG= Yaquina Graven. Note that north of 5°N, the seismicity is significantly reduced west of 76°W. However, there is a subtle N-S change in the distribution of seismicity across the white dashed line, which represents the southern edge of the Caribbean plate as interpreted in this study (see section 5 of this manuscript for details).

143 While arrangement of seafloor ages is relatively simple west of the Panama fracture zone (PFZ) (Fig.2),
 144 with rock age increasing with distance from the Nazca-Cocos spreading Center (NCS) (Wilson and Hey,
 145 1995), to the east of the PFZ (northern Nazca plate), the seafloor ages reveal a complex history. The
 146 youngest rocks in the northern Nazca plate (9 Ma) are located next to the eastward-trending Sandra and
 147 Malpelo rifts (Fig.2) (Lonsdale, 2005). Moving away from these rifts, the seafloor becomes older until
 148 reaching the Coiba, Malpelo and Carnegie ridges (Fig.2), where the rocks range between 16 and 20 Ma
 149 (Barckhausen et al., 2001; Sallarès et al., 2003; Lonsdale, 2005). Furthermore, given that there is rem-
 150 nant seismicity associated with the Sandra and Malpelo rifts (Lonsdale, 2005), some authors have pro-
 151 posed that the Nazca plate in this region is fragmented into minor tectonic blocks known as the Coiba
 152 (Adamek et al., 1988; Hardy, 1991) and Malpelo (Zhang et al., 2017) microplates (Fig.2).

153 The Nazca slab geometry is well constrained to the south of 5.5°N by geophysical methods (e.g. Cortes
 154 and Angelier, 2005; Syracuse et al., 2016). The termination of the northern volcanic zone (Fig.3) (Wagner
 155 et al., 2017) and the abrupt change in the distribution of seismicity (Wadati-Benioff Zones, WBZs) has
 156 been interpreted as a slab tear (Fig.2) (e.g. Vargas and Mann, 2013). Although a flat-slab has been con-
 157 sidered north of this tear (e.g. Chiarabba et al., 2015; Wagner et al., 2017), the northernmost edge of the
 158 Nazca plate, and its transition beneath Central America is not understood. The presence of the South
 159 Panama Deformed Belt (SPDB, Fig.2) has been regarded as strong evidence of oblique subduction of the

160 Nazca plate beneath the Panama isthmus (e.g. Moore et al., 1995; Mann and Kolarsky, 1995). This is
 161 supported by young adakitic volcanism in eastern Panama that has been associated with shallow subduc-
 162 tion of the Nazca plate (Gutscher et al., 2000). Nonetheless, Johnston and Thorkelson (1997) proposed
 163 that this adakitic signature could be the result of slab windows or localized tears in the Nazca slab that
 164 facilitated the migration of mantle melts from the lower plate.

165

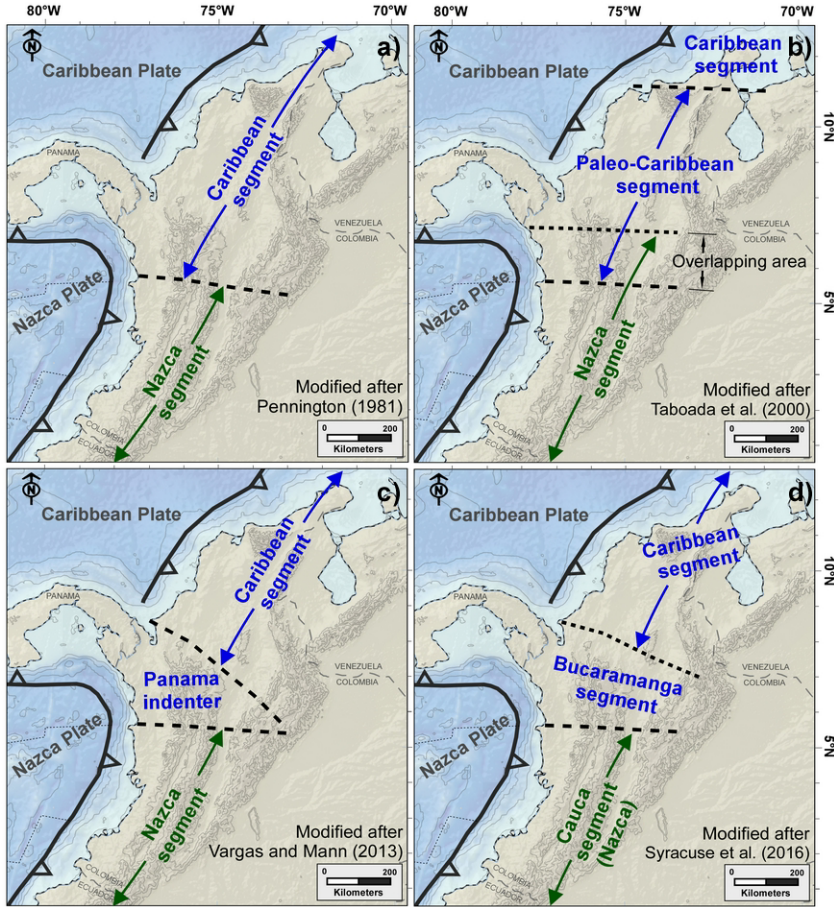


Fig. 4. Some previous interpretations showing the existing ambiguity in the definition of the slab boundaries beneath South America. While several authors consider the northern edge of the Nazca plate to be at about 5.5°N (e.g. Pennington, 2013), others prefer more northerly positions (Taboada et al., 2000; Cortes and Angelier., 2005; Sun et al., 2022). The southern edge of the Caribbean plate is also ambiguous, as some interpretations delineate this boundary at 5.5°N. In contrast, other authors consider the Caribbean slab to be as south as 4°N (Kellogg et al., 2019; Sun et al., 2022), in agreement with the southern occurrence of Miocene accreted rocks of the PCA. The Panama indenter and the Bucaramanga segment (c and d) are derived from the Caribbean plate after its convergence against South America (Vargas and Mann, 2013; Syracuse et al., 2016).

168

169 **2.3 The Northwestern South America (NWSA) Plate**

170 The Late Cretaceous to recent geodynamics in NWSA are associated with three mountain belts devel-
 171 oped north of 2°N, separated by along-strike topographic depressions (Fig.2). This area is comprised by
 172 an assemblage of terranes (e.g., Restrepo and Toussaint, 1988; Cediel et al., 2003) that may be consid-
 173 ered in terms of two broad domains separated by the Romeral fault system (RFS), which extends along
 174 the western flank of the Central Cordillera (Fig.2). East of the RFS, the crust is constituted by a Precam-
 175 brian to Paleozoic continental basement related to the Guiana Craton (Cediel et al., 2003) (Fig.1). Con-
 176 versely, west of the RFS the crust corresponds to relict slivers of oceanic plateau rocks of the Caribbean
 177 Large Igneous Province (CLIP; Fig 2) (Kerr et al., 1997; Sinton et al., 1998), accreted during the Late
 178 Cretaceous to the continental Ecuadorian-Colombian margin. Further to the west, and bounded by the
 179 Uramita fault system (UFS; Fig.2), the CLIP plateau rocks are replaced by intra-oceanic arc rocks that
 180 define the continuation of the Panamanian magmatic arc within South America (León et al., 2018). This

181 terrain, known as the Panama-Choco Arc (PCA; Fig.2) (Duque-Caro, 1990), has been interpreted as re-
182 sult of a Miocene accretion event (e.g. Pindell and Kennan, 2009; Montes et al., 2019; Kellogg et al.,
183 2019). As result of this complex history, the northern Andean range evolved from a diachronic and hetero-
184 geneous orogenic advance (Parra et al., 2009; Bayona et al., 2013, 2020; Mora et al., 2010, 2020). The
185 collision of the PCA against South America after the late Oligocene was a determining factor in the Ande-
186 an Orogeny (e.g. Córtes and Angelier, 2005; Mora et al., 2015; Montes et al., 2019). However, the role of
187 other driving mechanisms that controlled the mountain building in the Northern Andes remains controver-
188 sial (e.g. Reyes-Harker et al., 2015; Mora et al., 2015).

189

190 **3. Data and Methods**

191 **3.1 Paleo-Tectonic Reconstruction**

192 Using the GPlates open access software v. 2.3 (Boyden et al., 2011; Müller et al. 2018; Gurnis et al.,
193 2018; <https://www.gplates.org>), we modeled the relative motion of the Caribbean and Farallon/Nazca
194 plates from 60 Ma to recent times. Our regional model was built upon the global hierarchy of plate mo-
195 tions and mantle reference frame proposed by Müller et al. (2019), by following the methodology of
196 Gurnis et al. (2012) for building deforming plate boundaries through time. For visualization purposes, the
197 South American plate was anchored and, consequently, the tectonic plate convergence velocities and
198 obliquities presented in this paper are relative to fixed South America (Fig.1). Considering that our study
199 area is focused in the southwestern corner of the Caribbean plate and its interaction with the South Amer-
200 ican and Farallon/Nazca plates, we give more relevance to the PCA kinematics. To this end, we relied
201 mainly on the regional reconstruction by Boschman et al. (2014), who used local block rotations for the
202 Panama isthmus proposed in previous studies (Di Marco et al., 1995; Farris et al., 2011; Montes et al.,
203 2012). We also used global plate models (Seton et al., 2012; Matthews et al., 2016; Müller et al., 2019),
204 who made improvements to the regional model of Boschman et al. (2014) and allow for better integration
205 with the kinematics of the Farallon plate.

206 The kinematics calculated for the Farallon/Nazca plate in southern latitudes (motion tracks in Fig.1) (e.g.
207 Pardo-Casas and Molnar, 1987; Müller et al., 2019); are only applicable for the Ecuadorian - Colombian
208 offshore domain for geological times prior to the Farallon breakup (Lonsdale, 2005). Therefore, we used
209 the rotation poles of Müller et al. (2019) for the time period between 60 and 23 Ma. For the Miocene to
210 recent period, we used published variations in the relative positions of the Nazca-Cocos spreading center
211 and the Galapagos hotspot (NCS and GHS in Fig.2), as well as rates of spreading calculated from paleo-
212 omagnetic anomalies (Barckhausen et al., 2001; Werner et al., 2003; Lonsdale, 2005), to propose an
213 alternative kinematic reconstruction of the northern Nazca plate. Although there is uncertainty about the
214 trend of the spreading centers along the already subducted slab (McGirr et al., 2020), we assume that the
215 trend of these features in these areas do not have significant changes to those observed in the preserved
216 area.

217 **3.2 Upper Plate Record and Geometrical Reconstruction**

218 Although there are several factors that influence volcanic distribution in continental arcs, different studies
219 in the Andes have postulated that past changes in subduction angle can be estimated from spatial varia-
220 tions, width and age of the magmatic arc (e.g., Coira et al. 1993; Ramos et al. 2002; Trumbull et al., 2006;

221 Wagner et al., 2017). Indeed, Tatsumi and Eggins (1995) found an empirical relationship between arc-
222 trench distance and slab dip and stated that the slab is between 110 and 140 km below the arc. In this
223 study we use this empirical dependence to constrain the depth isocontours of subducting plates. We em-
224 ploy the paleogeographic reconstruction of the plate margins and the spatiotemporal distribution of Ceno-
225 zoic arc magmatism. We used the recently published Cenozoic arc magmatism records along the Colom-
226 bian margin (Lara et al., 2013; Wagner et al., 2017; Leal-Mejía et al., 2019; Marín-Cerón et al., 2019;
227 Cardona et al., 2018; Barbosa et al., 2019; Weber et al., 2020), the Ecuadorian Andes (Schütte et al.,
228 2010) and the Panamanian isthmus (Lissinna, 2005; Wegner et al., 2011; Montes et al., 2012; Rooney et
229 al., 2015).

230 The resulting geometric models were integrated with published evidence of deformation in the upper
231 plate, which allowed us to identify possible correlations between the regional plate geodynamics and first-
232 order phases of deformation in the Northern Andes during the Cenozoic (Table S1). These deformation
233 episodes are based on recently published interpretations for the Northern Andes (e.g. Parra et al., 2009;
234 Mora et al., 2010; Caballero et al., 2013; Mora et al 2013a; Mora et al 2013b; Moreno et al., 2013; Silva et
235 al., 2013; Montes et al., 2012; Bayona et al., 2013; Villagómez and Spikings, 2013; Horton et al., 2015;
236 Reyes-Harker et al., 2015; Mora-Bohórquez et al., 2017a; León et al., 2018; Pardo-Trujillo et al., 2020)
237 and eastern Panama (Montes et al., 2012; Barat et al., 2014). Due to the complex interaction between the
238 subducting Caribbean and Farallon/Nazca plates throughout the Cenozoic, the geometrical restoration of
239 these slabs requires a three-dimensional approach. In this study we achieved this by using the Petrel
240 software (<https://www.software.slb.com/products>). The results are shown in different time-step structural
241 contour maps and three-dimensional diagrams. Although there is uncertainty about the actual structural
242 evolution, we draw detailed contour maps (20 km contour interval), only for the purpose of emphasizing
243 the geometrical changes between the different tectonic episodes.

244

245 **4. Results**

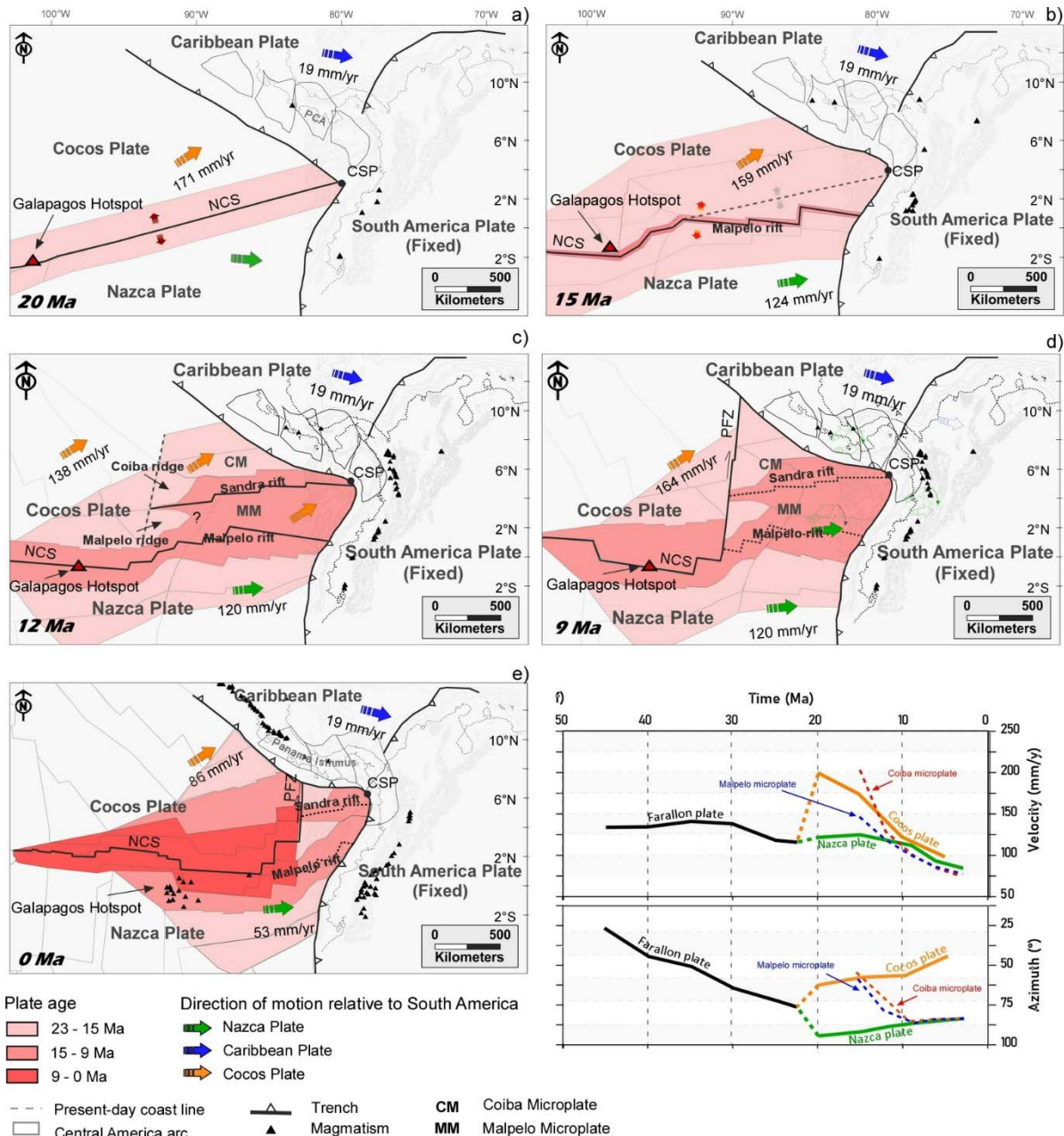
246 **4.2 Plate Kinematic Reconstruction**

247 Below we integrate the results of our kinematic reconstruction of the Northern Nazca plate (Fig.5) and
248 Southwestern Caribbean plate (Fig.6) with a compilation of observations made by different authors.

249 **4.2.1 Nazca Plate Reconstruction**

250 Previous studies suggest that the Farallon kinematics were relatively homogeneous during the Paleogene
251 (Figs.1, 5f) (e.g. Müller et al., 2019). However, by the late Oligocene the Galapagos hotspot got aligned
252 with a preexisting fractured or weakened zone triggering the Farallon plate breakup and the origin of the
253 Nazca and Cocos plates at 23 Ma (Fig.5a) (Lonsdale, 2005). The initial oceanic spreading along the new
254 Nazca-Cocos plate boundary prompted a differential direction of displacement for the Nazca and Cocos
255 plates, representing a more orthogonal convergence against Central and South America (Fig.5a). This
256 motion scheme changed at around 18 Ma, when the spreading center jumped to a more southern position
257 (note shift in spreading-axis position between Figs.5a and 5b) (Barckhausen et al., 2001; Werner et al.,
258 2003). From a kinematic point of view, this E-W spreading center was the northern edge of the Nazca
259 plate during the middle Miocene, and as a consequence, the segment converging against NWSA (the
260 proto-Coiba and proto-Malpelo microplates) exhibited similar kinematics as the Cocos plate at that time

261 (Fig. 5f). After 15 Ma, the spreading axis in the easternmost Pacific shifted to the Malpelo rift (Figs.5b)
262 and shortly after, but with concurrent activity, to the Sandra rift (5c) (Lonsdale, 2005). This complex oce-
263 anic spreading generated a northward motion to the north of the Malpelo spreading center (Fig.5c). Final-
264 ly, the spreading along the Sandra and Malpelo rifts abruptly ended at 9 Ma, and as a consequence, the
265 Coiba (CM) and Malpelo (MM) microplates became part of the Nazca plate (Fig.5d) (Sallarès et al., 2003;
266 Lonsdale, 2005), leading to the establishment of a transform fault boundary between the Cocos and
267 Nazca plates (the Panama fracture zone, PFZ, Fig.2) (Sallarès et al., 2003; Lonsdale, 2005; Morell,
268 2015). As a consequence of this late Miocene coupling of the Coiba and Malpelo microplates to the
269 Nazca plate, the convergence direction became more oblique against the Panama isthmus (Morell, 2015;
270 Rooney et al., 2015) and more orthogonal against the northern South American margin (Figs.5d,e). In
271 other words, the modern Nazca-Cocos plate boundary and the current tectonic configuration in the Pacif-
272 ic, offshore Colombia and Panamá, were established after 9 Ma.



273

Fig. 5. a-e) Paleotectonic reconstruction of the Nazca-Cocos plate boundary (NCS) from the early Miocene to the present-day. Red colors indicate the age of the ocean-floor according to previous paleomagnetic studies (Barkhausen et al., 2001; Werner et al., 2003; MacMillan et al., 2004; and Lonsdale, 2005). f) Estimated evolution of the motion direction and velocity of the Farallon, Nazca and Cocos plates, and the Coiba and Malpelo microplates.

274

275

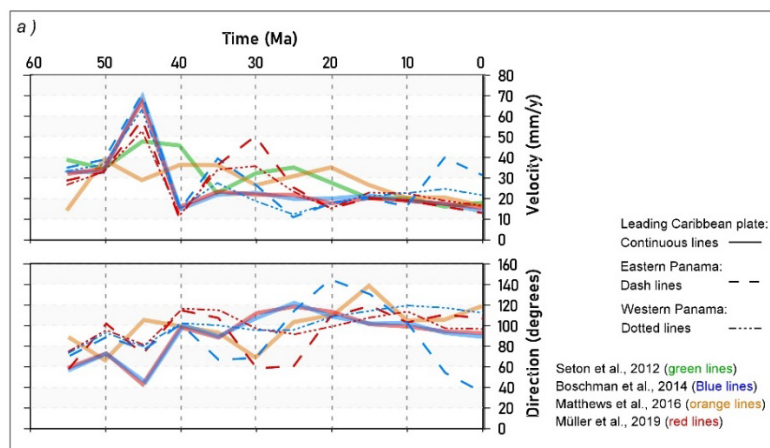
276 4.2.2 Southwestern Caribbean Plate Reconstruction

277 The Panama-Choco arc (PCA) was located about 1000 km in a southwestern position of its current loca-
 278 tion during the Paleocene (60 Ma) (Figs.2, 6b) (e.g. Pindell and Kennan, 2009) and was moving towards
 279 the NE, defining a highly oblique convergence with the South American margin (Fig.6b). During the

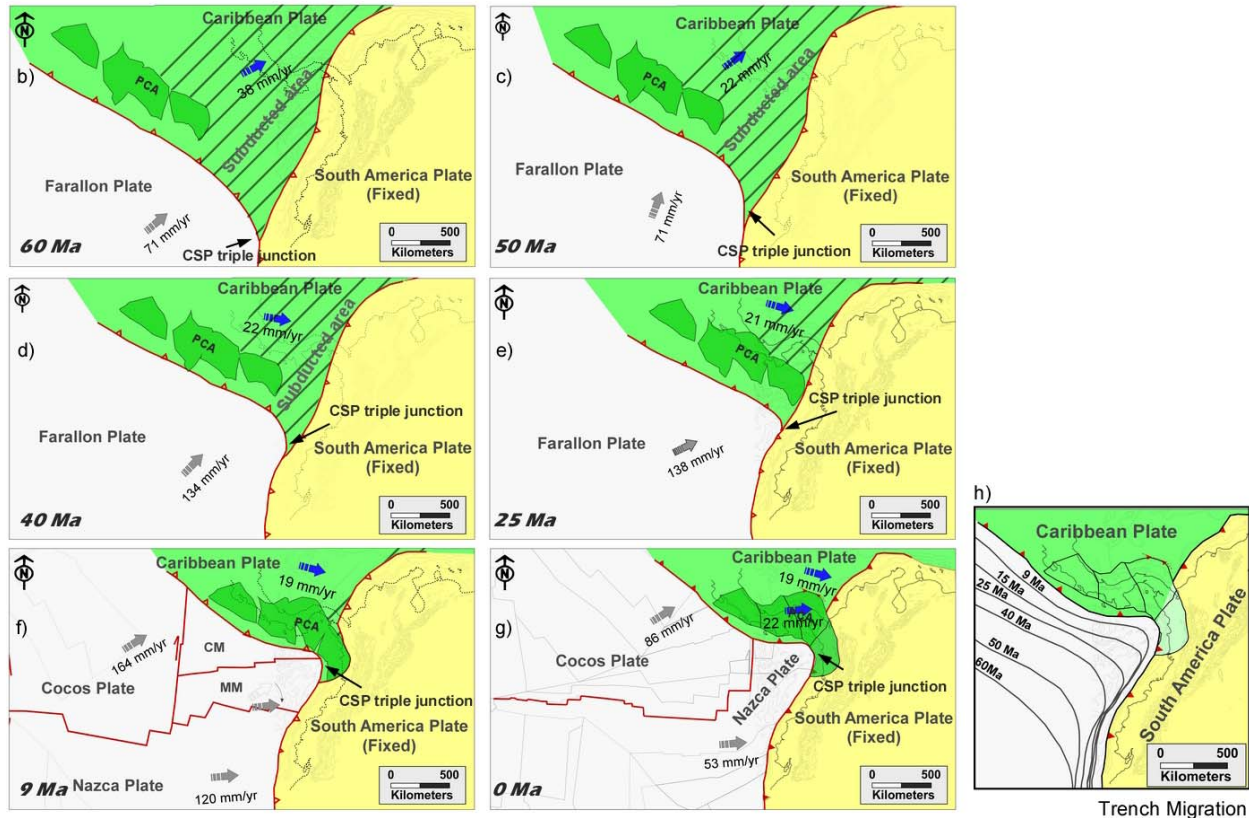
280 Paleocene, the Farallon plate margin, defined by its boundary with the Caribbean plate to the northwest
 281 and the South American plate to the southeast, formed a subtle curved trend (Fig.6b). Throughout the
 282 Paleocene-early Eocene, the southwestern Caribbean plate continued moving in SW-NE direction at an
 283 average speed of 36 mm/yr (Fig.6a) (Boschman et al., 2014; Müller et al., 2019). During the middle Eo-
 284 cene there was an abrupt shift towards the SE (Boschman et al., 2014; Müller et al., 2019) (Fig.6a), that
 285 implied a more orthogonal convergence direction against South America. As a result, the CSP triple junc-
 286 tion moved northeastward during the Eocene and the vertical-axis curvature between the Farallon-
 287 Caribbean and Farallon-Peruvian trenches significantly increased to become almost orthogonal
 288 (Figs.6c,h).

289 During the late Eocene-Oligocene, the Caribbean plate continued moving in an eastward direction at an
 290 average rate of 22 mm/yr (Fig.6a), moving the PCA toward the Colombian margin (Fig.6d). At ca. 23 Ma,
 291 the eastward motion of the Caribbean plate culminated in the onset of collision of the intra-oceanic PCA
 292 against the Colombian margin at about 300 km to the south of the present-day CSP triple junction
 293 (Fig.6e) (Duque-Caro, 1990) (4.5°N in Fig7a). Although the Caribbean kinematics during the Miocene,
 294 after initial collision, were dominated by eastward plate motion, the resulting arc fragmentation and rota-
 295 tion of blocks (Farris et al., 2011; Montes et al., 2012, 2019) caused the continued northward migration of
 296 the accretion front with South America (Figs.6f,g).

297



298



299

Fig. 6. a) Kinematics of the Caribbean plate relative to stable South America. b, c, d, e, f, g) Paleotectonic reconstruction of the southwestern Caribbean plate motion throughout the Cenozoic showing the migration and convergence of the PCA against SA. Note that as a consequence of the Caribbean kinematics, the triple junction with the Farallon/Nazca and South American plates migrated in northward direction. h) Migration of the Caribbean-Pacific trench. CM= Coiba microplate, LMV= Lower Magdalena Valley, MM= Malpelo microplate, PCA= Panama-Choco arc, SA= South America.

300

301 5. Discussion

302 5.1 Farallon/Nazca Plate Geodynamics

303 The evolution of the Farallon/Nazca plate convergence against the NWSA can be divided into three major
 304 episodes separated by the breakup of the Farallon plate during the late Oligocene and the establishment
 305 of the modern northern Nazca plate kinematics during the late Miocene.

306 5.1.1 Paleocene to late Oligocene (65 – 23Ma).

307 The continuity of the Farallon slab to the northeast of the South American margin is critical for under-
 308 standing the geodynamics prior to the Farallon breakup. However, geophysical methods do not allow a
 309 clear definition of this transition (e.g. Wagner et al., 2017). For this reason, most previous models have
 310 assumed that there is no continuity between the South and Central American margin. On the contrary,
 311 below we argue that the Farallon plate evolved as a continuous slab segment, conditioning the geody-
 312 namics at the triple-junction.

313 The Farallon kinematics during the Paleogene (Figs.1, 5f) defined an oblique convergence against the
314 PCA and South American margins. Although the oceanic crust of the Caribbean plate east of the PCA
315 during the Paleocene is already subducted (see subducted area in Fig.6a), the most likely geometrical
316 interpretation is that the trench followed a continuous trend, linking the PCA and South American
317 trenches during the Paleocene (Fig.6a). This is supported by the spatiotemporal distribution of
318 magmatism along the PCA and South American margins during the Paleogene-Eocene (Figs.7a,b) (e.g.
319 Wegner et al., 2011; Leal-Mejía et al., 2019; Cardona et al., 2018). The Paleocene configuration of the
320 Farallon margin defined a lateral transition between ocean-continent (South America) and ocean-ocean
321 (Caribbean) subduction that, in agreement with Cardona et al. (2018), resembled an Aleutian type margin
322 (Fig.7a). Cardona et al. (2018) and Barbosa-Espitia et al. (2019) provide geochemical evidence of this
323 magmatic transition. Assuming these intrusions occurred at a distance of 300 km from the trench, similar
324 to the present-day volcanic zone, the Farallon plate was subducting below the margin at a steep angle (>
325 25° dip) during the Paleocene (green contour lines on Fig.7a).

326 This configuration changed during the middle-late Eocene (Figs.7b,c), when the curvature of the Farallon
327 trench strongly increased at the CSP triple junction, shaping a nearly orthogonal corner (green contour
328 lines on Fig.7b). The coincidence between this trench constriction and the contemporaneous decrease in
329 magmatic activity throughout the late Eocene-Oligocene on the northern South American margin (Leal-
330 Mejía et al., 2019; Bayona et al., 2012) and the eastern PCA (Figs.7c,d) (Lissinna, 2005; Wegner et al.,
331 2011) suggests that the slab segments beneath these margins formed a continuous subduction system.
332 We propose that depending on the angle of subduction, there are two possible end-members scenarios
333 for the subducting slab geometry beneath the PCA and South America margins from the late Eocene
334 (Fig.9). Considering that the Farallon plate evolved as a single subducting element implies that the slab
335 bent tightly to the east of the CSP triple junction. This leads to an accommodation-space problem in the
336 hinge zone, that causes trench-parallel shortening strain in the bent slab, resulting either in subsequent
337 rupture and overlapping of slab segments (Fig.9b) or in a reduced subduction angle with a regional flat-
338 slab around the hinge zone (Fig.9c). A similar flat-slab setting associated with a convergent triple junction
339 has been reported beneath Japan (Faccenna et al., 2018). It is interesting to note that a regional onset of
340 inversion of rift structures in the Eastern Cordillera of Colombia, associated with an eastward migration of
341 the deformation front toward the backarc region (Table S1) (eg. Gómez et al., 2003; Parra et al., 2009;
342 Mora et al., 2010, 2013; Saylor et al., 2012; Sánchez et al., 2012; De la Parra et al., 2015; Martínez et al.,
343 2022; Rosero et al., 2022) could support an Oligocene episode of flat-slab subduction (Fig.7d). This Oli-
344 gocene event is also concurrent with a deformation phase in eastern Panama (Montes et al., 2012; Barat
345 et al., 2014). However, future work is required to determine if there is a causal relationship between these
346 events.

347 The approximate simultaneity of decreased magmatic activity during the late Eocene-Oligocene
348 (Figs.7c,d) on both the PCA and South America margins (Wegner et al., 2011; Leal-Mejía et al., 2019;
349 Cardona et al., 2018; Barbosa-Espitia et al., 2019) suggests that the subduction zones along these mar-
350 gins did not evolve independently. Instead, the Farallon plate subducted as a single slab beneath these
351 margins during the Oligocene, favoring the flat-slab model proposed in Fig.9c.

352 **5.1.2 Early to latest middle Miocene (23 – 9 Ma)**

353 The Oligocene flat-slab subduction during the Oligocene is in line with the hypothesis formulated by
354 Lonsdale (2005), which suggests that the stress that broke the Farallon plate was preceded by the exten-
355 sional pull between the Central and South American subduction zones (as conceptualized in Fig.9c) and

356 the alignment of this weakness zone with the Galapagos hotspot by the early Miocene (Fig.5a). Neverthe-
357 less, there is no evidence in South America of this breakup and initial spreading during the early Miocene.
358 This lack of evidence can be explained by the fact that during the Oligocene-Miocene, the subducted
359 Farallon/Nazca slab at this position was overlapped by the subducting Caribbean slab (Fig.7d), implying
360 that the Caribbean plate must have acted as a blanket that inhibited the rise of magmatic fluids to the
361 South American plate. This interpretation is different from that of McGirr et al. (2020), which considers the
362 Azuero zone in Panama as the initial rupture point of the Farallón plate. However, if that scenario were
363 correct, a magmatic record associated with the initial crustal spreading would indeed be in that region.

364 Interestingly, subduction-related magmatism renewed during the late Oligocene in the PCA and South
365 America (Fig.7e) (Wegner et al., 2011; Wagner et al., 2017; Leal-Mejía et al., 2019; Marín-Cerón et al.,
366 2019) suggesting a re-steepening of the now separated Nazca and Cocos plates in the Panamanian and
367 Colombian margins. This steepening, and the increasing curvature of the trenches at the CSP triple junc-
368 tion (Fig.7e), may have resulted in the above-mentioned zone of compressive stress in the subducting
369 slab, indicating an evolution between the model shown in Fig.9c to the model shown in Fig.9b during the
370 early Miocene. This compressive stress in the inflexion point (Fig.9b) may have prevented the oceanic
371 spreading along the original rupture zone (Fig.5a), forcing the southward migration of the spreading cen-
372 ter by 18 Ma (Fig.5b) (Barkhausen et al., 2001; Werner et al., 2003). Possibly, this gave way to the San-
373 dra and Malpelo rifts, and in turn to the Coiba and Malpelo microplates during the early- middle Miocene
374 (Figs.5b,c and 7f).

375 From a kinematic point of view, the southward migration of the spreading center implies that the eastward
376 motion of the Nazca plate during most of the early-middle Miocene was limited to offshore southern Ec-
377 uador, Peru and Chile (Fig.7f). Conversely, the Sandra and Malpelo spreading centers imprinted a north-
378 ward component of motion to the Coiba and Malpelo microplates. As a result, the plate beneath NWSA
379 and the Panamá isthmus had a Cocos-like motion during most of the early-middle Miocene, which implied
380 an orthogonal convergence against the Panama isthmus (Morell, 2015; Rooney et al., 2015) and an
381 oblique convergence against South America (Fig.7f). This interpretation, however, differs from the model
382 by McGuirr et al. (2020), who assume that the Sandra and Malpelo rifts did not project eastward beneath
383 South America due to the flat-slab subduction of the Nazca plate. Nonetheless, there is no evidence of
384 Nazca flat-slab subduction during the middle Miocene (Chiarabba et al., 2015; Wagner et al., 2017).

385 While the moderate exhumation rates reported in the northern Andes throughout the early-middle Mio-
386 cene (Table S1) (Mora et al., 2020a) is consistent with the continued oblique convergence during most of
387 that time span (Fig.7f), the accelerated Andean deformation during the late Miocene could be associated
388 with a major tectonic event. Morell (2015) and Rooney et al. (2015) recognize a kinematic change in the
389 northern Nazca plate by 9 Ma with implications for the Central American tectonic history. The influence of
390 this kinematic event on the South American plate has not been studied until now.

391 **5.1.3 Late Miocene to Recent (9 – 0Ma)**

392 The kinematic change at 9 Ma due to the attachment of the Coiba and Malpelo microplates to the Nazca
393 plate, represented a major tectonic event that modified the convergence directions and the subduction
394 system beneath Eastern Panama (Morell, 2015) and Northern South America. The eastward migration of
395 the arc-related magmatism in the Central Cordillera of Colombia during the Miocene (Figs.7e-h) (Wagner
396 et al., 2017; Leal-Mejía et al., 2019; Marín-Cerón et al., 2019) has been associated with a progressive
397 shallowing of the Nazca slab (Wagner et al., 2017). Particularly, the magmatic migration north of 5.5°N

398 (Fig.7g) that initiated the volcanism in the Eastern Cordillera at 6 Ma (Pardo et al, 2005; Bernet et al.,
399 2016), supports a shallow subduction of the Nazca plate during the late Miocene (Fig.7h) (Chiarabba et
400 al., 2015; Wagner et al., 2017). However, the uninterrupted magmatism in the South American arc south
401 of 3°N (Figs.7g, 8), indicates that the late Miocene shallow subduction was operating only in the most
402 northern Nazca slab segment, but not in southern latitudes. The change in convergence direction, in
403 combination with the already subducted slab beneath Panama, and the complicated subduction geometry
404 east of the CSP triple junction (Fig.7g), very likely triggered this new phase of flattening behind the triple
405 junction (Figs.7g,h, 9b). Therefore, this mechanism of slab flattening supports a Nazca plate behaving as
406 a single subduction system beneath the Eastern Panama units (Gutscher et al., 2000) and the Northern
407 Andes. Though the present-day northward motion of the Nazca plate beneath Panama is minimal, the
408 amount of crust subducted before 9 Ma in northward direction was significantly more important (see con-
409 tours of subducted ages in Fig.8), which weakens the model of a slab window beneath Panama (John-
410 ston and Thorkelson, 1997; McGirr et al., 2020).

411 It is very likely that the change in convergence obliquity, and the flat-slab subduction of the northern
412 Nazca plate during the late Miocene (Figs.7h,8) played a major role in the onset of accelerated defor-
413 mation and the main phase of Andean orogeny (e.g. Parra et al., 2009; Mora et al., 2006, 2010, 2020a,b;
414 Carrillo et al., 2016) (Table S1). During the late Pliocene, the renewed volcanism in the Central Cordillera
415 south of 5.5°N indicates steepening of the Nazca slab after its tearing (Caldas tear) and separation from
416 the northern segment that stayed flattened (Fig.8) (Wagner et al., 2017). As the geometrical conditions
417 shown in Fig.9c prevailed only in the northernmost segment, the slab steepening was induced merely in
418 the southern segment (Fig.8), triggering the modern volcanism south of 5.5° N (Fig.8) (Vargas and Mann,
419 2013; Wagner et al., 2017; Leal-Mejia et al., 2019; Marín-Cerón et al., 2019).

420 Nonetheless, while there is agreement of late Miocene to recent flat-slab subduction of the Nazca plate
421 north of 5.5°N in South America, on the Panamanian side there is controversy on the presence (Gutscher
422 et al., 2000) or absence of the Nazca plate (e.g. Johnston and Thorkelson, 1997). Even though previous
423 studies do not interpret the continuity of the Nazca plate beneath Central and South America, our recon-
424 struction suggests that this plate is continuous east of the CPS triple junction, connecting both margins by
425 means of a flat slab.

426 **5.2 Caribbean Plate Geodynamics**

427 The convergent geodynamics of the Caribbean plate against NWSA were dominated by two events dur-
428 ing the Cenozoic: the abrupt kinematic change during the middle Eocene and the accretion of the PCA to
429 South America.

430 **5.2.1 Kinematic Change during the middle Eocene**

431 The highly oblique subduction of the Caribbean plate during the late Cretaceous to middle Eocene
432 (Figs.7a,b) prompted the arc-related magmatism in the northern Central Cordillera of Colombia and the
433 Santa Marta Massif (Cardona et al., 2011; Bayona et al., 2012; Jaramillo et al., 2017; Leal-Mejia et al.,
434 2019). Although there is consensus that the Caribbean plate shifted from northeastward to eastward mi-
435 gration during the middle Eocene (Figs.6a,d) (Seton et al., 2012; Matthews et al., 2016; Müller et al.,
436 2019), the implications on the convergence with South America are not well understood. Several authors
437 propose that this kinematic change coincided in time with the initial subduction of a thicker lithosphere,
438 which defined the onset of flat-slab subduction of the Caribbean plate (Cardona et al., 2011; Bayona et

439 al., 2012). Below we propose that the Eocene change in convergence obliquity was additionally associat-
440 ed with a break-off in the Caribbean slab.

441 Although the distribution of magmatism suggests at least 300 km of subducted slab of the Caribbean
442 plate between the Late Cretaceous and middle Eocene (Fig.7a,b), an implication of this protracted obliqu-
443 uity is that the slab may have been unstable due to its negligible downward (eastward) motion. We specu-
444 late that the abrupt change in Caribbean plate convergence, that became more orthogonal by the middle
445 Eocene (Figs.6c and 6d) (Boschman et al., 2014; Müller et al., 2019), may have led to the break-off and
446 collapse of this nearly stagnant slab segment (Fig.7c). This is supported by the paradoxical cessation of
447 magmatism when the Caribbean convergence became orthogonal after the middle Eocene (Figs.7c,d).
448 Although this magmatic shutting down has been interpreted as initial flat-slab subduction of the Caribbean
449 plate (e.g. Bayona et al., 2012), this cannot explain the late Eocene regional tectonic quiescence in the
450 northern Andes (Table S1) (e.g. Mora et al., 2013a). On the contrary, a missing Caribbean slab (Fig.7c),
451 and in turn the lack of plate coupling during the late Eocene may have accounted for both the magmatic
452 and tectonic quiescence during the late Eocene. Furthermore, the northward reduction in exhumation
453 rates from the Ecuadorian to the Colombian Andes (Spikings et al., 2010; Restrepo–Moreno et al., 2009,
454 Mora et al., 2020a) (Table S1) is consistent with the area of influence of the Caribbean plate during the
455 late Eocene (Fig.7c).

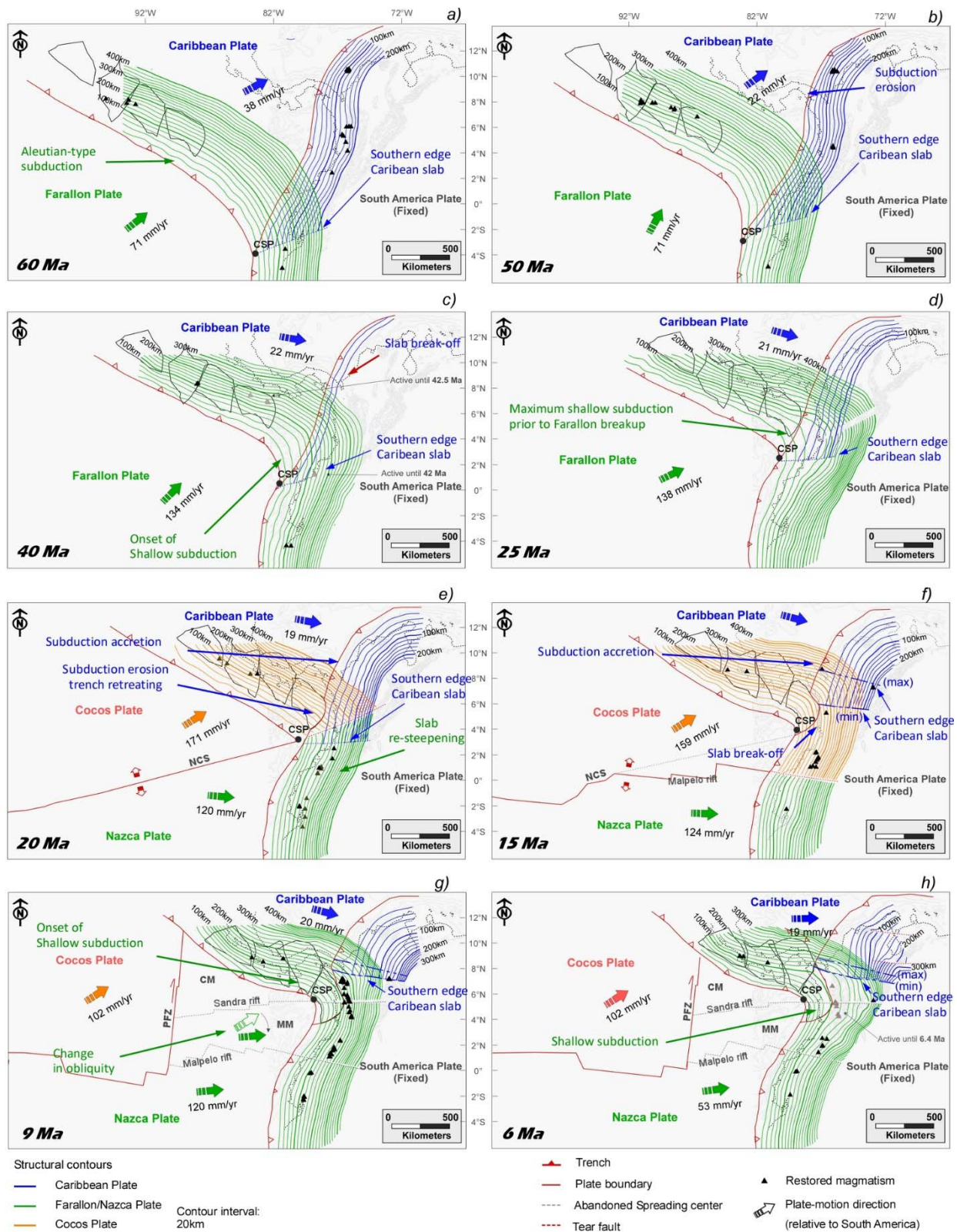


Fig. 7. a-h) Suggested reconstruction of the northwestern South America and Panama subduction systems considering the development of magmatism, the change of geometry of the trenches and other concepts discussed in this paper. Farallon/Nazca (green), Cocos (green), and Caribbean (blue) slabs. Black triangles show active magmatism. Big arrows indicate

the direction of plate motion relative to stable South America. Blue dashed lines show the suggested alternatives for the southern boundary of the Caribbean plate, minimum resulting from the development of magmatism east of the PCA, and maximum derived from the Caribbean kinematics after initial contact between the PCA and SA. Note that the purpose of showing this relatively detailed interpretation (contour interval 20 km) is to emphasize the geometric changes between the different tectonic episodes.

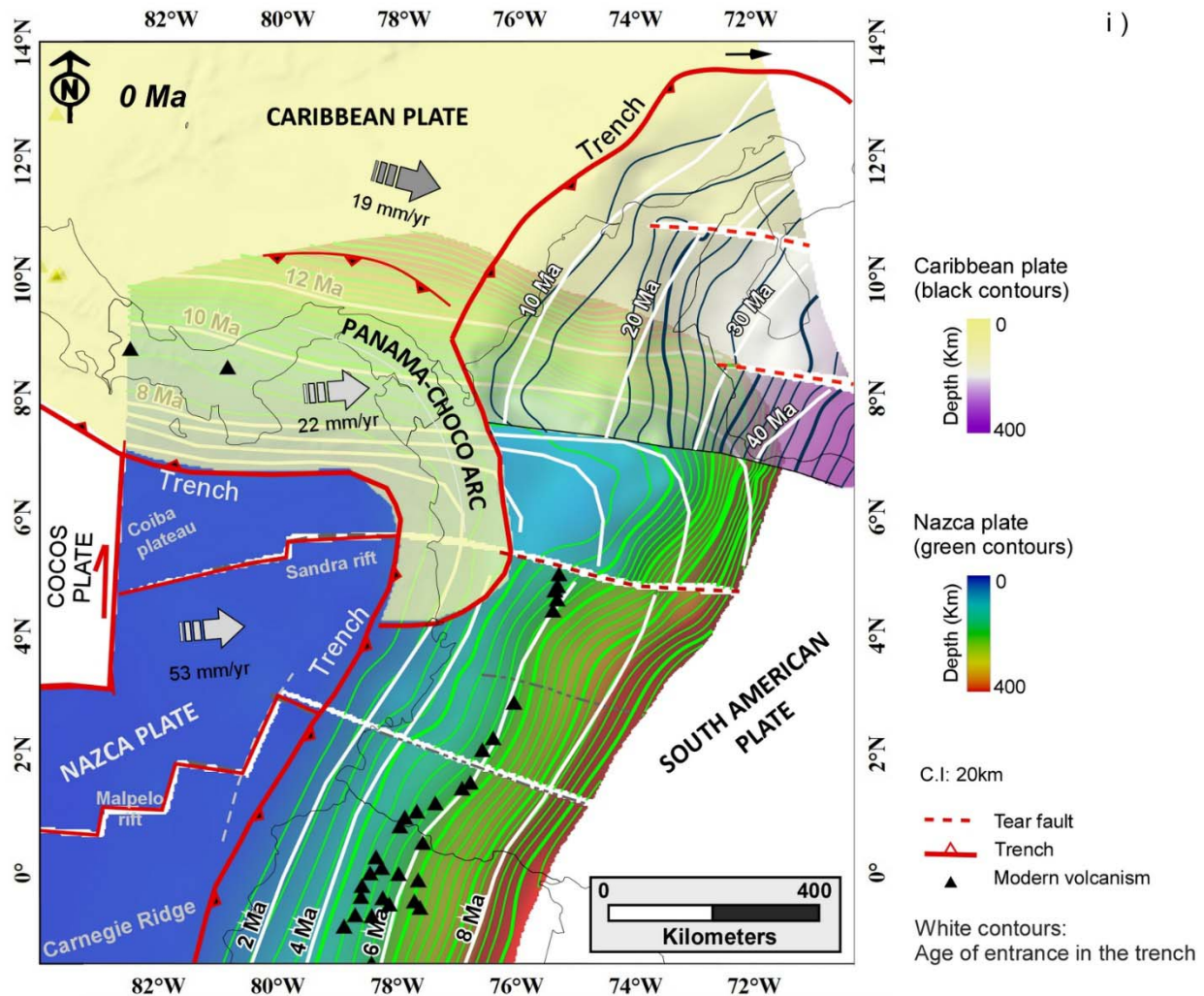


Fig. 8. Present-day structural map of the Nazca and Caribbean slabs beneath NWSA. Farallon/Nazca (green), Cocos (green), and Caribbean (blue) slabs. White contours indicate the age of entrance in the trench. Black triangles show active magmatism. Big arrows indicate the direction of plate motion relative to stable South America.

457 Another implication of the new Caribbean kinematics after the middle Eocene (Fig.7c), is that since that
 458 moment, the margin laterally transitioned between an orthogonal subduction to a highly oblique boundary
 459 below NWSA (Fig.10b). Although this geometric configuration may prompt the formation of subduction-
 460 transform edge propagators (STEP faults) (Mora-Bohórquez, et al., 2017b; Govers & Wortel, 2005), un-
 461 der low convergence rates, the slab could not be torn apart in the transform margin, which would result in
 462 shallow subduction by slab-pulling (Fig.10c) (Govers & Wortel, 2005). We consider that this was the case
 463 in northern South America, where the shape of the continental margin, and the direction of motion
 464 (Fig.6a), may have forced the shallow subduction of the Caribbean plate since the middle Eocene

465 (Figs.7c, 10c). The previous break-off of the slab and the buoyant nature of this lithosphere (Pindell et al.,
 466 2005; Bayona et al., 2012) may have favored this process.

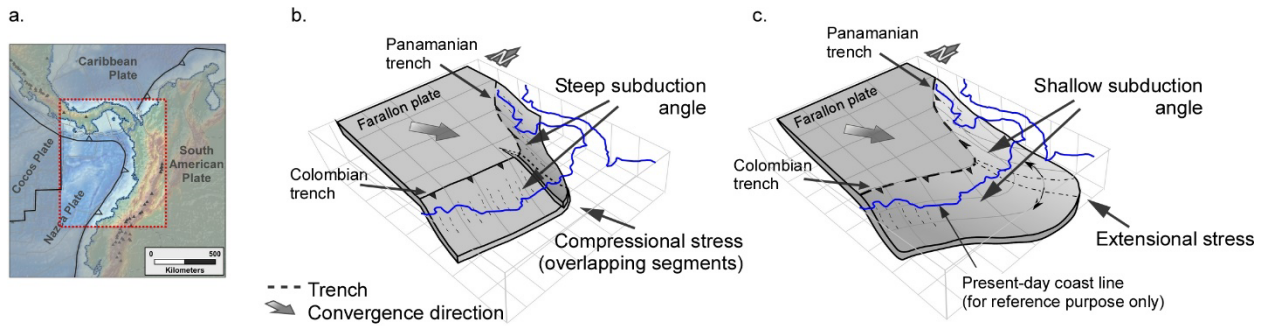
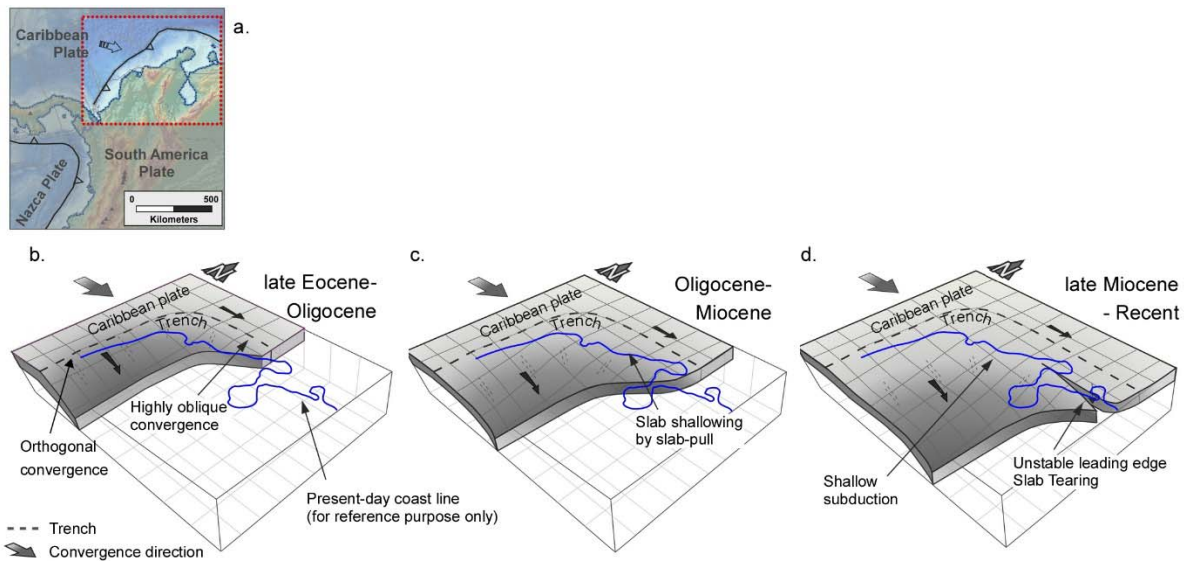


Fig. 9. Simplified sketch showing two end-member scenarios for the subduction geometry of a single slab obliquely subducting under two orthogonal margins. These settings depict the Farallon plate at the corner between Central and South America (a). In the first model (b) it is assumed that the slabs subduct with steep angles on both margins, prompting the compressional stress behind the trench due to a reduced accommodation space. In the second model (c) it is assumed that the slab horizontal folding is accommodated by reducing the angle of subduction at the inflexion point, favoring the slab flattening on both margins. It is important to note that the stress behind the hinge zone in c) could be related to slab rupture at advanced stages of flattening.



467 Fig. 10. Simplified sketch showing three time-steps of the convergence of the Caribbean plate against NWSA (in this sketch the effect of the PCA accretion is not considered). Given the curved trench geometry and the direction of convergence, the southernmost segment is characterized by orthogonal subduction, while the northeastern segment by a highly oblique convergence. Although this configuration is similar to other models that account for Subduction-Transform Edge Propagators (STEP faults) (Govers and Wortel, 2005), the very slow convergence could inhibit the faulting and favor the slab shallowing near the oblique margin. We consider that this is the case in the area shown in a), as the low convergence rate of the Caribbean plate, in combination with the margin shape induced the flat-slab subduction by slab-pull from the northeastern side of the margin (b,c). At advanced stages, the cumulative shallow subduction may have not been sustainable, which possibly prompted the faulting in the leading edge of the slab (d).

468 **5.2.2 Accretion of the Panama-Choco Arc (PCA) to NWSA**

469 Though the accretion of the PCA to South America is widely mentioned in the literature (e.g. Duque-Caro,
 470 1990; Montes et al., 2012), the geodynamic mechanism of this event is not understood (Fig.12). Most

471 previous interpretations agree that the Caribbean plate is subducting east of the PCA (Figure S3) (e.g.
472 Vargas and Mann, 2013; Kellogg et al., 2019), which has been interpreted as a renewed subduction after
473 the initial collision between the PCA and South America during the early-middle Miocene (León et al.,
474 2018). Although the acquisition of additional data is required, in the following lines we explain why our
475 preferred interpretation is that there is not a Caribbean slab east of the PCA.

476 The initial point of collision of the PCA against South America was approximately 400 kilometers to the
477 south of the present Panama Isthmus during the late Oligocene (Fig.12a). However, during the Miocene,
478 the PCA was virtually forced into the continent defining a concave suture ((Fig.12a). The paleogeographic
479 reconstruction (Fig.12) indicates that the deformation was not symmetrical on both sides of the suture
480 after first contact of the PCA with South America. On the one hand, the compressive strain fragmented
481 the PCA and rotated the resulting blocks forming an orocline (Montes et al., 2012), the northeastward
482 advance of the southern edge of the Caribbean plate, and the northward migration of the accretion front
483 against South America. It is very likely that this behavior was prompted by the northeastward pushing of
484 the Pacific plates (Figs.12a-c). On the other hand, the most important change on the continental side was
485 the eastward retreat of the margin by at least 200 km (Fig.12). In spite of this retreat, several recent stud-
486 ies indicate that horizontal shortening and exhumation rates were not significantly increased in the north-
487 ern Andes during the early-middle Miocene (Restrepo–Moreno et al., 2009; Mora et al., 2020a; Zapata et
488 al., 2021; Pérez-Consuegra., 2022). For instance, shortening estimates of 40 ± 10 km in the Eastern Cor-
489 dillera and Magdalena basin during the Miocene to recent between 6° and 8°N (Mora et al., 2013a), and a
490 maximum ~ 10 km of shortening in the Central Cordillera during the same time span (range dominated by
491 transpressive structures) give a total maximum shortening of ~ 60 km, which cannot explain the 200 km of
492 margin retreat. Moreover, León et al. (2018) recognize that the suture zone evolved as a negative topo-
493 graphic area, with the continuous accumulation of fine-grained hemipelagic sediments, precluding crustal
494 thickening as a consequence of this contraction. The lack of known Miocene metamorphic rocks near the
495 suture zone, also suggests that this accretional process did not take place as a typical collisional event
496 (Zheng et al., 2015). This is also confirmed by crustal thickness estimation from receiver functions by
497 Poveda et al. (2015), showing no crustal thickening in the suture zone. In the contrary, the Moho depth
498 slightly decreases west of the Central Cordillera toward the suture.

499 Given that most of the original Paleogene forearc area is missing on the continental side (Fig.11a) (do-
500 main between the Uramita and the Romeral fault systems), we suggest that most parts of the forearc
501 terrane (up to 200 km) were removed by subduction erosion during the emplacement of the PCA into the
502 margin (Fig.11b). This tectonic erosion and fast retreating margin was likely a consequence of the ham-
503 pered subduction of the highly buoyant lithosphere associated with the PCA, and the oceanic nature of
504 the continental margin (mafic terrane accreted during the Late Cretaceous). Subduction erosion is a ma-
505 jor factor in removing material from active plate margins (von Huene & Scholl, 1991; Clift and Vannucchi,
506 2004; Kukowsky and Oncken, 2006; Bruce et al., 2011). Furthermore, the loss of at least 200 km of fore-
507 arc material and trench retreat since 20 Ma to the east of the PCA is similar to the average rate of 10
508 mm/yr of subduction erosion reported in the Peruvian margin associated with the subduction of the ero-
509 sive Nazca ridge (Clift and Vannucchi, 2004). Also, from numerical modeling Keppie et al. (2009) find that
510 regionally focused subduction erosion may occur in an unsteady fast mode that they show to have oc-
511 curred along the Andean margin. Finally, the lack of relevant exhumation episodes before the late Mio-
512 cene could be due to the fact that erosive subduction systems are typically associated with subsidence in
513 the forearc (e.g. von Huene & Scholl 1991; Clift and Vannucchi, 2004; Kukowsky and Oncken, 2006),
514 which supports the accumulation of an important Miocene sedimentary sequence west of the Romeral
515 fault system (Gomez et al., 2015; León et al., 2018), simultaneous with the initial accretion of the PCA.

516 Nonetheless, the forced subduction of a highly buoyant lithosphere could also lead to the rupture of the
517 already subducted slabs (Fig.11b) (Zheng et al., 2015). The clearest evidence which points to a slab
518 break-off beneath the NWSA margin is the development of Miocene arc-related magmatism in close prox-
519 imity to the suture zone between the PCA and South America (Figs.11a, 12). These magmatic intrusions,
520 ranging in age from 15 to 7 Ma (e.g. Leal-Mejía et al., 2019), with heterogeneous compositions including
521 tholeiitic, calc-alkaline, and shoshonitic signatures (Weber et al., 2020), have been regarded as originat-
522 ing from fluids from the Nazca slab (Wagner et al., 2017; Weber et al., 2020). Under the premise of an
523 existing Caribbean slab, however, this magmatism would not be possible, as the fluids rising from the
524 Nazca plate would be stopped by the overlying Caribbean slab (which may have been subducting shal-
525 lower than 50 kilometers) (Fig. S1f,g,h). Therefore, the emplacement of these magmatic intrusions re-
526 quires a breakoff in the Caribbean slab east of the PCA at about 15 Ma. This interpretation is corroborat-
527 ed by the regional trend of Miocene magmatism related to the Nazca plate (Figs.7 f,g) and additionally, by
528 the adakitic signature of these Miocene bodies (Weber et al., 2020). The latter could be related to the
529 subduction of the active Sandra spreading center and with the complicated Nazca plate geometry behind
530 the CSP triple junction. Moreover, the distribution of shallow seismicity indicates that the current defor-
531 mation is not symmetrical on both sides of the suture, but it is significantly reduced east of the PCA side
532 (east of the Uramita fault) (Fig.3a), coinciding with the area of no coupling by a subducting slab.

533 We propose that the PCA was forced into the South American margin by means of a major subduction
534 erosion event of the forearc during the early Miocene (Fig.11b), with the consequent advance of the plate
535 boundary (Fig.12). Subsequently, the hampered subduction of the highly buoyant arc resulted in the
536 breakoff of the slab to the east of the PCA at about 15 Ma, favoring initial margin subsidence and em-
537 placement of Nazca-derived magmas in the upper plate. This interpretation, however, raises the question
538 about the driving mechanism that supported the eastward motion of the PCA after initial collision. As sug-
539 gested by published geodetic data, the Panama isthmus is currently moving at 22 mm/yr relative to stable
540 South America, slightly faster than the current motion of the Caribbean plate (e.g. Trenkamp et al., 2002)
541 (Fig.12f). Considering the late Miocene shallow subduction and the much faster Nazca plate, we specu-
542 late that the Nazca kinematics boosted the motion of the overriding PCA microplate from below. Besides
543 explaining the current kinematics of the PCA, this mechanism accounts for the continued approaching
544 between the intra-oceanic and continental arcs (Mandé and Antioquia batholiths in Figs.12d-f), and the
545 increased deformation rate in the northern Andes.

546 Even though the subduction mode of the Caribbean plate associated with the PCA accretion was highly
547 erosive, it is interesting that the adjacent area to the north corresponds to a contemporaneous accretion-
548 ary margin (Sinu accretionary prism) (Fig.12). Mora-Bohórquez et al. (2017a) argue that the onset of the
549 Sinu accretionary prism during the early Miocene following an earlier stage of subduction erosion was
550 triggered by the initiation of massive influx of sediments from the Magdalena river to the trench. The PCA
551 accretion could also play a role in this tectonic evolution. As suggested by Montes et al. (2015), the pro-
552 gressive closure of the Pacific-Atlantic seaway changed the oceanic currents during the Miocene, leading
553 to the definitive separation of the Pacific and Atlantic oceans. The incremental restraining of oceanic cur-
554 rents, could have favored the accumulation of the deltaic Magdalena sediments to the north of the PCA,
555 favoring the formation of the Sinu accretionary prism in the Northern margin.

556 Finally, the kinematic reconstruction provides key arguments to propose that the southern Caribbean
557 boundary beneath South America is located north of the accreted PCA. As previously suggested, follow-
558 ing the initial erosive subduction during the early Miocene, the physical impossibility of subducting thick
559 and buoyant arc-related units (Mandé Batholith), may have induced the slab breakup east of the PCA by

560 the middle Miocene. An additional fact that restricts the Caribbean lithosphere to the north of 8°N, is that
 561 the PCA, as an island-arc is made up of a thick continental crust (e.g. Pindell et al., 2005) and underlain
 562 by sub-arc mantle lithosphere that is likely both, very thin as well as weak due to its thermal state. If this
 563 thick arc is stacked against the South American plate, then there is no strong and thick mantle lithosphere
 564 to be subducted beneath South America east of the PCA. However, apart from the middle Miocene mag-
 565 matism in northern Colombia (Figs. 7f,g), there is no additional evidence to date the onset of this condi-
 566 tion. In Figs. 7f,g,h are shown the maximum southern edge of the Caribbean plate, estimated according
 567 to the magmatic development on SA; and the minimum southern edge derived from tracing the boundary
 568 of the PCA with the Caribbean lithosphere into the subduction zone using the Caribbean plate displace-
 569 ment since collision of the PCA with South America.

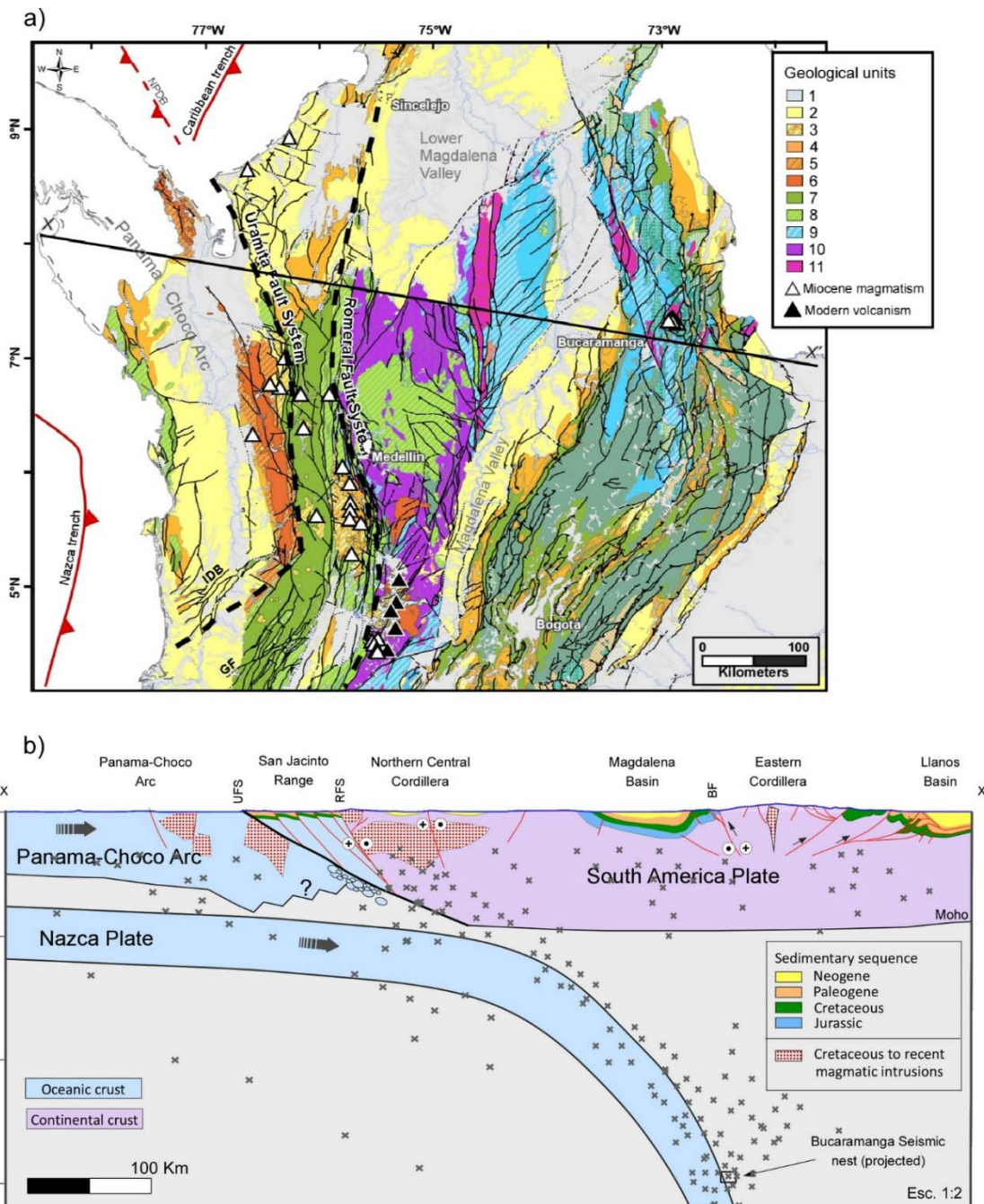
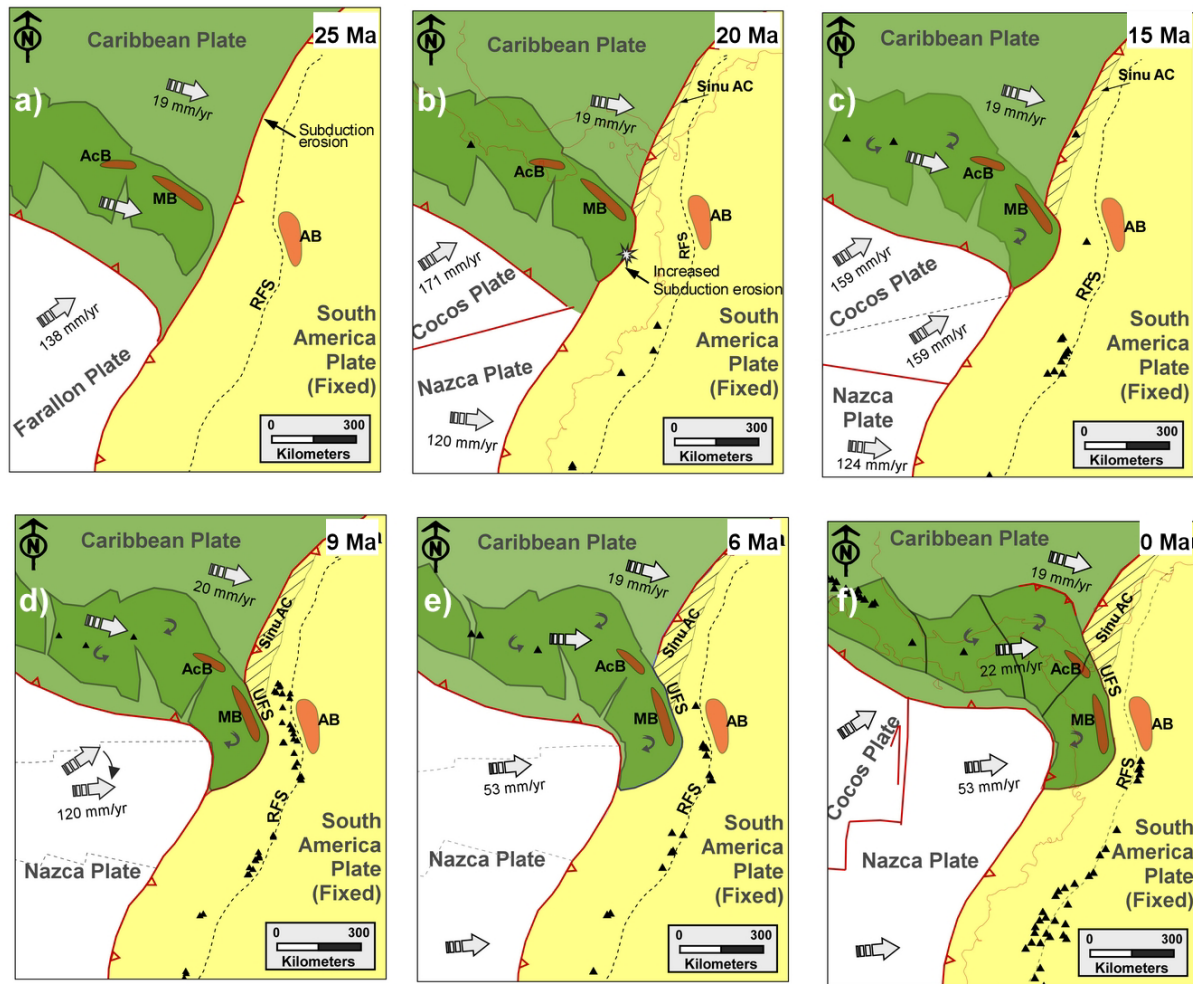


Fig. 11. a) Geological map of NWSA, modified after Gómez et al. (2015). Geological units: 1- Quaternary sedimentites, 2- Neogene sedimentites, 3- Neogene volcanosedimentary rocks, 4- Paleogene sedimentites, 5- Paleogene extrusive rocks, 6- Paleogene plutonic rocks, 7- Upper Cretaceous oceanic platform rocks, 8- Upper Cretaceous intrusive arc rocks, 9- Jurassic sedimentites, 10- Triassic and Jurassic metamorphic rocks, 11- Paleozoic igneous and metamorphic rocks, BF: Bucaramanga fault, GF: Garrapatas fault, IDF: Isthma deformed belt, NPFD: North Panama deformed belt, PCA: Panama-Choco arc, RFZ: Romeral fault system, UFZ: Uramita fault system. b) Simplified cross section showing the tectonic configuration. Black dots correspond to seismic events located within 8 km of the section. Crustal thickness for the South American plate taken from Poveda et al. (2015). Structural interpretation in the South American plate modified after Tesón et al. (2013) and Mora-Bohorquez et al. (2017).



571

Fig. 12. Detailed paleogeographic reconstruction of the Panama-Choco arc (PCA) convergence and accretion to the South American margin. While the continued eastward motion of the PCA (relative to South America) resulted in the vertical axis rotation of blocks and orocline formation (Montes et al., 2012), in the continental side the subduction of the highly buoyant crust prompted the severe subduction erosion and the trench retreat toward the continent. Simultaneously, north of the collisional zone the slow convergence rate and increased sediment accumulation coincide with the formation of the Sinu accretionary prism. Black triangles show the location of active magmatism. Red polygons show the restored location of Paleogene plutons. AB: Antioquia batholith and associated Paleogene stocks, AcB: Acandi batholith, MB: Mande batholith, RFS: Romeral fault system, Sinu Ac: Sinu accretionary prism, UFS: Uramita fault system.

572 **5.3 Present-Day Tectonic Geometry**

573 In order to validate the tectonic configuration resulting from the geometrical reconstruction of subduction,
574 we developed a three-dimensional interpretation of the Nazca and Caribbean slabs based on existing
575 seismicity data and a recent tomographic model. As a result of this analysis, we obtained a model that is
576 consistent not only with the geologic record, but also with observables of the current configuration, such
577 as seismicity, tomography, magmatism and geodetic vectors.

578 The seismicity dataset comprises a catalogue of 177,000 seismic events (magnitude < 6.8) during the
579 period 2003–2018 taken from the National Seismological Network of Colombia (RSNC; Fig.3). The tomo-
580 graphic data that we use correspond to the recently published finite-frequency velocity model for the
581 Northern Andean region developed by Sun et al., (2022) (Fig.13). In that tomography they obtained a P
582 wave velocity model based on seismic events retrieved from 165 stations in Colombia and 65 stations in
583 Venezuela (Sun et al., 2022). We are using dVp/Vp anomalies, which according to Sun et al. (2022), pro-
584 vide a reliable resolution for interpreting regional and continuous high-velocity anomalies that could be
585 related to distinct slab segments. The visualization -interpretation of this slabs within the tomographic
586 model was made with the commercial software MOVE v. 2019 (<https://www.petex.com>) by using an or-
587 thogonal projection.

588 **5.3.1 The Nazca Plate**

589 The present-day Nazca slab can be separated into two domains separated by the Caldas tear at 5.5°N
590 (Figs.8, 13) (Vargas and Mann, 2013). The seismic distribution suggests that south of this position the
591 Nazca plate subducts at a steep angle (>25°) (Fig.3), which is further supported by the trend of the Ande-
592 an magmatic arc (Andean Volcanic Zone), that is continuous south of this location (Pennington, 1981;
593 Vargas and Mann, 2013; Wagner et al., 2017) (Figs.2 and 3). Nonetheless, some authors have identified
594 a velocity discontinuity at 3°N (N1 and N2 in Figs.13b,c,d) (Vargas and Mann, 2013, Sun et al., 2022).
595 However, as the cross section i (Fig.13) and seismicity data are not clear indicators of a significant
596 change in geometry (Fig.3), we regard this anomaly as related to a thermal perturbation, possibly related
597 to the subduction of the extinct Malpelo rift (Fig.8).

598 North of 5.5°N the tomographic model shows a greater number of minor velocity anomalies which makes
599 it more difficult to differentiate between the Nazca and Caribbean slabs (N3 in Figs.13b,c,d and cross
600 section 1). Although these anomalies could be interpreted as artifacts, it is possible that they are related
601 to an inclined-axis bending of the Nazca slab subducting at shallow depth following a similar shape to that
602 of the trench at the CSP triple junction, as suggested by our reconstruction (Fig.8). In the cross-section e
603 of Fig.13 there is a complex pattern of high velocity anomalies (N3 in Fig. 12). While the shallowest
604 anomaly can be associated with a shallow subducting Caribbean plate (due to its proximity to the Carib-
605 bean trench), the deeper ones define a parabolic shape that could be regarded as a geophysical artifact
606 (N3 in Fig. 12e). Considering that this pattern is also observed between 6°N and 9°N (Fig.13 b,c,d), and
607 that other tomographic studies have also identified anomalies in this region at depths below 50 km (Yarce
608 et al., 2014; Bernal-Olaya et al., 2015; Syracuse et al., 2016; Sun et al., 2022), we ruled out that this
609 anomaly is a geophysical artifact. Based on synthetic modeling, Sun et al. (2022) showed that this com-
610 plex array of velocity anomalies to the north of 5.5°N is the result of overlapping slabs. Following this
611 analysis, we consider that this pattern could be related to a subducting slab north of 5.5°N that seems to
612 be connected to the Nazca trench, east of the CSP triple junction (GIF image in Fig. S1). Furthermore, it
613 is important to consider that subduction along this narrow corner of the Nazca plate may have resulted in
614 different phases of slab rupture (Fig.9a), which together with the subduction of the Sandra rift may be
615 related to an anomalously hot slab, which would explain the weak nature of these velocity anomalies.

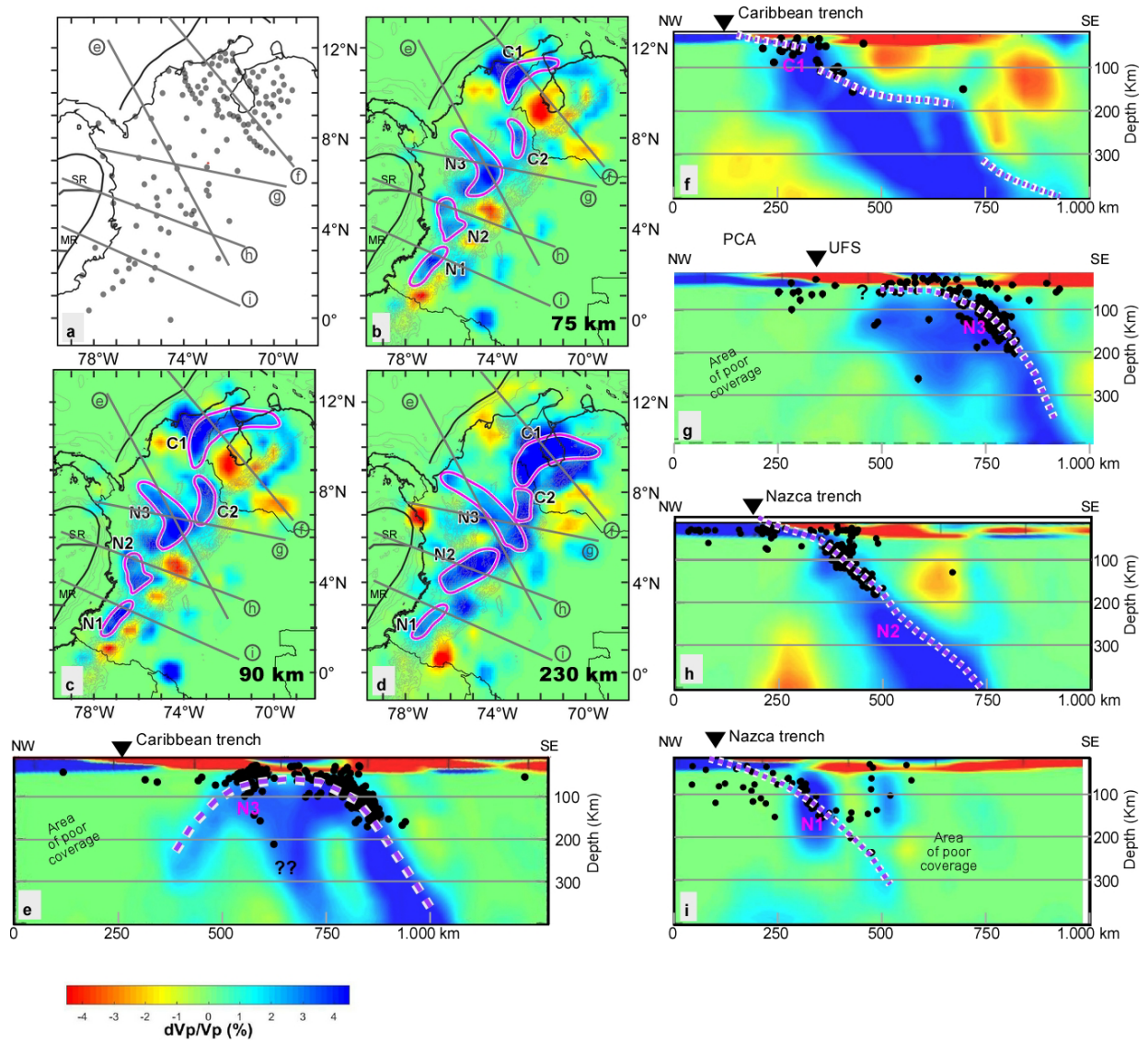
616 Additionally, this interpretation is supported by the adakitic magmatic signature in eastern Panama (de
617 Boer et al., 1988; Gutscher et al., 2000); the faster eastward motion of the Panama isthmus as compared
618 to the Caribbean plate (as result of the Nazca slab pushing from below) (Figs.11, 12f); the Miocene sub-
619 duction-related magmatism north of 5.5°N (Weber et al., 2020), and the origin of the Farallon plate
620 boundary as an Aleutian type margin (Cardona et al., 2018).

621 The Bucaramanga seismic nest (Fig.11) has been related to either the Caribbean or the Nazca plate
622 (Fig.3) (e.g. Taboada et al., 2000; Zarifi et al., 2007; Vargas and Mann, 2013; Prieto et al., 2012; Chiar-
623 abba et al., 2015, Sun et al.,2022). According to our reconstruction, the Bucaramanga seismic nest is
624 associated with the Nazca slab (Fig.11b). This interpretation is consistent with the high eastward rate of
625 subduction, as well as localized dehydration processes proposed by Chiarabba et al. (2015) and Siravo et
626 al. (2019) in the inflection point of the Nazca plate, which could increase the intermediate-depth seismici-
627 ty. In addition, the possible high strain rates at this bending geometry, as well as the complex mantle fluid
628 dynamics that could be expected beneath this vertical-axis curved slab, may be associated with thermal
629 runaway processes as suggested by Prieto et al. (2013) in the Bucaramanga seismic nest. However, the
630 lack of Nazca-related seismicity west of the vertical-axis bending and beneath Panama (Fig.3) poses a
631 challenge, which could be explained by the fact that today, the Nazca slab has a negligible subduction
632 velocity in the northward direction (Fig.8).

633 **5.3.2 The Caribbean Plate**

634 In agreement with previous studies, our interpretation confirms that most of the Caribbean plate corre-
635 sponds to a flat-slab (e.g. Cornthwaite et al., 2021; Sun et al., 2022) that decreases its dip towards the
636 north (Figs.8, 13). This shallow geometry is supported by a continuous northward trend of intermediate-
637 depth seismicity (WBZ) at about 73°W (Fig.3), which defines the position where the shallow subduction
638 ends and the slab starts to sink into the mantle. In line with this observation, the kinematic reconstruction
639 predicts that east of the WBZ, the current Caribbean slab may be fragmented as result of cumulative in-
640 stability in its leading edge (Figs.8, 9d). This interpretation is confirmed (C1 and C2 in Figs. 13b,c,d) and
641 cross section f in Fig.13, which show that east of 73°W the Caribbean slab is composed of three distinct
642 step segments that are deeper to the south, possibly separated by E-W tear faults.

643 Nonetheless, not all the intermediate-depth seismicity running from 5° to 10°N (Fig.3b) corresponds to the
644 Caribbean plate. The southern edge of the Caribbean plate beneath South America is perhaps the most
645 debated question that has not been resolved. Even though rocks of the Caribbean plate and PCA, ac-
646 creted to the continental margin during the Miocene are found between 4.5°N and 8°N (Duque-Caro,
647 1990), we conclude that it is not geodynamically possible to have remnants of the Caribbean slab sub-
648 ducting to the east of the accreted PCA (see discussion above). The simplest explanation is that there is
649 no oceanic lithosphere beneath the stacked arc to feed the subduction system, nor is there a subduction
650 trench (instead there is the Uramita suture zone, see Fig.11). In addition to the deformation and magmatic
651 record in the upper plate that supports this hypothesis (see discussion above), the shallow and intermedi-
652 ate-depth seismicity, north of the Caldas tear, shows a subtle reduction between the Uramita fault zone
653 and the WBZ at about 74°E (Fig. 4). This pattern of reduced seismicity is consistent with a missing Carib-
654 bean slab in that position. The white dashed line in Fig. 4 indicates the proposed southern edge of the
655 Caribbean slab. Finally, it is important to remark that there is an area of close overlapping between the
656 Nazca and Caribbean plates as suggested in other studies (Figs.8, 13) (e.g. Sun et al., 2022).



657

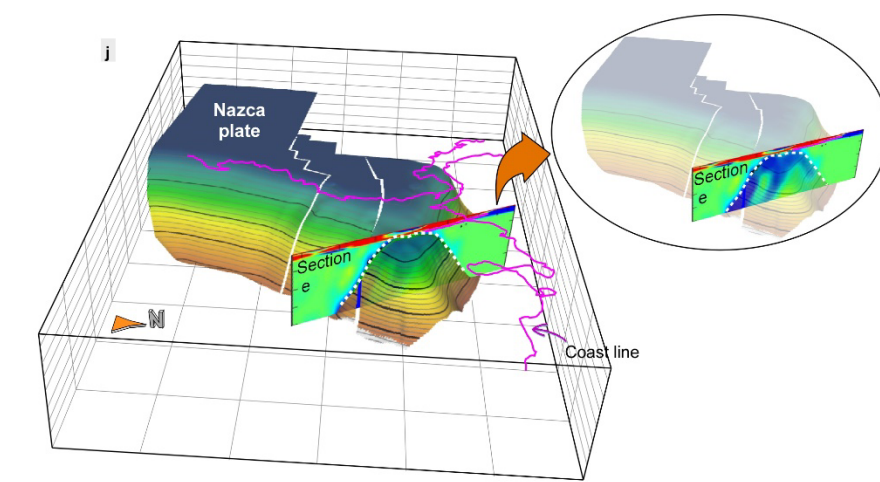


Fig. 13. Tomographic model taken from Sun et al. (2022) beneath NWSA (dV_p/V_p). a) Location of seismic stations and location of cross sections. b, c, d) depth slices at 75, 90 and 230 km. e, f, g, h, i show tomographic cross sections. The purple lines and texts underscore well-resolve velocity anomalies interpreted in this study. Black dots in cross sections show seismicity within 10 km from the profiles. j) Three-dimensional view of the interpreted Nazca plate, highlighting the intercept between the section “e” and the Nazca slab

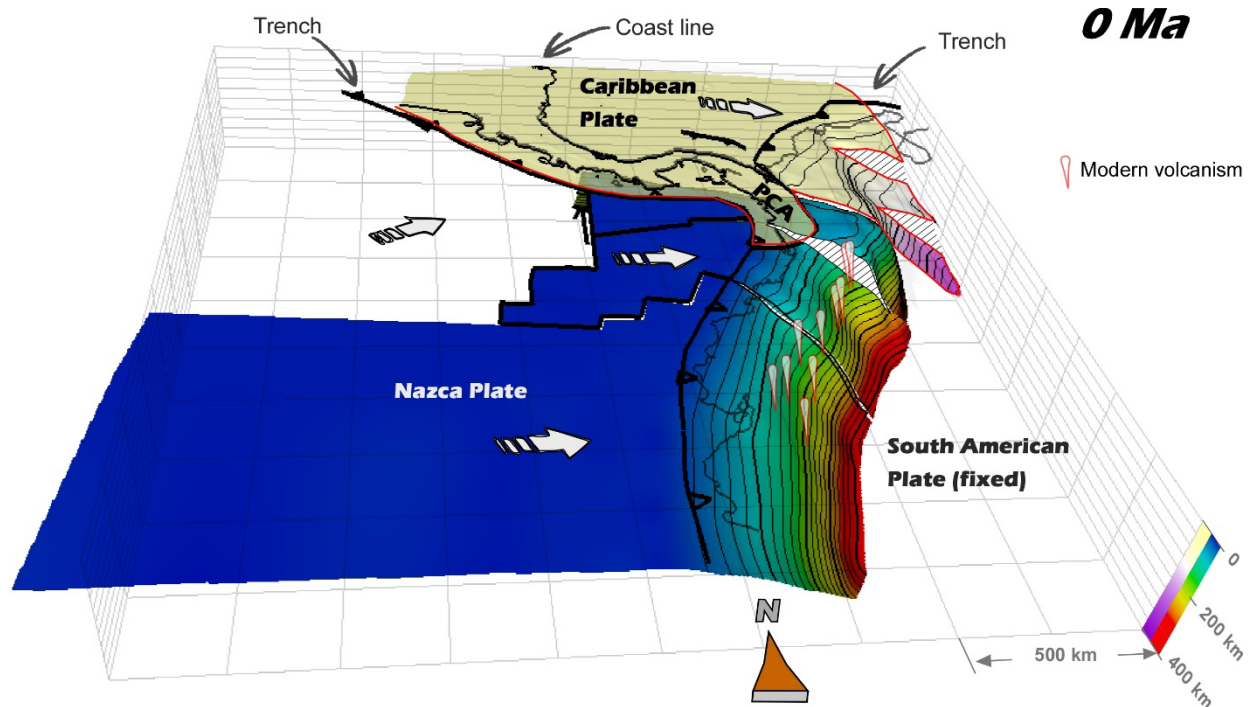
at its vertical-axis bending. MR: Malpelo ridge, SR: Sandra ridge, PCA: Panama-Choco arc.

659 **6. Conclusions**

660 Our reconstruction indicates that the northeastward motion of the southern Caribbean edge caused a
661 progressive change in geometry of the Pacific trench, and in turn of the Farallon plate subduction. This
662 change induced the flat-slab subduction of the Farallon plate throughout the late Eocene-late Oligocene,
663 which inhibited the Farallon-related magmatism in the South American and PCA margins and facilitated
664 the rupture of the Farallon plate. The subsequent plate kinematics during the early-middle Miocene in-
665 duced a plate reorganization that included further plate fragmentation, change in convergence obliquity,
666 steepening of the subducting slabs and renewing of magmatism. During the late Miocene, the Coiba and
667 Malpelo microplates were attached to the Nazca plate, resulting in an abrupt change in convergence di-
668 rections against eastern Panama and northern South America. This event correlates with the late Mio-
669 cene onset of shallow subduction of the northernmost Nazca plate and the accelerated deformation in the
670 Andes. Finally, during the late Pliocene, the flattened slab broke along the Caldas tear triggering the
671 modern volcanism south of 5.5° N.

672 On the other side, the highly oblique convergence of the Caribbean plate during the Paleocene-Eocene,
673 allowed arc-related magmatism in northernmost South America. This configuration changed by the middle
674 Eocene, when the Caribbean plate began to migrate in eastward direction relative to stable South Ameri-
675 ca. This change triggered the breakoff of the slab and meant a significant lateral variation in obliquity
676 along the margin. These factors prompted the slab-pull and flat-slab subduction from that moment on-
677 wards. By the late Oligocene-early Miocene, the approaching of the buoyant PCA triggered the fragmen-
678 tation and rotation of the PCA and a phase of rapid subduction erosion of the mafic forearc, accompanied
679 by nearly 200 km of trench advance. By the middle Miocene, the Caribbean slab subduction could not
680 continue, breaking this slab east of the PCA, and initiating a phase of tectonic collision in NWSA.

681 In summary, this contribution presents a paleotectonic reconstruction of the interacting Caribbean and
682 Farallon/Nazca plates against NWSA, that integrates the spatiotemporal distribution of magmatism and
683 the first-order history of deformation in the northern Andes. The results of this reconstruction allowed us
684 to constrain a new geometrical model of the subducting Caribbean and Nazca plates (Fig.14), which addi-
685 tionally explains key observables, such as seismicity and mantle velocity anomalies. Further works, in-
686 cluding acquisitions of new seismological data and three-dimensional numerical and analog experiments,
687 are required to test the proposed conceptual models and plate tectonic geometries.



688

Fig. 14. Three-dimensional view of the tectonic configuration of the Nazca and Caribbean plates at the junction between Central and South America. The Nazca slab can be separated in two domains, a southern one with steep angle of subduction ($>25^\circ$), and a northern one with flat-slab subduction that turns horizontally behind the PCA (Panama-Choco arc), following a similar geometry than the trench. On the other hand, the Caribbean slab consists of a shallow subducting slab that is tore apart to the east in three different segments. Note that the Caribbean slab is absent east of the PCA due to its breakoff during the middle Miocene. Nevertheless, the southern Caribbean edge overlaps the Nazca plate in its more northern segment. Directions of plate motion are relative to stable South America. Contour interval: 20 km.

689

690 7. Acknowledgements

This manuscript is part of the PhD research of R. Gonzalez at the Freie Universität Berlin and the GFZ Potsdam. R. González is especially grateful to Ecopetrol for funding this study. We acknowledge the GFZ Lithospheric Dynamics section for ongoing discussions, in particular Sabrina Metzger. We thank Robert Trumbull for his clarifications on subduction geodynamics and German Bayona for fruitful discussions. Finally, R. Gonzalez show gratitude to Robert Ondrack and Alejandro Mora for their support in initiating this research.

691 8. Open research

GPlates files from the paleotectonic reconstruction presented in this research are accessible as a Source Data file [<https://zenodo.org/deposit/7411340>]. The Data file additionally contains information including a compilation of the main tectonic events in the South American plate, and figures in three-dimensional view.

692 9. References

- 693 Adamek, S., C. Frohlich, and W. D. Pennington, 1988, Seismicity of the Caribbean-Nazca Boundary: Constraints on microplate
694 tectonics of the Panama region: *Journal of Geophysical Research: Solid Earth*, v. 93, p. 2053-2075.
- 695 Amante, C., and B. W. Eakins, 2009, ETOPO1 arc-minute global relief model: procedures, data sources and analysis. NOAA /
696 National Oceanic and Atmospheric Administration. National Environmental Satellite, Data, and Information Service

697 Anderson, V. J., B. K. Horton, J. E. Saylor, A. Mora, E. Tesón, D. O. Breecker, and R. A. Ketcham, 2016, Andean topographic
698 growth and basement uplift in southern Colombia: Implications for the evolution of the Magdalena, Orinoco, and Amazon river
699 systems: *Geosphere*, v. 12, p. 1235-1256.

700 Ayala-Calvo, R., G. Bayona, A. Cardona, C. Ojeda, O. C. Montenegro, C. Montes, V. Valencia, and C. Jaramillo, 2012, The
701 paleogene synorogenic succession in the northwestern Maracaibo block: Tracking intraplate uplifts and changes in sediment
702 delivery systems: *Journal of South American Earth Sciences*, v. 39, p. 93-111.

703 Barat, F., B. Mercier de Lépinay, M. Sosson, C. Müller, P. O. Baumgartner, and C. Baumgartner-Mora, 2014, Transition from the
704 Farallon Plate subduction to the collision between South and Central America: Geological evolution of the Panama Isthmus:
705 *Tectonophysics*, v. 622, p. 145-167.

706 Barbosa-Espitia, Á. A., G. D. Kamenov, D. A. Foster, S. A. Restrepo-Moreno, and A. Pardo-Trujillo, 2019b, Contemporaneous
707 Paleogene arc-magmatism within continental and accreted oceanic arc complexes in the northwestern Andes and Panama: *Lithos*,
708 v. 348-349, p. 105185.

709 Barckhausen, U., C. R. Ranero, R. von Huene, S. C. Cande, and H. A. Roeser, 2001, Revised tectonic boundaries in the Cocos
710 Plate off Costa Rica: Implications for the segmentation of the convergent margin and for plate tectonic models: *Journal of*
711 *Geophysical Research: Solid Earth*, v. 106, p. 19207-19220.

712 Bayona, G., A. Cardona, C. Jaramillo, A. Mora, C. Montes, V. Valencia, C. Ayala, O. Montenegro, and M. Ibañez-Mejía, 2012, Early
713 Paleogene magmatism in the northern Andes: Insights on the effects of Oceanic Plateau–continent convergence: *Earth and*
714 *Planetary Science Letters*, v. 331-332, p. 97-111.

715 Bayona, G., A. Cardona, C. Jaramillo, A. Mora, C. Montes, V. Caballero, H. Mahecha, F. Lamus, O. Montenegro, G. Jimenez, A.
716 Mesa, and V. Valencia, 2013, Onset of fault reactivation in the Eastern Cordillera of Colombia and proximal Llanos Basin; response
717 to Caribbean–South American convergence in early Palaeogene time: *Geological Society, London, Special Publications*, v. 377, p.
718 285.

719 Bayona, G., M. Baquero, C. Ramírez, M. Tabares, A. M. Salazar, G. Nova, E. Duarte, A. Pardo, A. Plata, C. Jaramillo, G.
720 Rodríguez, V. Caballero, A. Cardona, C. Montes, S. Gómez Marulanda, and A. L. Y. R. Cárdenas-Rozo, 2020, Unravelling the
721 widening of the earliest Andean northern orogen: Maastrichtian to early Eocene intra-basinal deformation in the northern Eastern
722 Cordillera of Colombia: *Basin Research*, v. 33, p. 809.

723 Bernal-Olaya, R., P. Mann, and C. Vargas, 2015, Earthquake, Tomographic, Seismic Reflection, and Gravity Evidence for a
724 Shallowly Dipping Subduction Zone beneath the Caribbean Margin of Northwestern Colombia: *AAPG Memoir*, v. 108, p. 22.

725 Bernet, M., C. Urueña, S. Amaya, and M. L. Peña, 2016, New thermo and geochronological constraints on the Pliocene-Pleistocene
726 eruption history of the Paipa-Iza volcanic complex, Eastern Cordillera, Colombia: *Journal of Volcanology and Geothermal Research*,
727 v. 327, p. 299-309.

728 Bezada, M. J., A. Levander, and B. Schmandt, 2010, Subduction in the southern Caribbean: Images from finite-frequency P wave
729 tomography: *Journal of Geophysical Research: Solid Earth*, v. 115.

730 Boschman, L. M., D. J. J. van Hinsbergen, T. H. Torsvik, W. Spakman, and J. L. Pindell, 2014, Kinematic reconstruction of the
731 Caribbean region since the Early Jurassic: *Earth-Science Reviews*, v. 138, p. 102-136.

732 Boyden, J. A., R. D. Müller, M. Gurnis, T. H. Torsvik, J. A. Clark, M. Turner, H. Ivey-Law, R. J. Watson, and J. S. Cannon, 2011,
733 Next-generation plate-tectonic reconstructions using GPlates, in C. Baru, and G. R. Keller, eds., *Geoinformatics: Cyberinfrastructure*
734 *for the Solid Earth Sciences*: Cambridge, Cambridge University Press, p. 95-114.

735 Burke, K., 1988, Tectonic Evolution of the Caribbean: *Annual Review of Earth and Planetary Sciences*, v. 16, p. 201-230.

736 Bruce, J., H. Shyu, Yih-Min Wu, Chien-Hsin Chang, Hsin-Hua Huang, 2011, Tectonic erosion and the removal of forearc lithosphere
737 during arc-continent collision: Evidence from recent earthquake sequences and tomography results in eastern Taiwan, *Journal of*
738 *Asian Earth Sciences*, Volume 42, Issue 3, p. 415-422.

739 Caballero, V., Parra, M., Mora, A., López, C., Rojas, L.E. and Quintero, I., 2013. Factors controlling selective abandonment and
740 reactivation in thick-skin orogens: a case study in the Magdalena Valley, Colombia. *Geological Society, London, Special*
741 *Publications*, 377(1), pp.343-367. Cardona, A., S. León, J. S. Jaramillo, C. Montes, V. Valencia, J. Vanegas, C. Bustamante, and S.
742 Echeverri, 2018, The Paleogene arcs of the northern Andes of Colombia and Panama: Insights on plate kinematic implications from
743 new and existing geochemical, geochronological and isotopic data: *Tectonophysics*, v. 749, p. 88-103.

744 Cardona, A., V. Valencia, M. Weber, J. Duque, C. Montes, G. Ojeda, P. Reiners, K. Domanik, S. Nicolescu, and D. Villagomez,
745 2011, Transient Cenozoic tectonic stages in the southern margin of the Caribbean plate: U-Th/He thermochronological constraints
746 from Eocene plutonic rocks in the Santa Marta massif and Serranía de Jarara, northern Colombia: *GEOLOGICA ACTA*, v. 9, p. 445-
747 +.

748 Cardona, A., M. Weber, V. Valencia, C. Bustamante, C. Montes, U. Cordani, and C. M. Muñoz, 2014, Geochronology and
749 geochemistry of the Parashi granitoid, NE Colombia: Tectonic implication of short-lived Early Eocene plutonism along the SE
750 Caribbean margin: *Journal of South American Earth Sciences*, v. 50, p. 75-92.

751 Cardona, A., S. León, J. S. Jaramillo, C. Montes, V. Valencia, J. Vanegas, C. Bustamante, and S. Echeverri, 2018, The Paleogene
752 arcs of the northern Andes of Colombia and Panama: Insights on plate kinematic implications from new and existing geochemical,
753 geochronological and isotopic data: *Tectonophysics*, v. 749, p. 88-103.

- 754 Carrillo, E., A. Mora, R. A. Ketcham, R. Amorocho, M. Parra, D. Costantino, W. Robles, W. Avellaneda, J. S. Carvajal, and M. F.
755 Corcione, 2016, Movement vectors and deformation mechanisms in kinematic restorations: A case study from the Colombian
756 Eastern Cordillera: Interpretation, v. 4, p. T31-T48.
- 757 Cedié, F., R. P. Shaw, and C. Cáceres, 2003, Tectonic Assembly of the Northern Andean Block, in C. Bartolini, R. T. Buffler, and J.
758 F. Blickwede, eds., The Circum-Gulf of Mexico and the Caribbean: Hydrocarbon Habitats, Basin Formation and Plate Tectonics,
759 American Association of Petroleum Geologists, p. 0.
- 760 Chiarabba, C., P. De Gori, C. Faccenna, F. Speranza, D. Seccia, V. Dionicio, and G. A. Prieto, 2015, Subduction system and flat
761 slab beneath the Eastern Cordillera of Colombia: Geochemistry, Geophysics, Geosystems, v. 17, p. 16-27.
- 762 Clift, P., and P. Vannucchi, 2004, Controls on tectonic accretion versus erosion in subduction zones: Implications for the origin and
763 recycling of the continental crust: Reviews of Geophysics, v. 42.
- 764 Coira, B., J. Davidson, C. Mpodozis, V. Ramos, 1982, Tectonic and magmatic evolution of the Andes of Northern Argentina and
765 Chile. *Earth Sci Rev* 18:302–332
- 766 Cornthwaite, J., M. J. Bezada, W. Miao, M. Schmitz, G. A. Prieto, V. Dionicio, F. Niu, and A. Levander, 2021, Caribbean Slab
767 Segmentation Beneath Northwest South America Revealed by 3-D Finite Frequency Teleseismic P-Wave Tomography:
768 *Geochemistry, Geophysics, Geosystems*, v. 22, p. e2020GC009431.
- 769 Cortés, M., and J. Angelier, 2005, Current states of stress in the northern Andes as indicated by focal mechanisms of earthquakes:
770 *Tectonophysics*, v. 403, p. 29-58.
- 771 de Boer, J. Z., M. J. Defant, R. H. Stewart, J. F. Restrepo, L. F. Clark, and A. H. Ramirez, 1988, Quaternary calc-alkaline volcanism
772 in western Panama: Regional variation and implication for the plate tectonic framework: *Journal of South American Earth Sciences*,
773 v. 1, p. 275-293.
- 774 de la Parra, F., A. Mora, M. Rueda, and I. Quintero, 2015, Temporal and spatial distribution of tectonic events as deduced from
775 reworked palynomorphs in the eastern Northern Andes: *Reworked Palynomorphs in the Eastern Northern Andes: AAPG Bulletin*, v.
776 99, p. 1455-1472.
- 777 Di Marco, G., P. O. Baumgartner, and J. E. Channell, 1995, Late Cretaceous-early Tertiary paleomagnetic data and a revised
778 tectonostratigraphic subdivision of Costa Rica and western Panama, in M. P., ed., *Geologic and Tectonic Development of the*
779 *Caribbean Plate Boundary in Southern Central America*, v. Special Paper 295: Boulder, Colorado, Geological Society of America.
- 780 Duque-Caro, H., 1990, The Choco block in the northwestern corner of South America: Structural, tectonostratigraphic, and
781 paleogeographic implications: *Journal of South American Earth Sciences*, v. 3, p. 71-84.
- 782 Escalona, A., and P. Mann, 2011, Tectonics, basin subsidence mechanisms, and paleogeography of the Caribbean-South American
783 plate boundary zone: *Marine and Petroleum Geology*, v. 28, p. 8-39.
- 784 Etayo-Serna, F., 1983, The Georgian heteromorph ammonite genera *Kutatissites* and *Pseudoaustraliceras* in Northwest
785 Southamerica: *Geología Norandina*, v. 7, p. 3-13.
- 786 Faccenna, C., Holt, A.F., Becker, T.W., Lallemand, S. and Royden, L.H., 2018. Dynamics of the Ryukyu/Izu-Bonin-Marianas double
787 subduction system. *Tectonophysics*, 746, pp.229-238.
- 788 Farris, D. W., C. Jaramillo, G. Bayona, S. A. Restrepo-Moreno, C. Montes, A. Cardona, A. Mora, R. J. Speakman, M. D. Glascock,
789 and V. Valencia, 2011, Fracturing of the Panamanian Isthmus during initial collision with South America: *Geology*, v. 39, p. 1007-
790 1010.
- 791 Gansser, A., 1973. Facts and theories on the Andes: twenty-sixth William Smith Lecture. *Journal of the Geological Society*, 129(2),
792 pp.93-131.
- 793 Geldmacher, J., T. W. Höfig, F. Hauff, K. Hoernle, D. Garbe-Schönberg, and D. S. Wilson, 2013, Influence of the Galápagos hotspot
794 on the East Pacific Rise during Miocene superfast spreading: *Geology*, v. 41, p. 183-186.
- 795 Gómez, E. a., T. E. Jordan, R. W. Allmendinger, K. Hegarty, S. Kelley, and M. Heizler, 2003, Controls on architecture of the Late
796 Cretaceous to Cenozoic southern Middle Magdalena Valley Basin, Colombia: *GSA Bulletin*, v. 115, p. 131-147.
- 797 Gómez, J., Montes, N.E., Nivia, Á. & Diederix, H., compilers. 2015. Geological Map of Colombia 2015. Scale 1:1 000 000. Servicio
798 Geológico Colombiano, 2 sheets. Bogotá. <https://doi.org/10.32685/10.143.2015.936>
- 799 Govers, R., and M. J. R. Wortel, 2005, Lithosphere tearing at STEP faults: response to edges of subduction zones: *Earth and*
800 *Planetary Science Letters*, v. 236, p. 505-523.
- 801 Gurnis, M., M. Turner, S. Zahirovic, L. DiCaprio, S. Spasojevic, R. D. Müller, J. Boyden, M. Seton, V. C. Manea, and D. J. Bower,
802 2012, Plate tectonic reconstructions with continuously closing plates: *Computers & Geosciences*, v. 38, p. 35-42.
- 803 Gurnis, M., T. Yang, J. Cannon, M. Turner, S. Williams, N. Flament, and R. D. Müller, 2018, Global tectonic reconstructions with
804 continuously deforming and evolving rigid plates: *Computers & Geosciences*, v. 116, p. 32-41.
- 805 Gutscher, M.-A., R. Maury, J.-P. Eissen, and E. Bourdon, 2000, Can slab melting be caused by flat subduction?: *Geology*, v. 28, p.
806 535-538.
- 807 Handschumacher, D. W., 1976, Post-Eocene Plate Tectonics of the Eastern Pacific: The Geophysics of the Pacific Ocean Basin
808 and Its Margin, p. 177-202.

809 Hardy, N. C., 1991, Tectonic evolution of the easternmost Panama basin: Some new data and inferences: *Journal of South*
810 *American Earth Sciences*, v. 4, p. 261-269.

811 Horton, B. K., V. J. Anderson, V. Caballero, J. E. Saylor, J. Nie, M. Parra, and A. Mora, 2015, Application of detrital zircon U-Pb
812 geochronology to surface and subsurface correlations of provenance, paleodrainage, and tectonics of the Middle Magdalena Valley
813 Basin of Colombia: *Geosphere*, v. 11, p. 1790-1811.

814 Jaramillo, J. S., A. Cardona, S. León, V. Valencia, and C. Vinasco, 2017, Geochemistry and geochronology from Cretaceous
815 magmatic and sedimentary rocks at 6°35' N, western flank of the Central cordillera (Colombian Andes): Magmatic record of arc
816 growth and collision: *Journal of South American Earth Sciences*, v. 76, p. 460-481.

817 Johnston, S. T., and D. J. Thorkelson, 1997, Cocos-Nazca slab window beneath Central America: *Earth and Planetary Science*
818 *Letters*, v. 146, p. 465-474.

819 Kellogg, J. N., G. B. F. Camelio, and H. Mora-Páez, 2019, Chapter 4 - Cenozoic tectonic evolution of the North Andes with
820 constraints from volcanic ages, seismic reflection, and satellite geodesy, in B. K. Horton, and A. Folguera, eds., *Andean Tectonics*,
821 Elsevier, p. 69-102.

822 Keppie, D. F., C. A. Currie, and C. Warren, 2009, Subduction erosion modes: Comparing finite element numerical models with the
823 geological record: *Earth and Planetary Science Letters*, v. 287, p. 241-254.

824 Kerr, A. C., J. Tarney, G. F. Marriner, A. Nivia, and A. D. Saunders, 1997, The Caribbean-Colombian Cretaceous igneous province:
825 The internal anatomy of an oceanic plateau: *Geophysical monograph-American Geophysical Union*, v. 100, p. 123-144.

826 Kukowski, N., and O. Oncken, 2006, Subduction erosion—The “normal” mode of fore-arc material transfer along the Chilean
827 margin?, *The Andes*, Springer, p. 217-236.

828 Lara, M., A. Cardona, G. Monsalve, J. Yarce, C. Montes, V. Valencia, M. Weber, F. De La Parra, D. Espitia, and M. López-Martínez,
829 2013, Middle Miocene near trench volcanism in northern Colombia: A record of slab tearing due to the simultaneous subduction of
830 the Caribbean Plate under South and Central America?: *Journal of South American Earth Sciences*, v. 45, p. 24-41.

831 Leal-Mejía, H., R. P. Shaw, and J. C. Melgarejo i Draper, 2019, Spatial-temporal migration of granitoid magmatism and the
832 Phanerozoic tectono-magmatic evolution of the Colombian Andes, *Geology and tectonics of Northwestern South America*, Springer,
833 p. 253-410.

834 León, S., A. Cardona, M. Parra, E. R. Sobel, J. S. Jaramillo, J. Glodny, V. A. Valencia, D. Chew, C. Montes, G. Posada, G.
835 Monsalve, and A. Pardo-Trujillo, 2018, Transition From Collisional to Subduction-Related Regimes: An Example From Neogene
836 Panama-Nazca-South America Interactions: *Tectonics*, v. 37, p. 119-139.

837 Lissinna, B., 2005, A profile through the central American landbridge in western Panama: 115 Ma interplay between the Galápagos
838 hotspot and the central American subduction zone.

839 Lonsdale, P., and K. D. Klitgord, 1978, Structure and tectonic history of the eastern Panama Basin: *GSA Bulletin*, v. 89, p. 981-999.

840 Lonsdale, P., 2005, Creation of the Cocos and Nazca plates by fission of the Farallon plate: *Tectonophysics*, v. 404, p. 237-264.

841 MacMillan, I., P. B. Gans, and G. Alvarado, 2004, Middle Miocene to present plate tectonic history of the southern Central American
842 Volcanic Arc: *Tectonophysics*, v. 392, p. 325-348.

843 Mann, P., and R. A. Kolarsky, 1995, East Panama deformed belt: Structure, age, and neotectonic significance: *SPECIAL PAPERS-*
844 *GEOLOGICAL SOCIETY OF AMERICA*, p. 111-111.

845 Mann, P., 1999, Chapter 1 Caribbean sedimentary basins: classification and tectonic setting from Jurassic to present, in P. Mann,
846 ed., *Sedimentary Basins of the World*, v. 4, Elsevier, p. 3-31.

847 Marín-Cerón, M. I., H. Leal-Mejía, M. Bernet, and J. Mesa-García, 2019, Late Cenozoic to modern-day volcanism in the Northern
848 Andes: A geochronological, petrographical, and geochemical review, *Geology and Tectonics of Northwestern South America*,
849 Springer, p. 603-648.

850 Martínez, J., M. Patiño, A. Mora, J. P. Arias Martínez, and E. Tesón, 2022, Chapter 13 - Structural styles and evolution of the
851 Colombian Eastern foothills Piedemonte triangle zone, in G. Zamora, and A. Mora, eds., *Andean Structural Styles*, Elsevier, p. 181-
852 193.

853 Matthews, K. J., K. T. Maloney, S. Zahirovic, S. E. Williams, M. Seton, and R. D. Müller, 2016, Global plate boundary evolution and
854 kinematics since the late Paleozoic: *Global and Planetary Change*, v. 146, p. 226-250.

855 McGirr, R., M. Seton, and S. Williams, 2021, Kinematic and geodynamic evolution of the Isthmus of Panama region: Implications for
856 Central American Seaway closure: *GSA Bulletin*, v. 133, p. 867-884.

857 Montes, C., G. Bayona, A. Cardona, D. M. Buchs, C. A. Silva, S. Morón, N. Hoyos, D. A. Ramírez, C. A. Jaramillo, and V. Valencia,
858 2012, Arc-continent collision and orocline formation: Closing of the Central American seaway: *Journal of Geophysical Research:*
859 *Solid Earth*, v. 117.

860 Montes, C., A. Cardona, C. Jaramillo, A. Pardo, J. C. Silva, V. Valencia, C. Ayala, L. C. Pérez-Angel, L. A. Rodríguez-Parra, V.
861 Ramírez, and H. Niño, 2015, Middle Miocene closure of the Central American Seaway: *Science*, v. 348, p. 226-229.

862 Montes, C., A. F. Rodríguez-Corcho, G. Bayona, N. Hoyos, S. Zapata, and A. Cardona, 2019, Continental margin response to
863 multiple arc-continent collisions: The northern Andes-Caribbean margin: *Earth-Science Reviews*, v. 198, p. 102903.

864 Moore, G. F., K. L. Sender, and P. Mann, 1995, Fracture zone collision along the South Panama margin: SPECIAL PAPERS-
865 GEOLOGICAL SOCIETY OF AMERICA, p. 201-201.

866 Mora, A., M. Parra, M. R. Strecker, A. Kammer, C. Dimaté, and F. Rodríguez, 2006, Cenozoic contractional reactivation of Mesozoic
867 extensional structures in the Eastern Cordillera of Colombia: *Tectonics*, v. 25.

868 Mora, A., B. K. Horton, A. s. Mesa, J. Rubiano, R. A. Ketcham, M. Parra, V. Blanco, D. Garcia, and D. F. Stockli, 2010, Migration of
869 Cenozoic deformation in the Eastern Cordillera of Colombia interpreted from fission track results and structural relationships:
870 Implications for petroleum systems: *AAPG Bulletin*, v. 94, p. 1543-1580.

871 Mora, A., Reyes-Harker, A., Rodriguez, G., Tesón, E., Ramirez-Arias, J.C., Parra, M., Caballero, V., Mora, J.P., Quintero, I.,
872 Valencia, V. and Ibañez, M., 2013. Inversion tectonics under increasing rates of shortening and sedimentation: Cenozoic example
873 from the Eastern Cordillera of Colombia. *Geological Society, London, Special Publications*, 377(1), pp.411-442.

874 Mora, A., Blanco, V., Naranjo, J., Sanchez, N., Ketcham, R.A., Rubiano, J., Stockli, D.F., Quintero, I., Nemčok, M., Horton, B.K. and
875 Davila, H., 2013. On the lag time between internal strain and basement involved thrust induced exhumation: The case of the
876 Colombian Eastern Cordillera. *Journal of Structural Geology*, 52, pp.96-118.

877 Mora, A., Parra, M., Forero, G.R., Blanco, V., Moreno, N., Caballero, V., Stockli, D., Duddy, I. and Ghorbal, B., 2015. What drives
878 orogenic asymmetry in the Northern Andes?: A case study from the apex of the Northern Andean Orocline. Mora, A., D. Villagómez,
879 M. Parra, V. M. Caballero, R. Spikings, B. K. Horton, J. A. Mora-Bohórquez, R. A. Ketcham, J. P. Arias-Martínez, and J. Gómez,
880 2020, Late Cretaceous to Cenozoic uplift of the northern Andes: Paleogeographic implications: *The Geology of Colombia*, v. 3, p.
881 89-121.

882 Mora, A., D. Villagómez, M. Parra, V. M. Caballero, R. Spikings, B. K. Horton, J. A. Mora-Bohórquez, R. A. Ketcham, and J. P.
883 Arias-Martínez, 2020a, Late Cretaceous to Cenozoic uplift of the northern Andes: Paleogeographic implications: *The Geology of*
884 *Colombia*, v. 3, p. 89-121.

885 Mora, A., E. Tesón, J. Martínez, M. Parra, A. Lasso, B. K. Horton, R. A. Ketcham, A. Velásquez, J. P. Arias-Martínez, and J.
886 Gómez, 2020b, The eastern foothills of Colombia: *The Geology of Colombia*, v. 3, p. 123-142.

887 Mora-Bohórquez, J. A., M. Ibáñez-Mejía, O. Oncken, M. de Freitas, V. Vélez, A. Mesa, and L. Serna, 2017a, Structure and age of
888 the Lower Magdalena Valley basin basement, northern Colombia: New reflection-seismic and U-Pb-Hf insights into the termination
889 of the central andes against the Caribbean basin: *Journal of South American Earth Sciences*, v. 74, p. 1-26.

890 Mora-Bohórquez, J. A., O. Oncken, E. Le Breton, M. Ibáñez-Mejía, C. Faccenna, G. Veloza, V. Vélez, M. de Freitas, and A. Mesa,
891 2017b, Linking Late Cretaceous to Eocene tectonostratigraphy of the San Jacinto fold belt of NW Colombia with Caribbean plateau
892 collision and flat subduction: *Tectonics*, v. 36, p. 2599-2629.

893 Mora-Bohórquez, J. A., O. Oncken, E. Le Breton, A. Mora, G. Veloza, V. Vélez, and M. de Freitas, 2018, Controls on forearc basin
894 formation and evolution: Insights from Oligocene to Recent tectono-stratigraphy of the Lower Magdalena Valley basin of northwest
895 Colombia: *Marine and Petroleum Geology*, v. 97, p. 288-310.

896 Mora-Páez, H., J. N. Kellogg, J. T. Freymueller, D. Mencin, R. M. S. Fernandes, H. Diederix, P. LaFemina, L. Cardona-Piedrahita,
897 S. Lizarazo, J.-R. Peláez-Gaviria, F. Díaz-Mila, O. Bohórquez-Orozco, L. Giraldo-Londoño, and Y. Corchuelo-Cuervo, 2019, Crustal
898 deformation in the northern Andes – A new GPS velocity field: *Journal of South American Earth Sciences*, v. 89, p. 76-91.

899 Morell, K. D., 2015, Late Miocene to recent plate tectonic history of the southern Central America convergent margin: *Geochemistry,*
900 *Geophysics, Geosystems*, v. 16, p. 3362-3382.

901 Moreno, N., Silva, A., Mora, A., Tesón, E., Quintero, I., Rojas, L.E., Lopez, C., Blanco, V., Castellanos, J., Sanchez, J. and Osorio,
902 L., 2013. Interaction between thin-and thick-skinned tectonics in the foothill areas of an inverted graben. *The Middle Magdalena*
903 *Foothill belt. Geological Society, London, Special Publications*, 377(1), pp.221-255

904 Müller, R. D., J. Cannon, X. Qin, R. J. Watson, M. Gurnis, S. Williams, T. Pfaffelmoser, M. Seton, S. H. J. Russell, and S. Zahirovic,
905 2018, *GPlates: Building a Virtual Earth Through Deep Time: Geochemistry, Geophysics, Geosystems*, v. 19, p. 2243-2261.

906 Müller, R. D., S. Zahirovic, S. E. Williams, J. Cannon, M. Seton, D. J. Bower, M. G. Tetley, C. Heine, E. Le Breton, S. Liu, S. H. J.
907 Russell, T. Yang, J. Leonard, and M. Gurnis, 2019, *A Global Plate Model Including Lithospheric Deformation Along Major Rifts and*
908 *Orogens Since the Triassic: Tectonics*, v. 38, p. 1884-1907.

909 Oncken, O., D. Hindle, J. Kley, K. Elger, P. Victor, and K. Schemmann, 2006, Deformation of the central Andean upper plate
910 system—Facts, fiction, and constraints for plateau models, *The Andes*, Springer, p. 3-27.

911 Pardo, N., H. Cepeda, and J. M. Jaramillo, 2005, The Paipa volcano, Eastern Cordillera of Colombia, South America: Volcanic
912 stratigraphy: *Earth Sciences Research Journal*, v. 9, p. 3-18.

913 Pardo-Casas, F., and P. Molnar, 1987, Relative motion of the Nazca (Farallon) and South American Plates since Late Cretaceous
914 time: *Tectonics*, v. 6, p. 233-248.

915 Pardo-Trujillo, A., S. Echeverri, C. Borrero, A. Arenas, F. Vallejo, R. Trejos, Á. Plata, J. A. Flores, A. Cardona, and S. Restrepo,
916 2020, Cenozoic Geologic Evolution of the Southern Tumaco Forearc Basin (SW Colombian Pacific): *The Geology of Colombia*, v. 3,
917 p. 215-247.

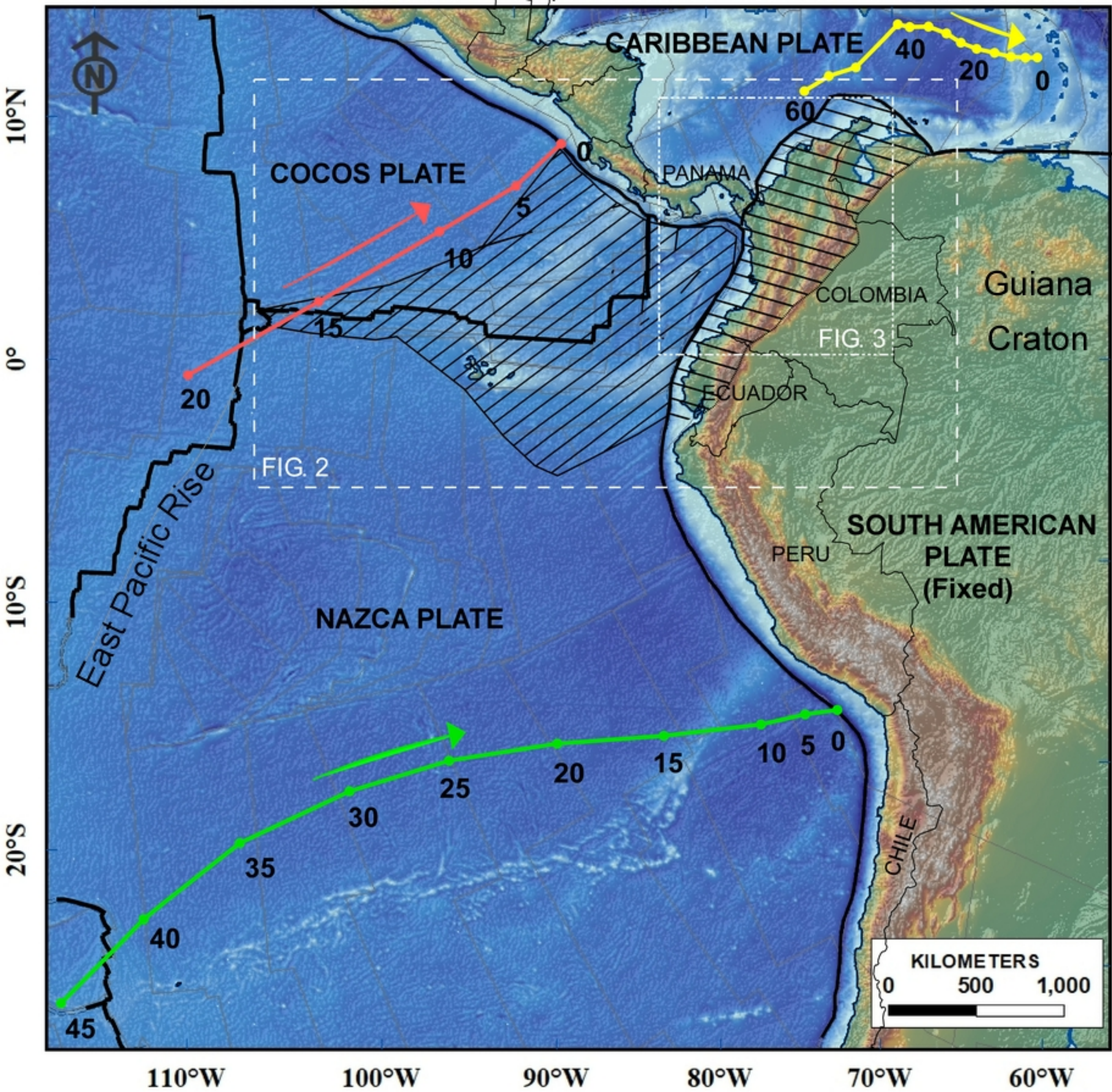
918 Parra, M., A. Mora, E. R. Sobel, M. R. Strecker, and R. González, 2009, Episodic orogenic front migration in the northern Andes:
919 Constraints from low-temperature thermochronology in the Eastern Cordillera, Colombia: *Tectonics*, v. 28.

- 920 Peacock, S. M., T. Rushmer, and A. B. Thompson, 1994, Partial melting of subducting oceanic crust: *Earth and Planetary Science*
921 *Letters*, v. 121, p. 227-244.
- 922 Pennington, W. D., 1981, Subduction of the Eastern Panama Basin and seismotectonics of Northwestern South America: *Journal of*
923 *Geophysical Research: Solid Earth*, v. 86, p. 10753-10770.
- 924 Pindell, J. L., and S. F. Barrett, 1990, Caribbean plate tectonic history: The Caribbean Region, volume H of *The Geology of North*
925 *America*, p. 405-432.
- 926 Pindell, J., L. Kennan, W. V. Maresch, K. Stanek, G. Draper, and R. Higgs, 2005, Plate-kinematics and crustal dynamics of circum-
927 Caribbean arc-continent interactions: Tectonic controls on basin development in Proto-Caribbean margins: *Special Papers-*
928 *Geological Society of America*, v. 394, p. 7.
- 929 Pindell, J. L., and L. Kennan, 2009, Tectonic evolution of the Gulf of Mexico, Caribbean and northern South America in the mantle
930 reference frame: an update: *Geological Society, London, Special Publications*, v. 328, p. 1-55.
- 931 Piraquive, A., E. Pinzón, A. Kammer, M. Bernet, and A. von Quadt, 2018, Early Neogene unroofing of the Sierra Nevada de Santa
932 Marta, as determined from detrital geothermochronology and the petrology of clastic basin sediments: *GSA Bulletin*, v. 130, p. 355-
933 380.
- 934 Poveda, E., G. Monsalve, and C. A. Vargas, 2015, Receiver functions and crustal structure of the northwestern Andean region,
935 Colombia: *Journal of Geophysical Research: Solid Earth*, v. 120, p. 2408-2425.
- 936 Prieto, G. A., G. C. Beroza, S. A. Barrett, G. A. López, and M. Florez, 2012, Earthquake nests as natural laboratories for the study of
937 intermediate-depth earthquake mechanics: *Tectonophysics*, v. 570-571, p. 42-56.
- 938 Prieto, G. A., M. Florez, S. A. Barrett, G. C. Beroza, P. Pedraza, J. F. Blanco, and E. Poveda, 2013, Seismic evidence for thermal
939 runaway during intermediate-depth earthquake rupture: *Geophysical Research Letters*, v. 40, p. 6064-6068.
- 940 Pérez-Consuegra, N., R. F. Ott, G. D. Hoke, J. P. Galve, V. Pérez-Peña, and A. Mora, 2021, Neogene variations in slab geometry
941 drive topographic change and drainage reorganization in the Northern Andes of Colombia: *Global and Planetary Change*, v. 206, p.
942 103641.
- 943 Ramos, V.A., E.O. Cristallini, and D.J. Pérez, 2002. The Pampean flat-slab of the Central Andes. *Journal of South American earth*
944 *sciences*, 15(1), pp.59-78.
- 945 Ramos, V. A., 2010, The tectonic regime along the Andes: Present-day and Mesozoic regimes: *Geological Journal*, v. 45, p. 2-25.
- 946 Restrepo, J., J., and J. F. Toussaint, 1988, Terranes and Continental Accretion in the Colombian Andes: *International Union of*
947 *Geological Sciences*, v. 11, p. 189-193.
- 948 Restrepo-Moreno, S. A., D. A. Foster, D. F. Stockli, and L. N. Parra-Sánchez, 2009, Long-term erosion and exhumation of the
949 "Altiplano Antioqueño", Northern Andes (Colombia) from apatite (U–Th)/He thermochronology: *Earth and Planetary Science*
950 *Letters*, v. 278, p. 1-12.
- 951 Reyes-Harker, A., C. F. Ruiz-Valdivieso, A. Mora, J. C. Ramírez-Arias, G. Rodriguez, F. de la Parra, V. Caballero, M. Parra, N.
952 Moreno, B. K. Horton, J. E. Saylor, A. Silva, V. Valencia, D. Stockli, and V. Blanco, 2015, Cenozoic paleogeography of the Andean
953 foreland and retroarc hinterland of Colombia: *AAPG Bulletin*, v. 99, p. 1407-1453.
- 954 Reyes-Santos, J. P., M. Mantilla-Monsalve, and J. S. Gonzalez, 2000, Regiones Tectono-Sedimentarias del Valle Inferior del
955 Magdalena, Colombia [PAPER IN SPANISH] *Tectono-Sedimentary Regions of the Lower Magdalena Valley, Colombia*.
- 956 Rooney, T. O., K. D. Morell, P. Hidalgo, and P. Franceschi, 2015, Magmatic consequences of the transition from orthogonal to
957 oblique subduction in Panama: *Geochemistry, Geophysics, Geosystems*, v. 16, p. 4178-4208.
- 958 Rosero, A., M. Carrero, C. Ceballos, and A. Mora, 2022, Seismic and structural analysis of the San Francisco oil field (Colombia).
959 *Structural controls on a complex hydrocarbon charge history, Andean Structural Styles*, Elsevier, p. 195-206.
- 960 Sallarès, V., P. Charvis, E. R. Flueh, and J. Bialas, 2003, Seismic structure of Cocos and Malpelo Volcanic Ridges and implications
961 for hot spot-ridge interaction: *Journal of Geophysical Research: Solid Earth*, v. 108.
- 962 Sánchez, J., B. K. Horton, E. Tesón, A. Mora, R. A. Ketcham, and D. F. Stockli, 2012, Kinematic evolution of Andean fold-thrust
963 structures along the boundary between the Eastern Cordillera and Middle Magdalena Valley basin, Colombia: *Tectonics*, v. 31.
- 964 Saylor, J. E., B. K. Horton, D. F. Stockli, A. Mora, and J. Corredor, 2012, Structural and thermochronological evidence for
965 Paleogene basement-involved shortening in the axial Eastern Cordillera, Colombia: *Journal of South American Earth Sciences*, v.
966 39, p. 202-215.
- 967 Schütte, P., M. Chiaradia, and B. Beate, 2010, Geodynamic controls on Tertiary arc magmatism in Ecuador: Constraints from U–Pb
968 zircon geochronology of Oligocene–Miocene intrusions and regional age distribution trends: *Tectonophysics*, v. 489, p. 159-176.
- 969 Seton, M., R. D. Müller, S. Zahirovic, C. Gaina, T. Torsvik, G. Shephard, A. Talsma, M. Gurnis, M. Turner, S. Maus, and M.
970 Chandler, 2012, Global continental and ocean basin reconstructions since 200Ma: *Earth-Science Reviews*, v. 113, p. 212-270.
- 971 Siebert, L., T. Simkin, and P. Kimberly, 2011, *Volcanoes of the World*, Univ of California Press.

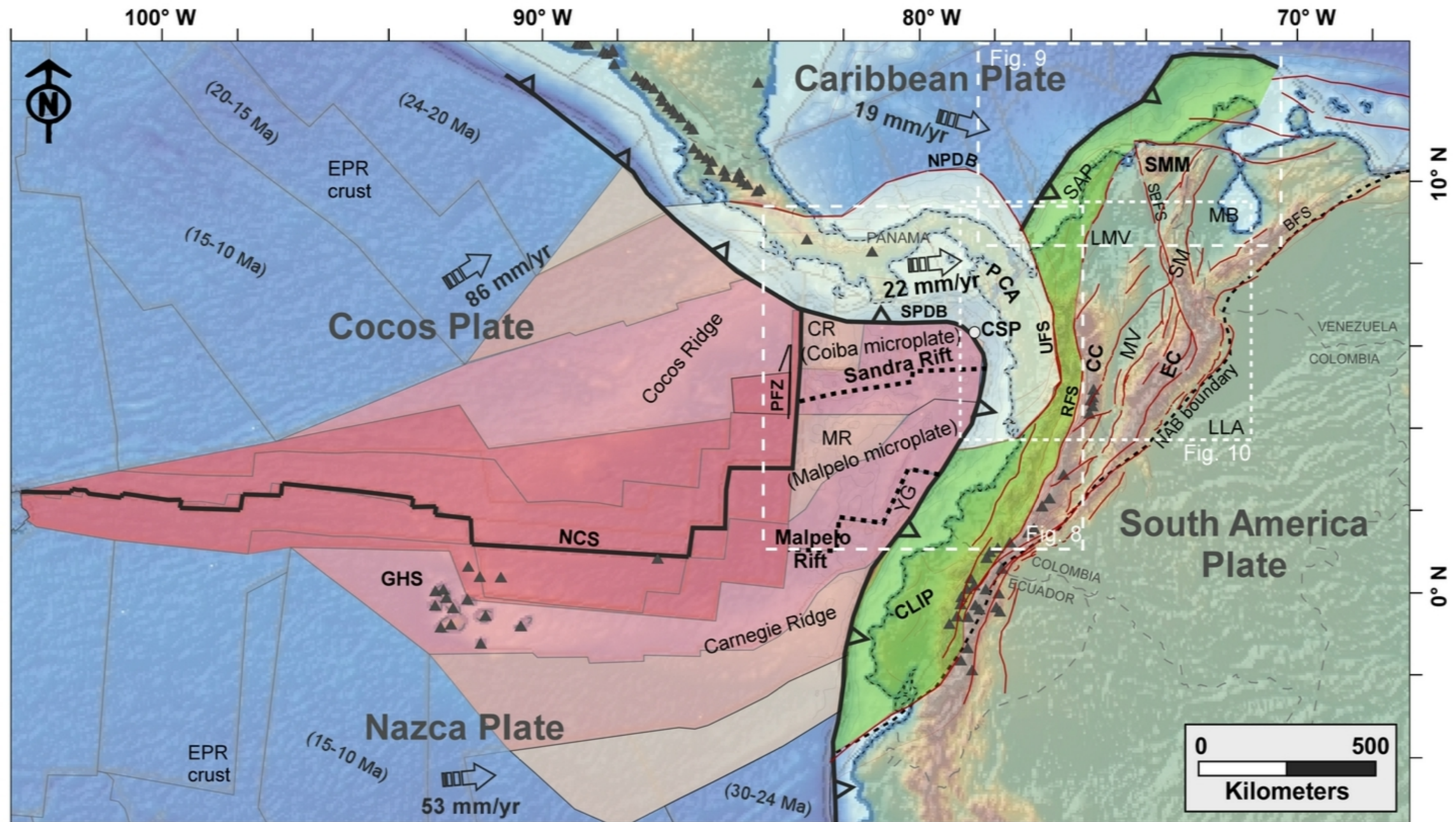
- 972 Silva, A., A. Mora, V. Caballero, G. Rodriguez, C. Ruiz, N. Moreno, M. Parra, J. C. Ramirez-Arias, M. Ibáñez, and I. Quintero, 2013,
973 Basin compartmentalization and drainage evolution during rift inversion: evidence from the Eastern Cordillera of Colombia:
974 Geological Society, London, Special Publications, v. 377, p. 369.
- 975 Sinton, C. W., R. A. Duncan, M. Storey, J. Lewis, and J. J. Estrada, 1998, An oceanic flood basalt province within the Caribbean
976 plate: *Earth and Planetary Science Letters*, v. 155, p. 221-235.
- 977 Siravo, G., C. Faccenna, M. G rault, T. W. Becker, M. G. Fellin, F. Herman, and P. Molin, 2019, Slab flattening and the rise of the
978 Eastern Cordillera, Colombia: *Earth and Planetary Science Letters*, v. 512, p. 100-110.
- 979 Somoza, R., and M. E. Ghidella, 2012, Late Cretaceous to recent plate motions in western South America revisited: *Earth and
980 Planetary Science Letters*, v. 331-332, p. 152-163.
- 981 Spikings, R. A., P. V. Crowhurst, W. Winkler, and D. Villagomez, 2010, Syn- and post-accretionary cooling history of the Ecuadorian
982 Andes constrained by their in-situ and detrital thermochronometric record: *Journal of South American Earth Sciences*, v. 30, p. 121-
983 133.
- 984 Sun, M., M. J. Bezada, J. Cornthwaite, G. A. Prieto, F. Niu, and A. Levander, 2022, Overlapping slabs: Untangling subduction in NW
985 South America through finite-frequency teleseismic tomography: *Earth and Planetary Science Letters*, v. 577, p. 117253.
- 986 Syracuse, E. M., M. Maceira, G. A. Prieto, H. Zhang, and C. J. Ammon, 2016, Multiple plates subducting beneath Colombia, as
987 illuminated by seismicity and velocity from the joint inversion of seismic and gravity data: *Earth and Planetary Science Letters*, v.
988 444, p. 139-149.
- 989 Taboada, A., L. A. Rivera, A. Fuenzalida, A. Cisternas, H. Philip, H. Bijwaard, J. Olaya, and C. Rivera, 2000, Geodynamics of the
990 northern Andes: Subductions and intracontinental deformation (Colombia): *Tectonics*, v. 19, p. 787-813.
- 991 Tatsumi Y, and S. Eggins, 1995, Subduction Zone Magmatism. *Frontiers in Earth Science* Blackwell, Cambridge
- 992 Toda, S., R. S. Stein, S. H. Kirby, and S. B. Bozkurt, 2008, A slab fragment wedged under Tokyo and its tectonic and seismic
993 implications: *Nature Geoscience*, v. 1, p. 771-776.
- 994 Trenkamp, R., J. N. Kellogg, J. T. Freymueller, and H. P. Mora, 2002, Wide plate margin deformation, southern Central America and
995 Northwestern South America, CASA GPS observations: *Journal of South American Earth Sciences*, v. 15, p. 157-171.
- 996 Trumbull, R. B., U. Riller, O. Oncken, E. Scheuber, K. Munier, and F. Hongn, 2006, The time-space distribution of Cenozoic
997 volcanism in the South-Central Andes: a new data compilation and some tectonic implications, *The Andes*, Springer, p. 29-43.
- 998 Vargas, C. A., and P. Mann, 2013, Tearing and Breaking Off of Subducted Slabs as the Result of Collision of the Panama Arc-
999 Indenter with Northwestern South America: *Bulletin of the Seismological Society of America*, v. 103, p. 2025-2046.
- 1000 Vargas, C. A., 2019, Subduction geometries in Northwestern South America. *The Geology of Colombia*, v. 4, p. 397-422. Bogotá.
1001 <https://doi.org/10.32685/pub.esp.38.2019.11>.
- 1002 Veloza, G., R. Styron, and M. Taylor, 2012, Open-source archive of active faults for northwest South America: *GSA TODAY*, v. 22.
- 1003 Villag mez, D., R. Spikings, T. Magna, A. Kammer, W. Winkler, and A. Beltr n, 2011, Geochronology, geochemistry and tectonic
1004 evolution of the Western and Central cordilleras of Colombia: *Lithos*, v. 125, p. 875-896.
- 1005 Villagomez, D., and R. Spikings, 2013, Unraveling The Complex Interaction Between The Southern Caribbean, Northwest South
1006 America And The Pacific Plates During The Cenozoic, p. T22A-08.
- 1007 Villamizar Escalante, N., 2017, Historia de exhumaci n del bloque este de la falla de Bucaramanga usando termocronolog a de baja
1008 temperatura, Santander, Colombia: *Geolog a*.
- 1009 Von Huene, R., and D. W. Scholl, 1991, Observations at convergent margins concerning sediment subduction, subduction erosion,
1010 and the growth of continental crust: *Reviews of Geophysics*, v. 29, p. 279-316.
- 1011 von Huene, R., C. s. R. Ranero, and P. Vannucchi, 2004, Generic model of subduction erosion: *Geology*, v. 32, p. 913-916.
- 1012 Wagner, L. S., J. S. Jaramillo, L. F. Ram rez-Hoyos, G. Monsalve, A. Cardona, and T. W. Becker, 2017, Transient slab flattening
1013 beneath Colombia: *Geophysical Research Letters*, v. 44, p. 6616-6623.
- 1014 Weber, M., J. F. Duque, S. Hoyos, A. L. C rdenas-Rozo, J. G mez, and R. Wilson, 2020, The Combia Volcanic Province: Miocene
1015 post-collisional magmatism in the northern Andes: *The Geology of Colombia*, v. 3, p. 355-394.
- 1016 Wegner, W., G. W rner, R. S. Harmon, and B. R. Jicha, 2011, Magmatic history and evolution of the Central American Land Bridge
1017 in Panama since Cretaceous times: *GSA Bulletin*, v. 123, p. 703-724.
- 1018 Werner, R., K. Hoernle, U. Barckhausen, and F. Hauff, 2003, Geodynamic evolution of the Gal pagos hot spot system (Central East
1019 Pacific) over the past 20 m.y.: Constraints from morphology, geochemistry, and magnetic anomalies: *Geochemistry, Geophysics,
1020 Geosystems*, v. 4.
- 1021 Wilson, D. S., and R. N. Hey, 1995, History of rift propagation and magnetization intensity for the Cocos-Nazca spreading Center:
1022 *Journal of Geophysical Research: Solid Earth*, v. 100, p. 10041-10056.
- 1023 Yarce, J., G. Monsalve, T. W. Becker, A. Cardona, E. Poveda, D. Alvira, and O. Ordo ez-Carmona, 2014, Seismological
1024 observations in Northwestern South America: Evidence for two subduction segments, contrasting crustal thicknesses and upper
1025 mantle flow: *Tectonophysics*, v. 637, p. 57-67.

- 1026 Zapata, S., M. Zapata-Henao, A. Cardona, C. Jaramillo, D. Silvestro, and F. Oboh-Ikuenobe, 2021, Long-term topographic growth
1027 and decay constrained by 3D thermo-kinematic modeling: Tectonic evolution of the Antioquia Altiplano, Northern Andes: Global and
1028 Planetary Change, v. 203, p. 103553.
- 1029 Zarifi, Z., J. Havskov, and A. Hanyga, 2007, An insight into the Bucaramanga nest: Tectonophysics, v. 443, p. 93-105.
- 1030 Zhang, T., R. G. Gordon, J. K. Mishra, and C. Wang, 2017, The Malpelo Plate Hypothesis and implications for nonclosure of the
1031 Cocos-Nazca-Pacific plate motion circuit: Geophysical Research Letters, v. 44, p. 8213-8218.
- 1032 Zheng, Y., Y. Chen, L. Dai, and Z. Zhao, 2015, Developing plate tectonics theory from oceanic subduction zones to collisional
1033 orogens: Science China Earth Sciences, v. 58, p. 1045-1069.

Location map.



Tectonic setting.



Age of crust erupted from the NCS

9 - 0 Ma	20 - 15 Ma
15 - 9 Ma	23 - 20 Ma

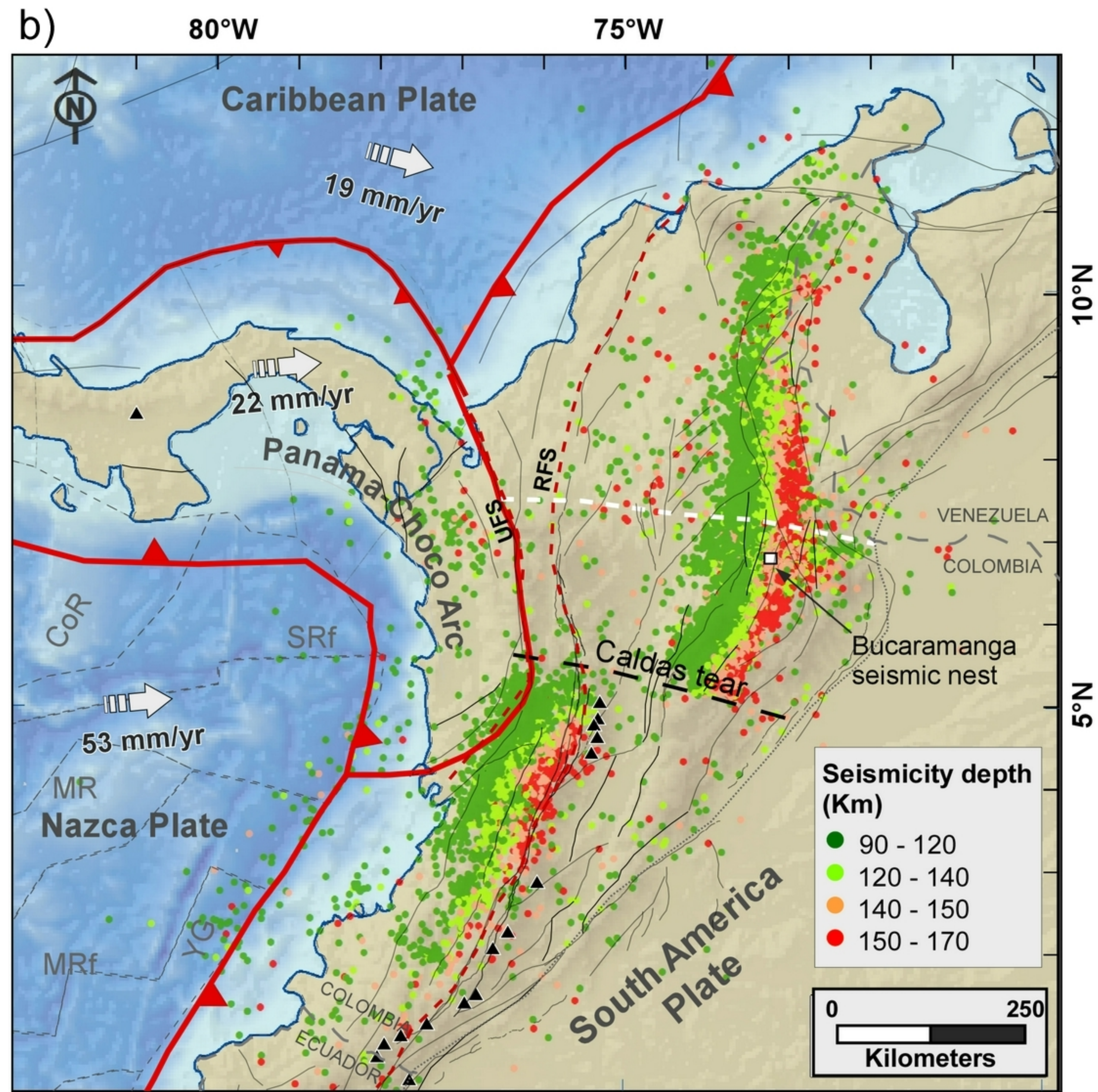
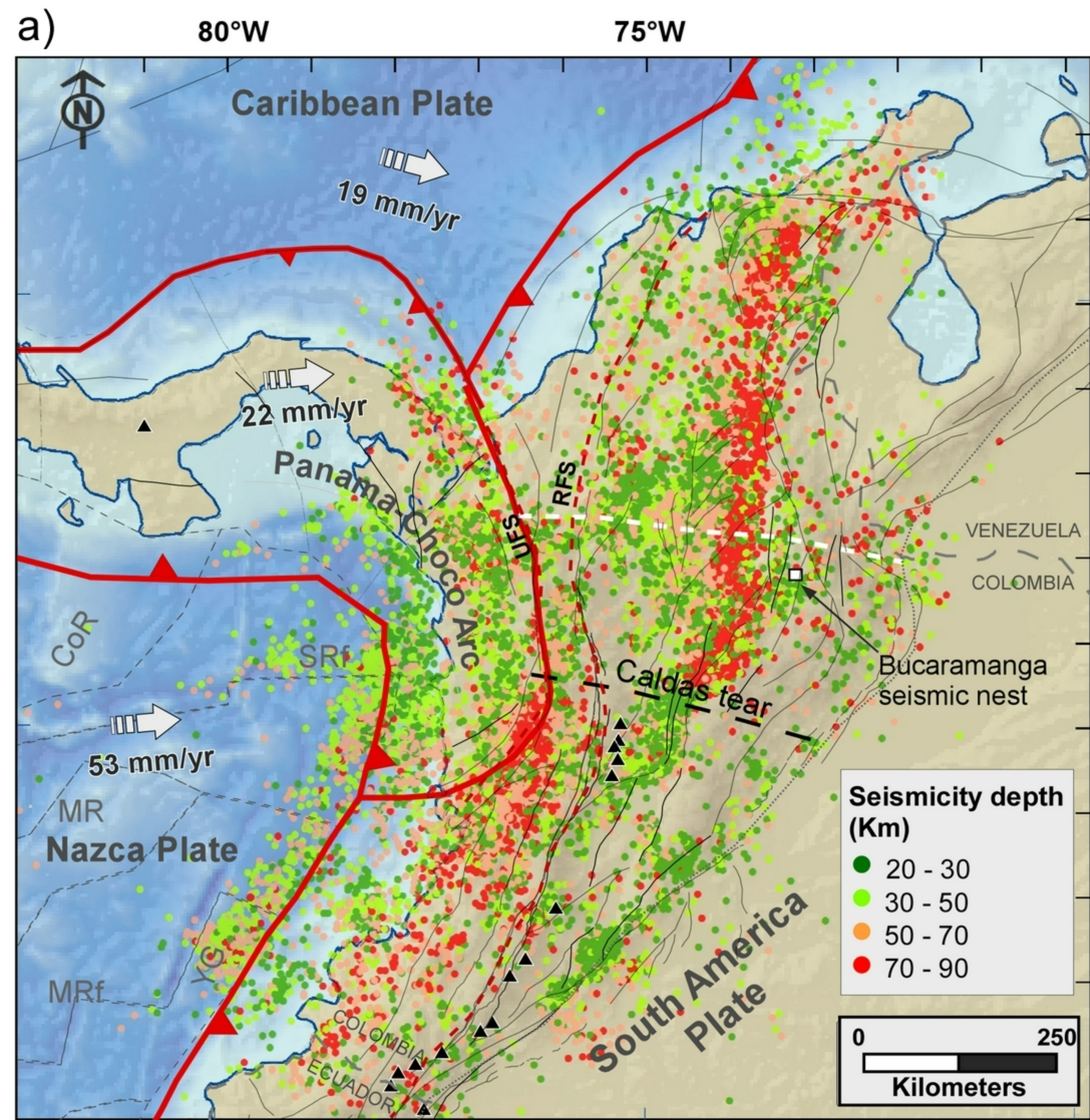
Accreted terrains

- Panama-Choco Arc
- Caribbean Large Igneous Province

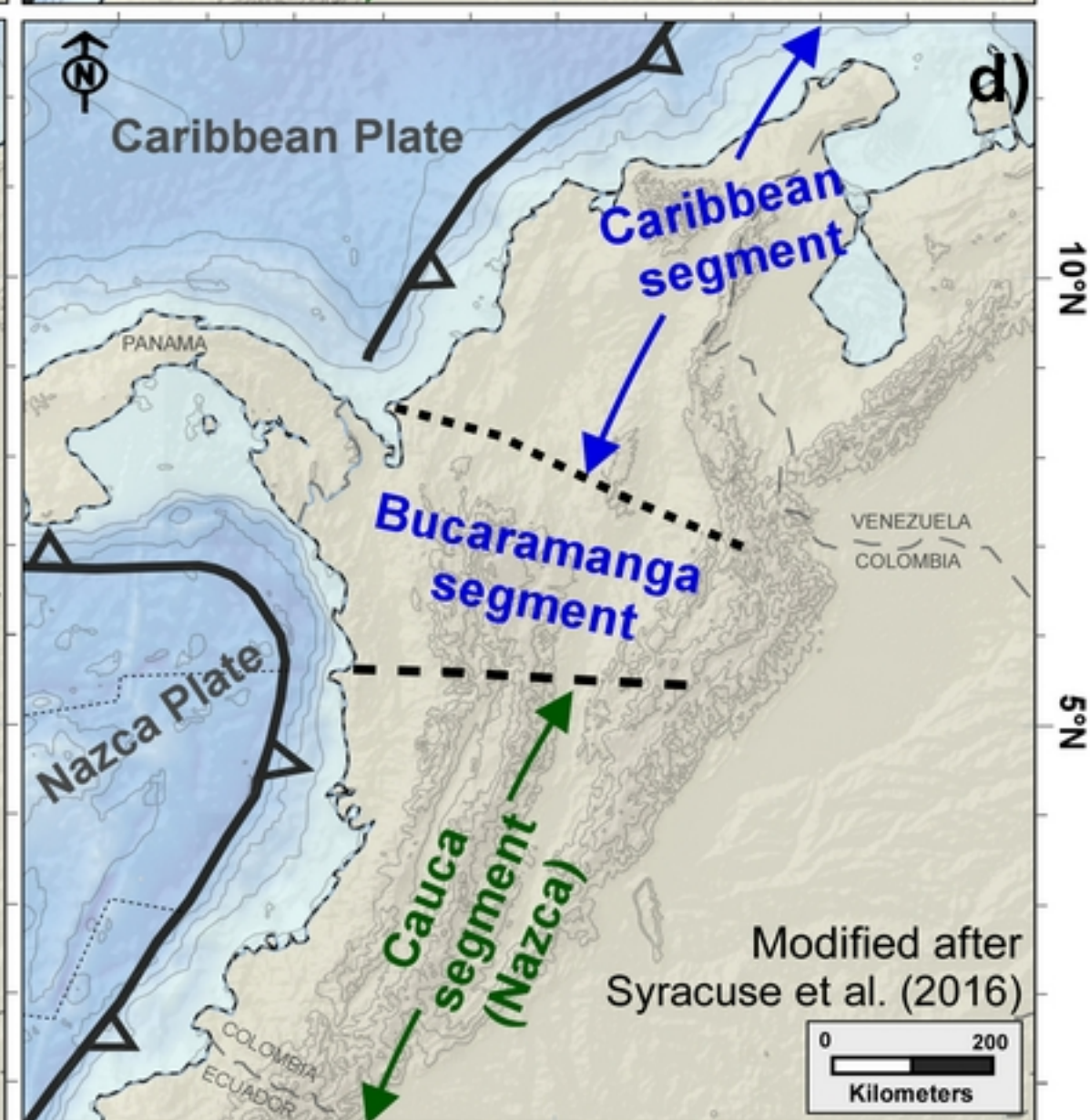
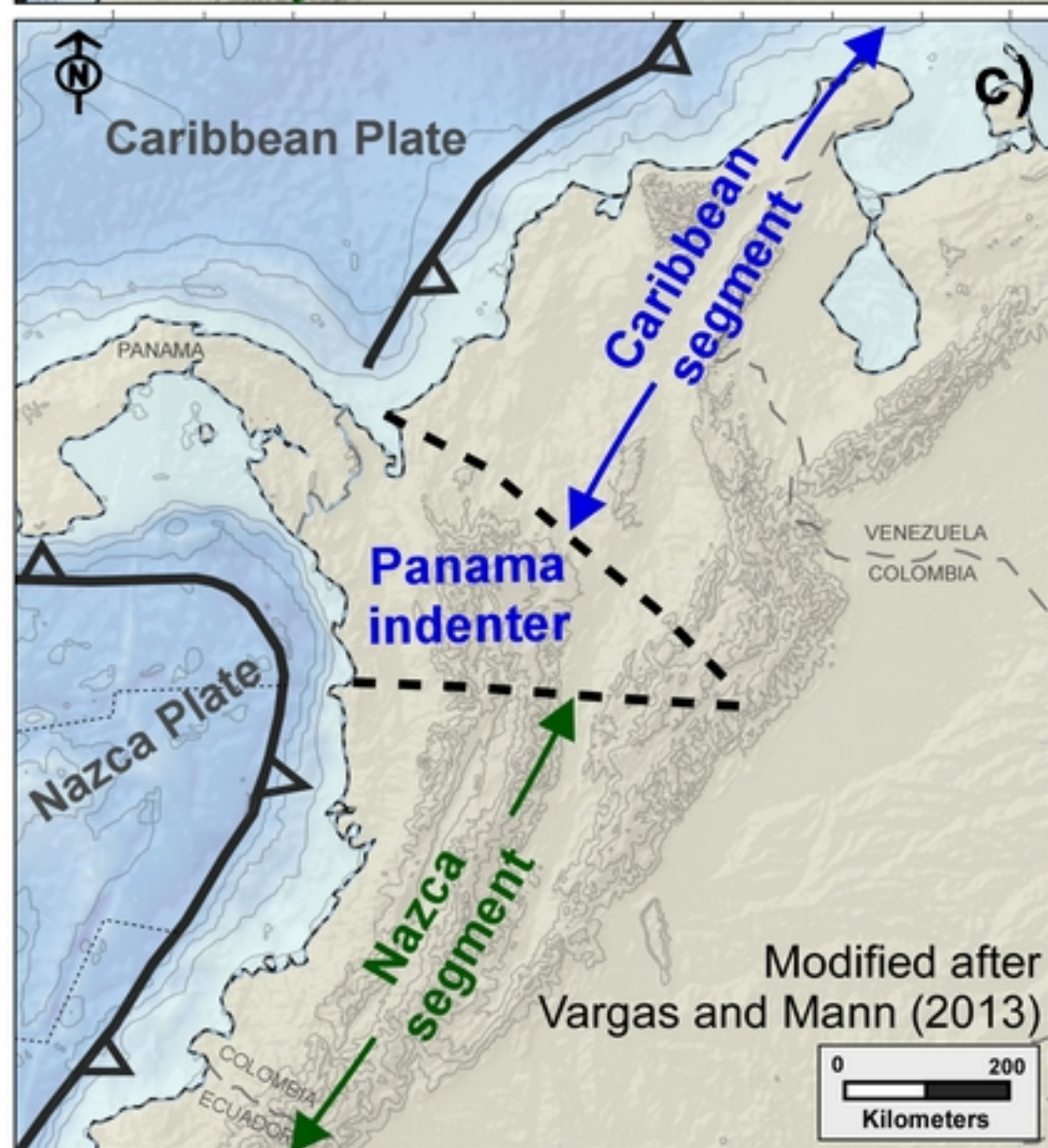
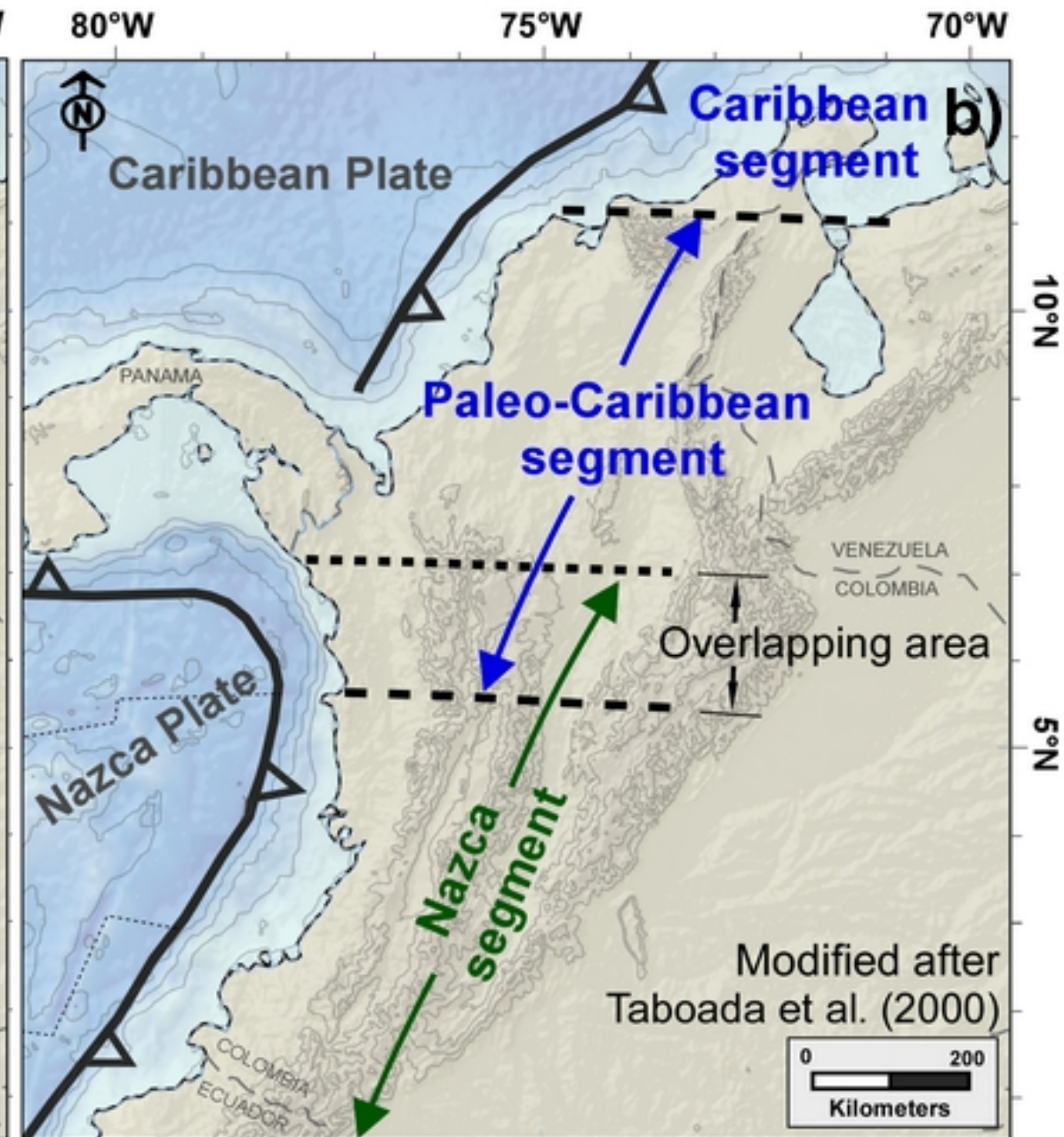
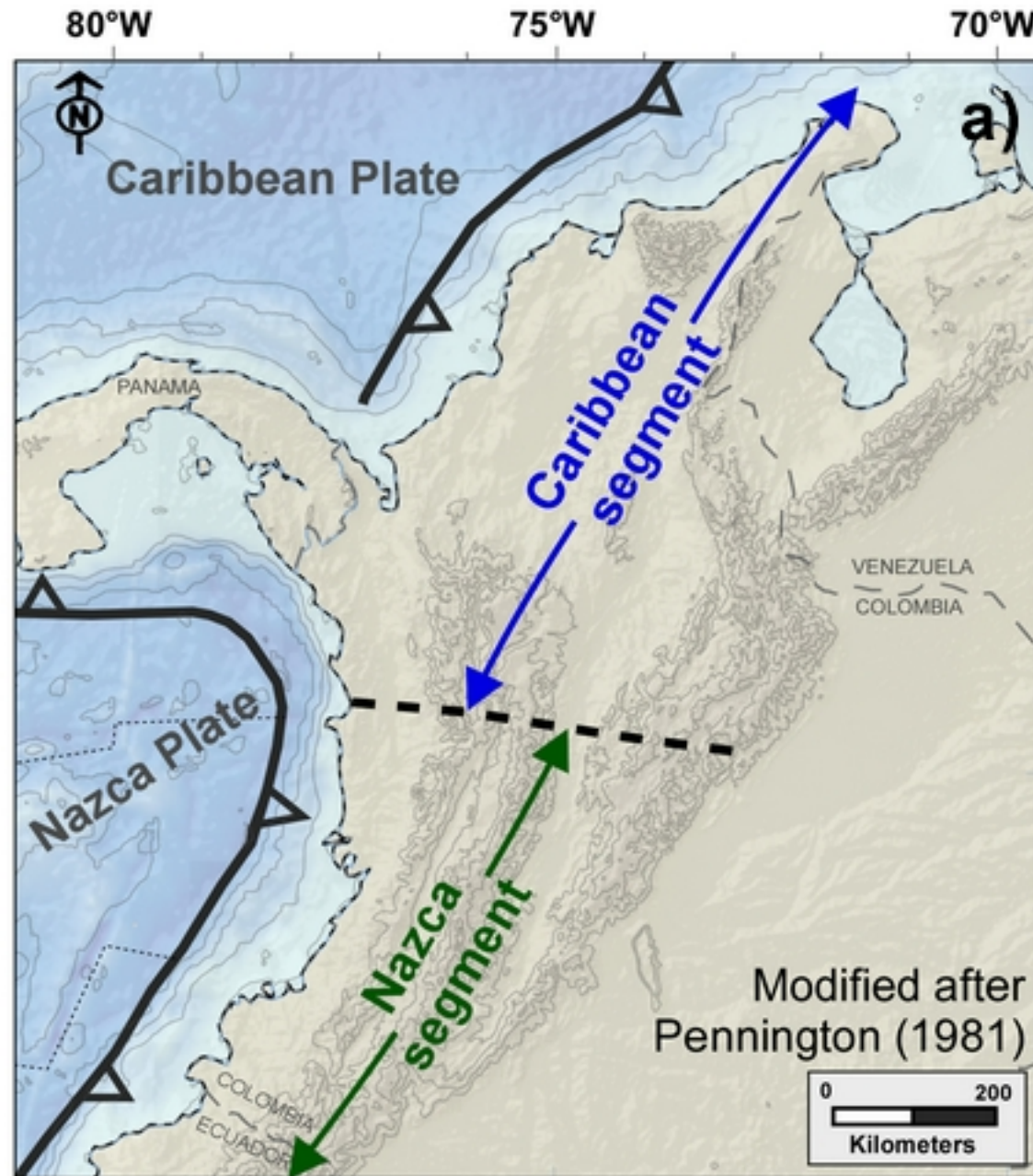
Main upper-plate faults

- NAB boundary
- Plate boundary
- Trench
- Modern volcanism

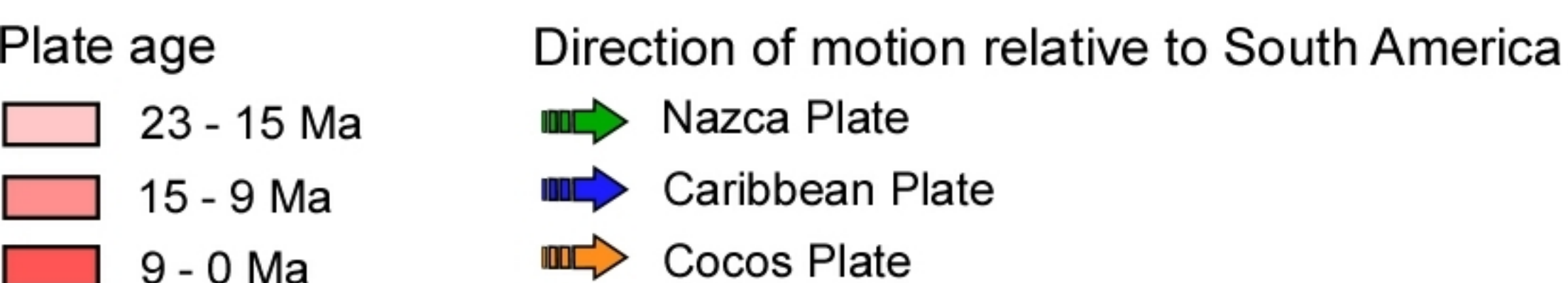
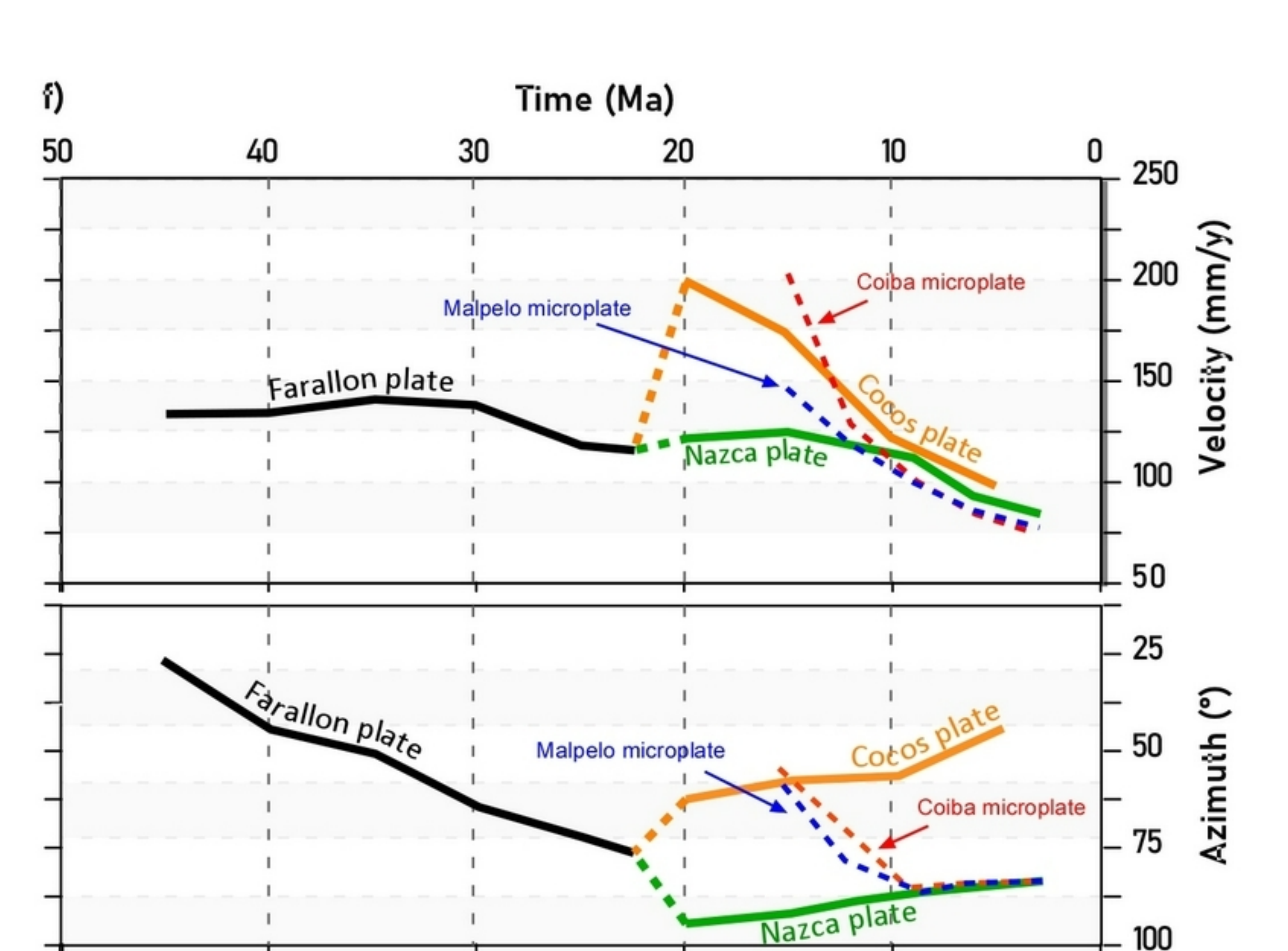
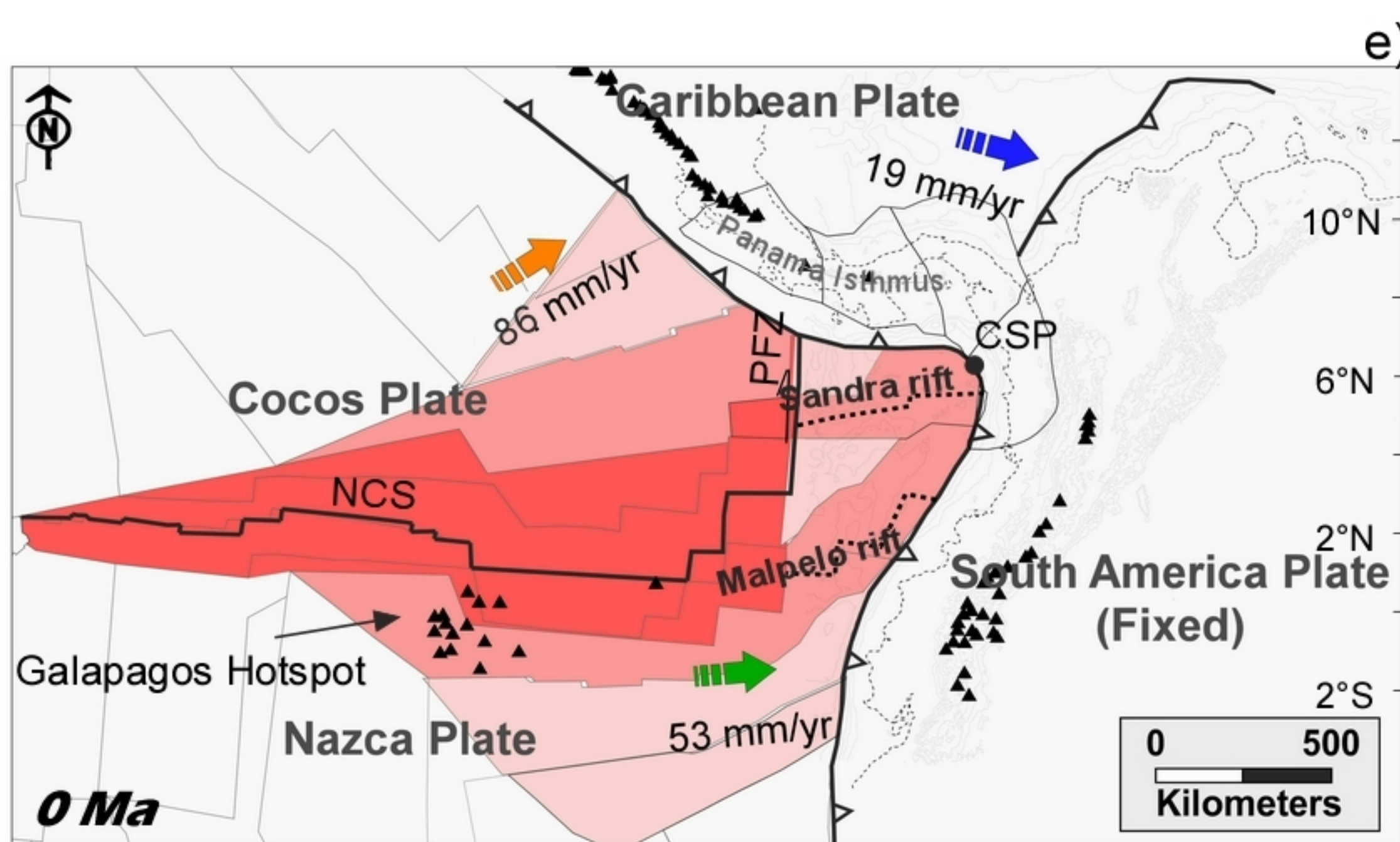
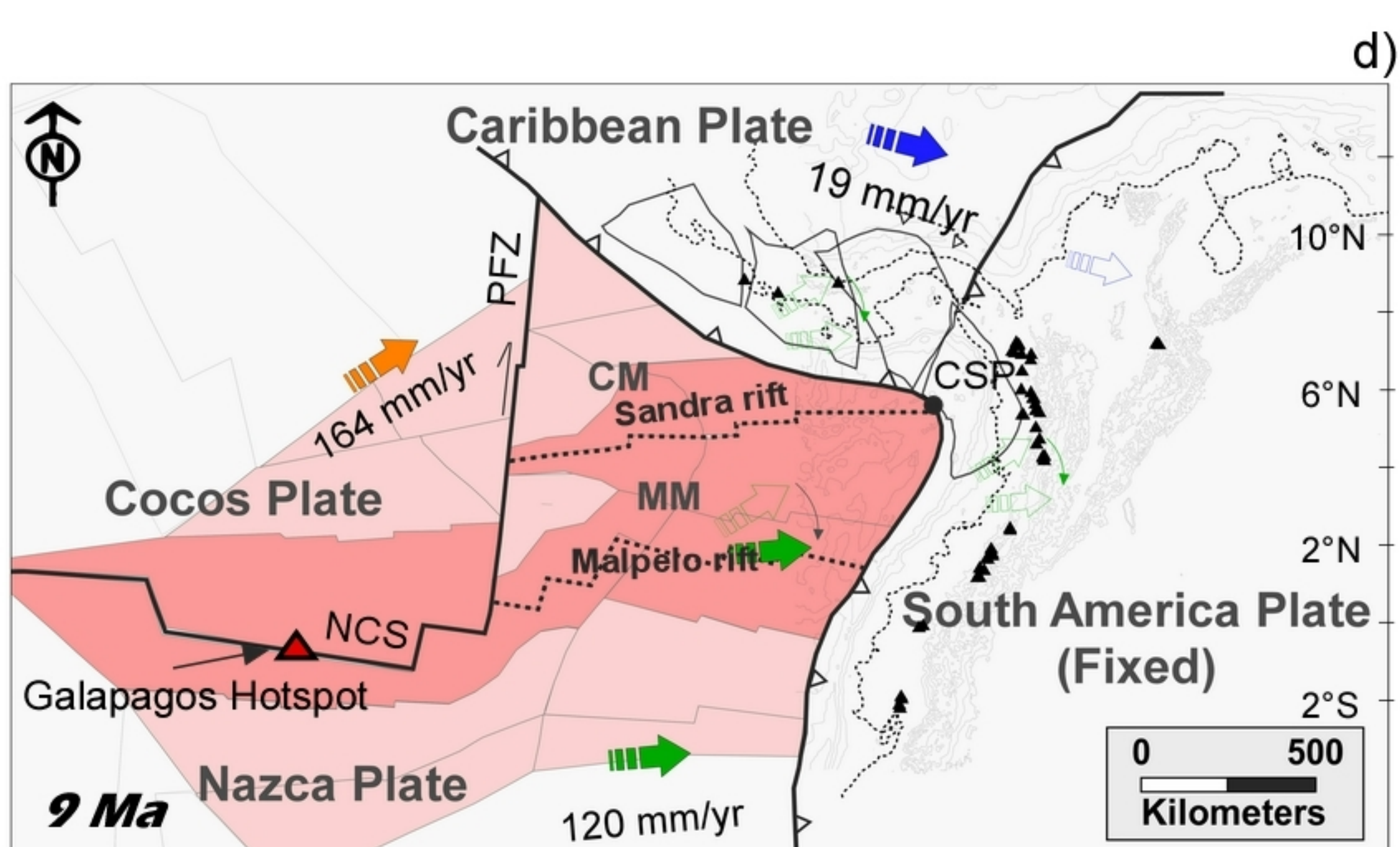
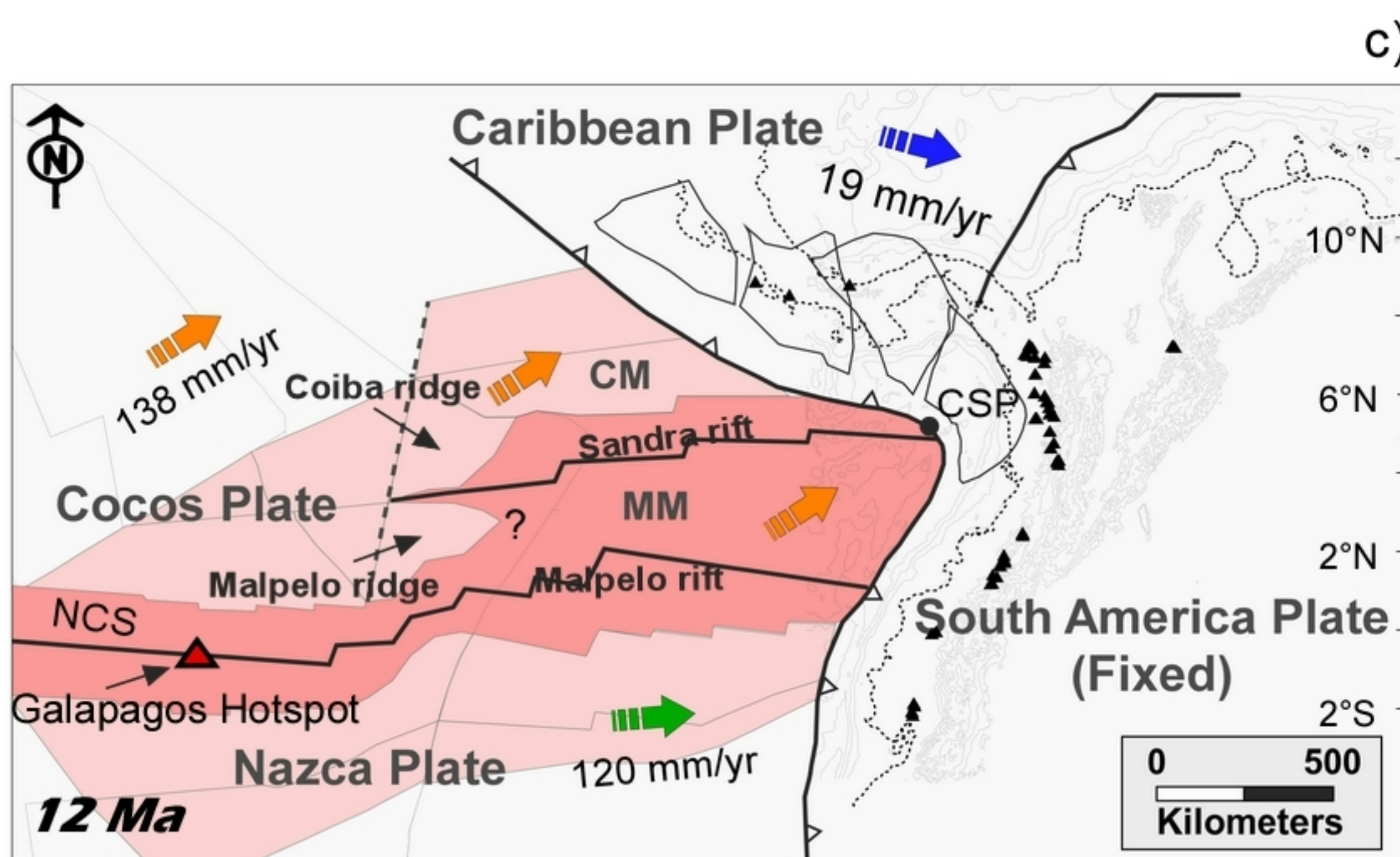
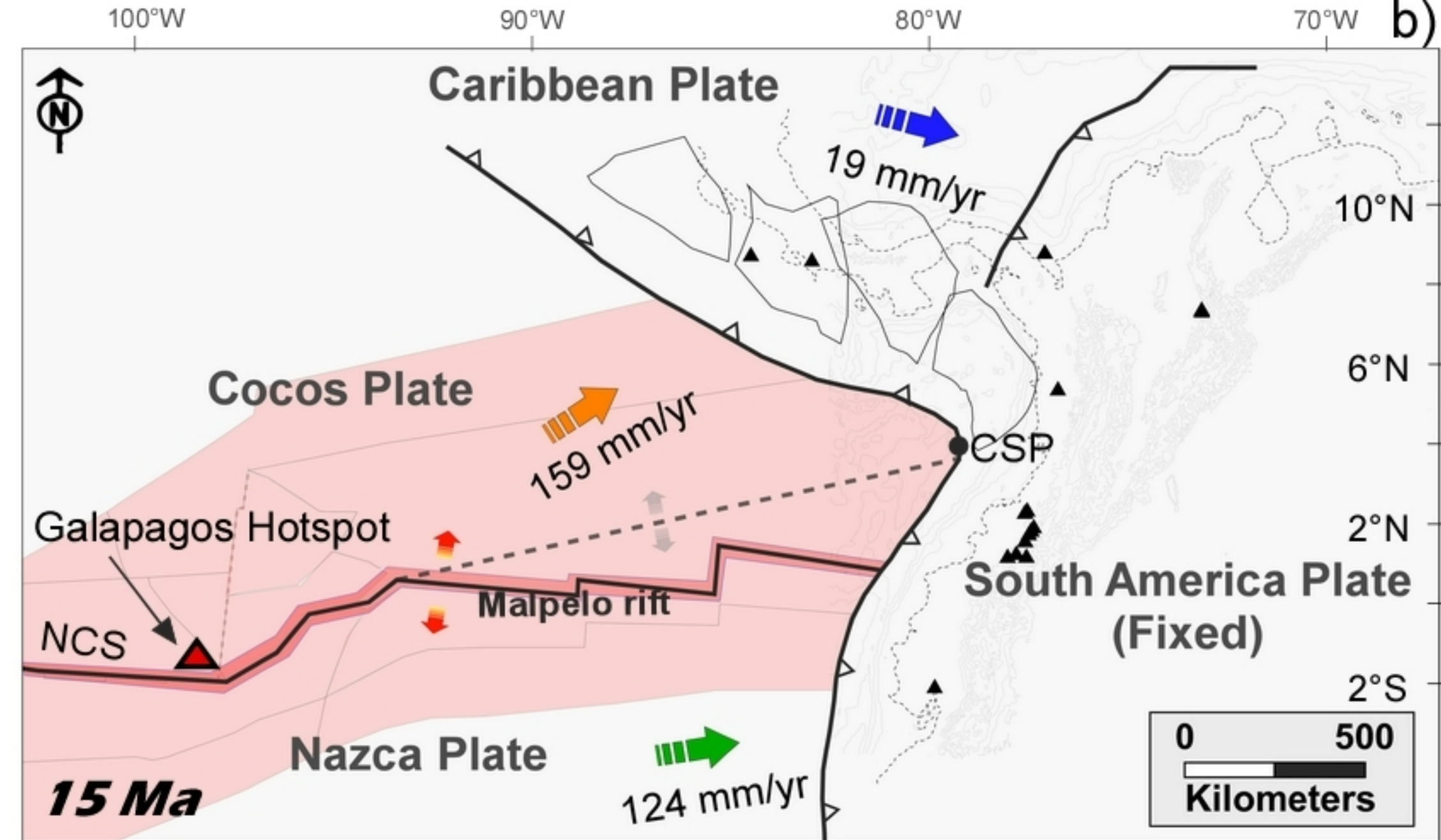
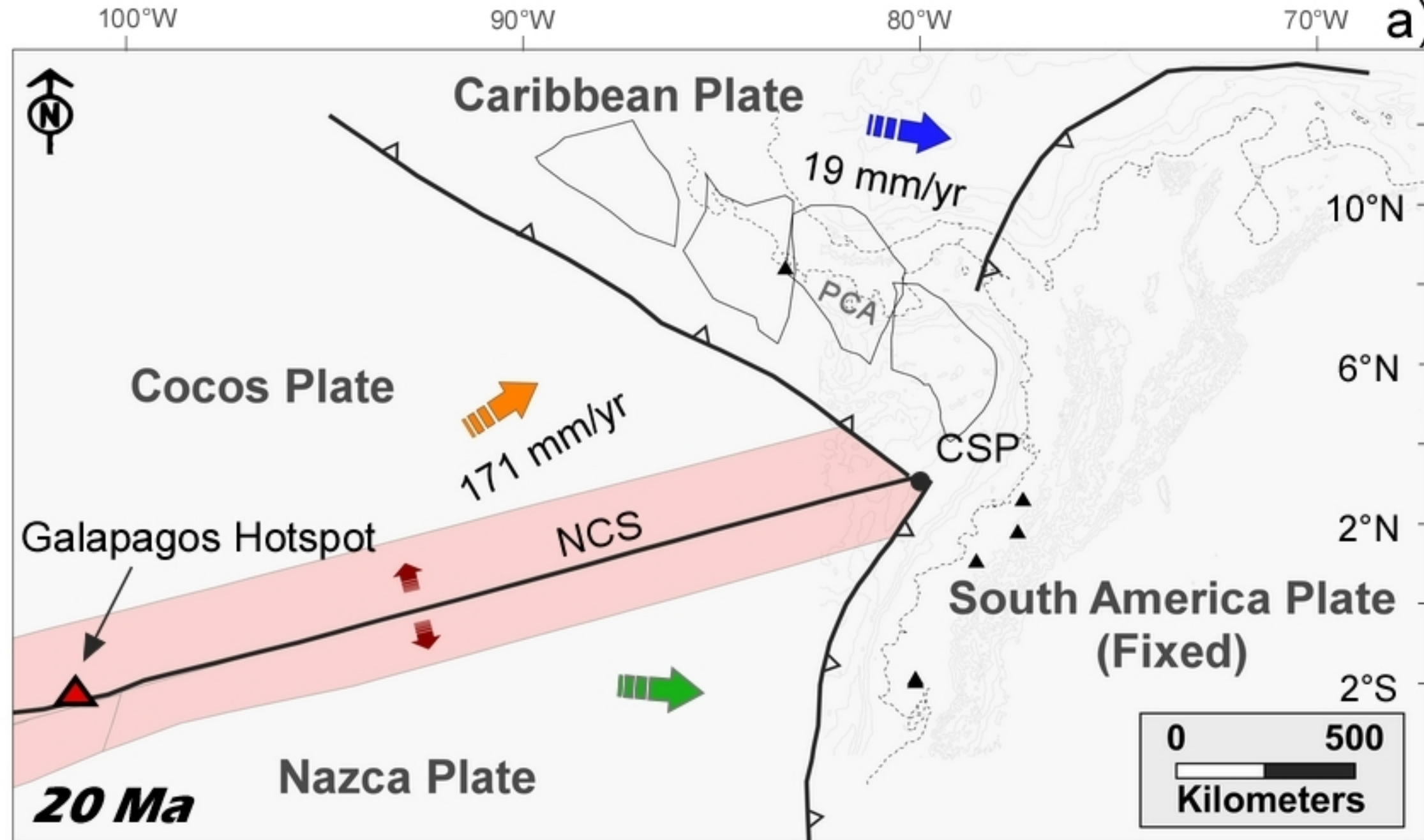
Seismicity map.



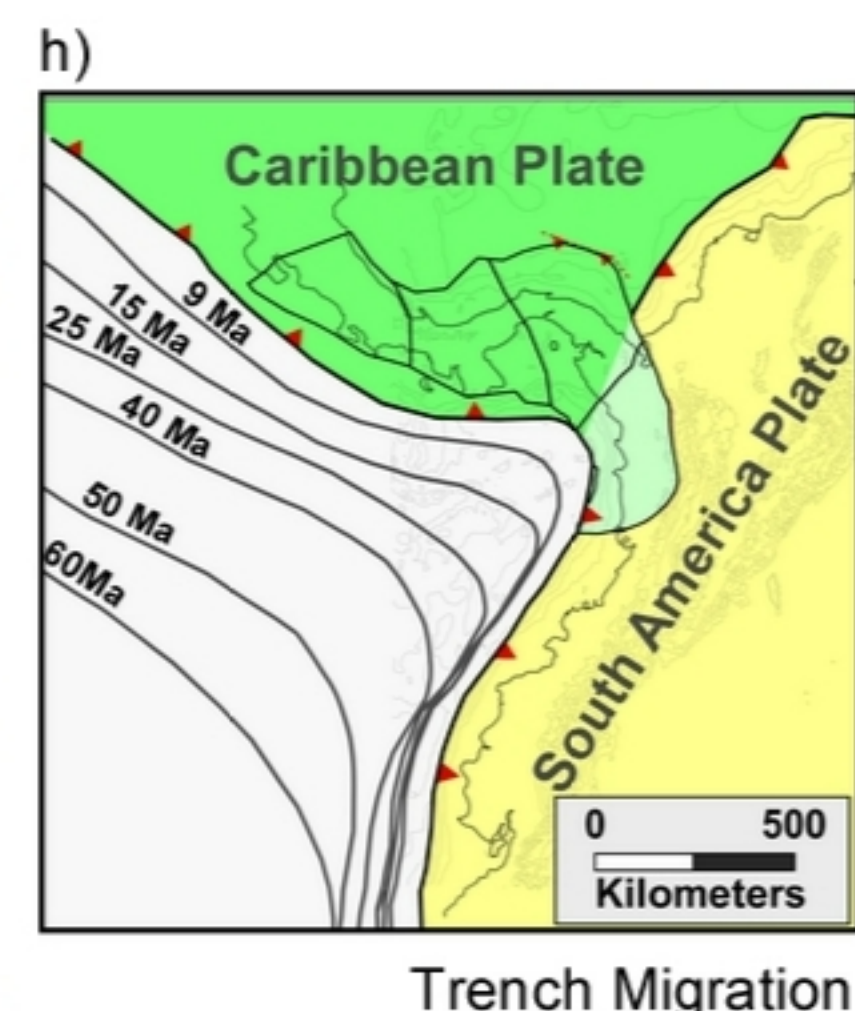
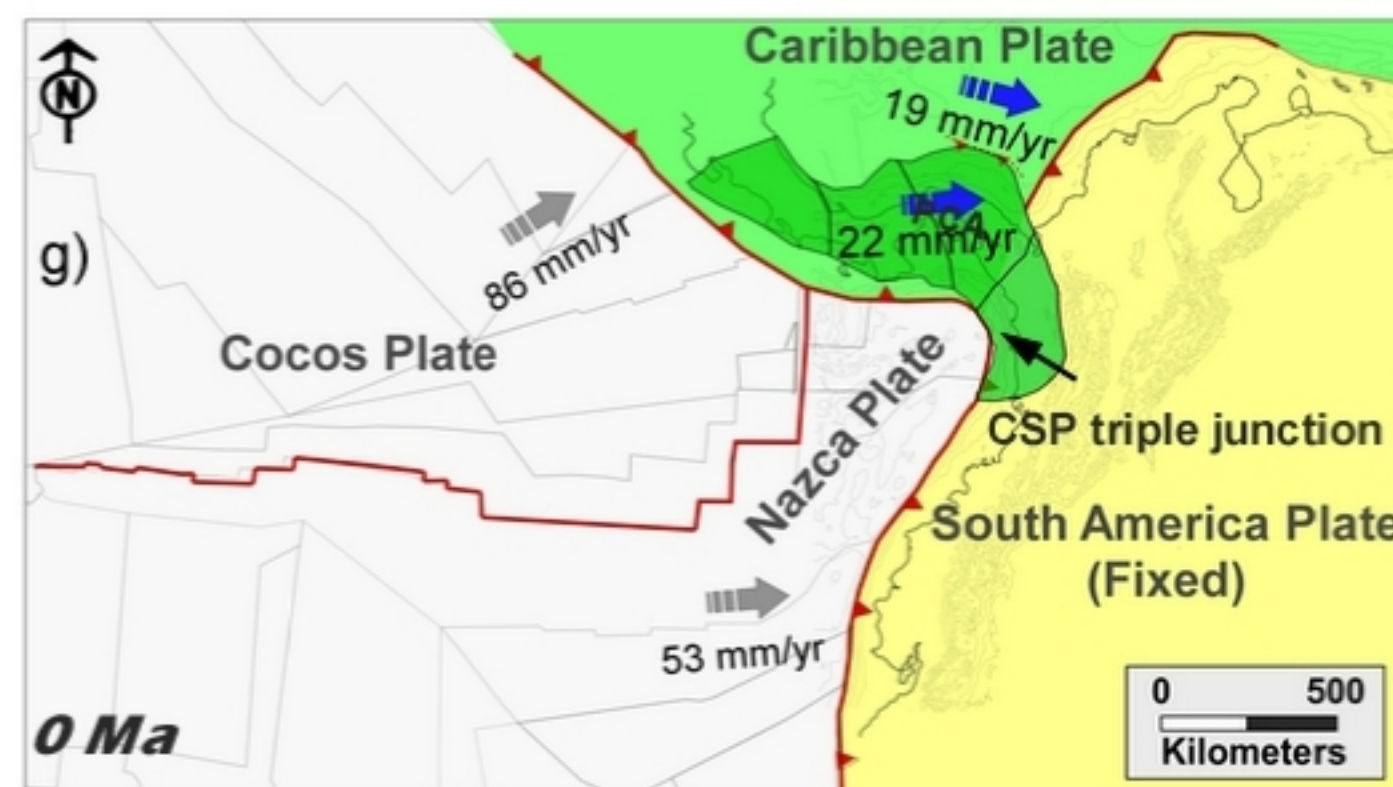
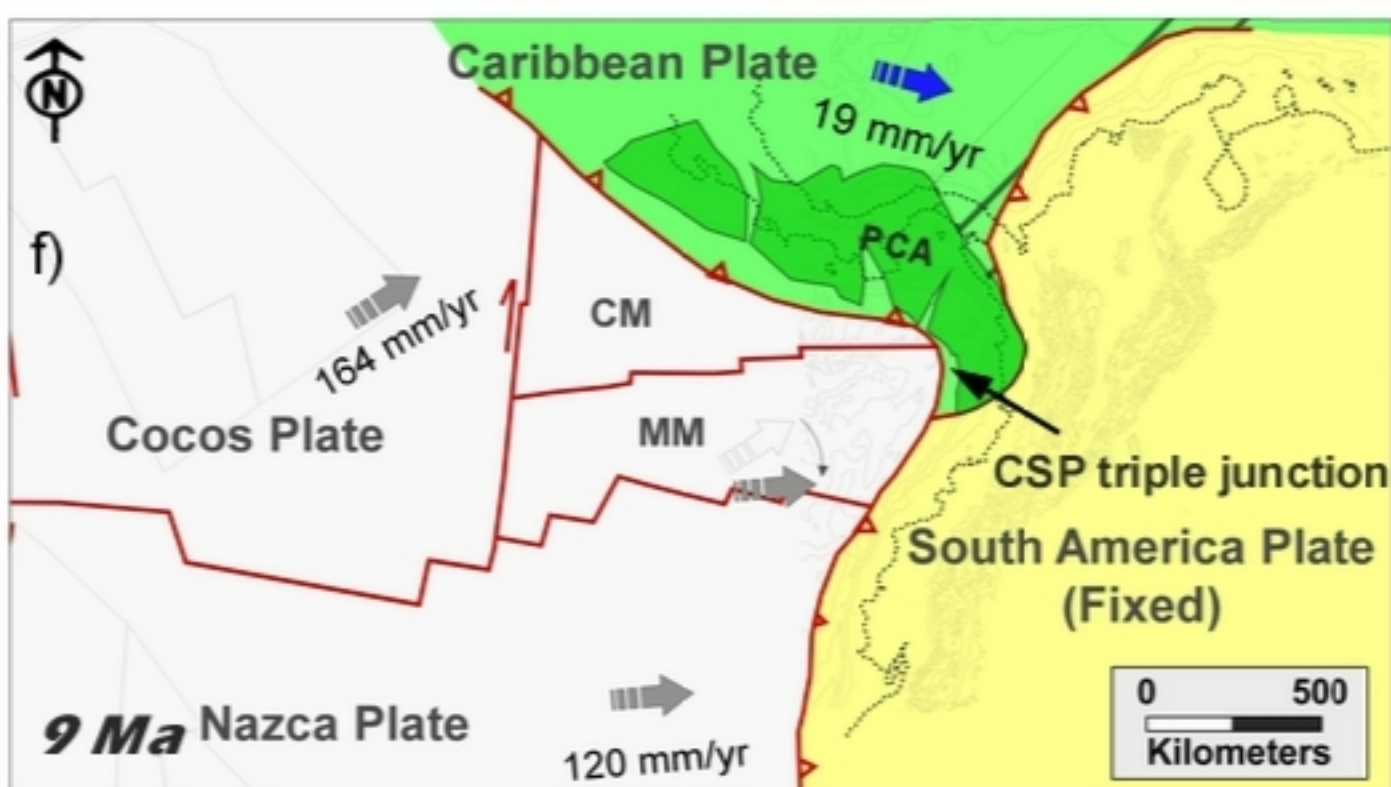
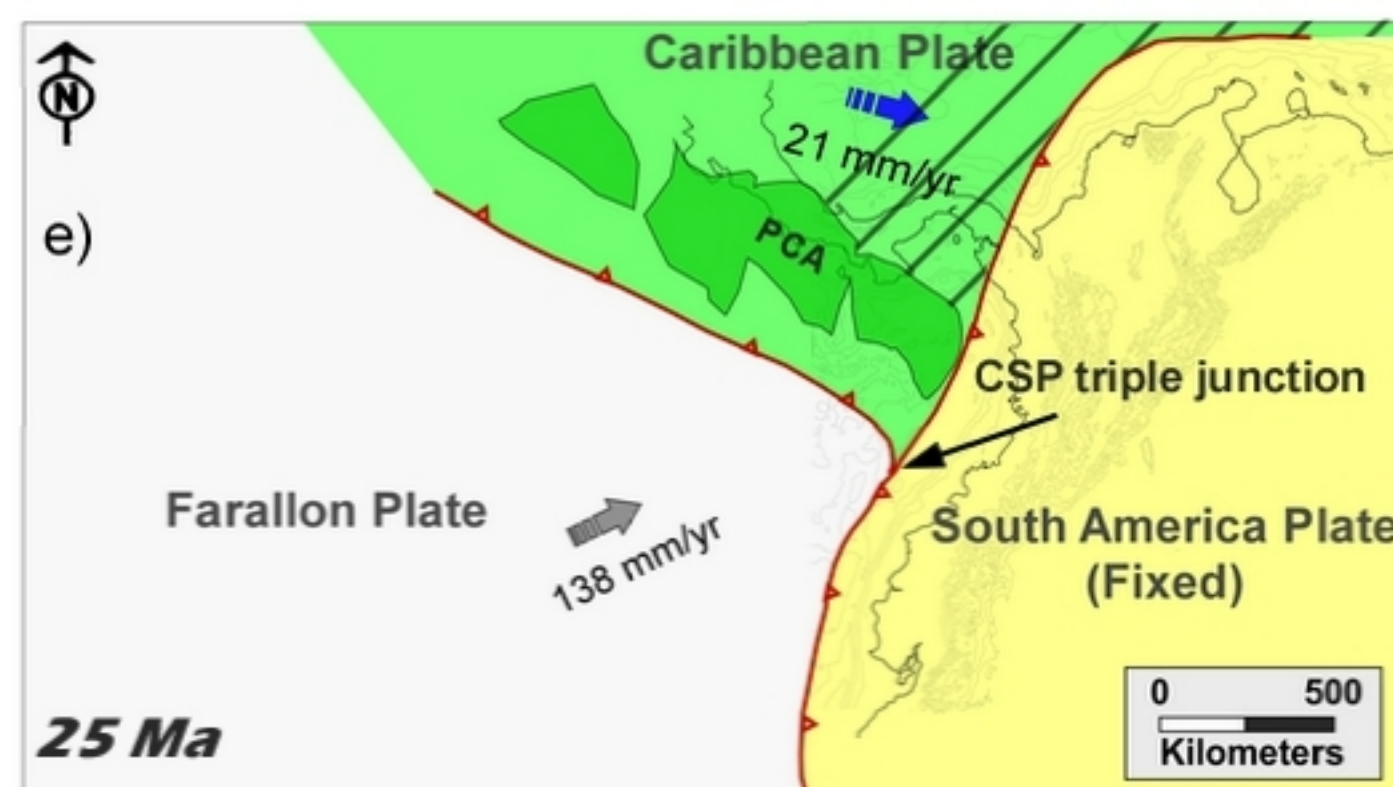
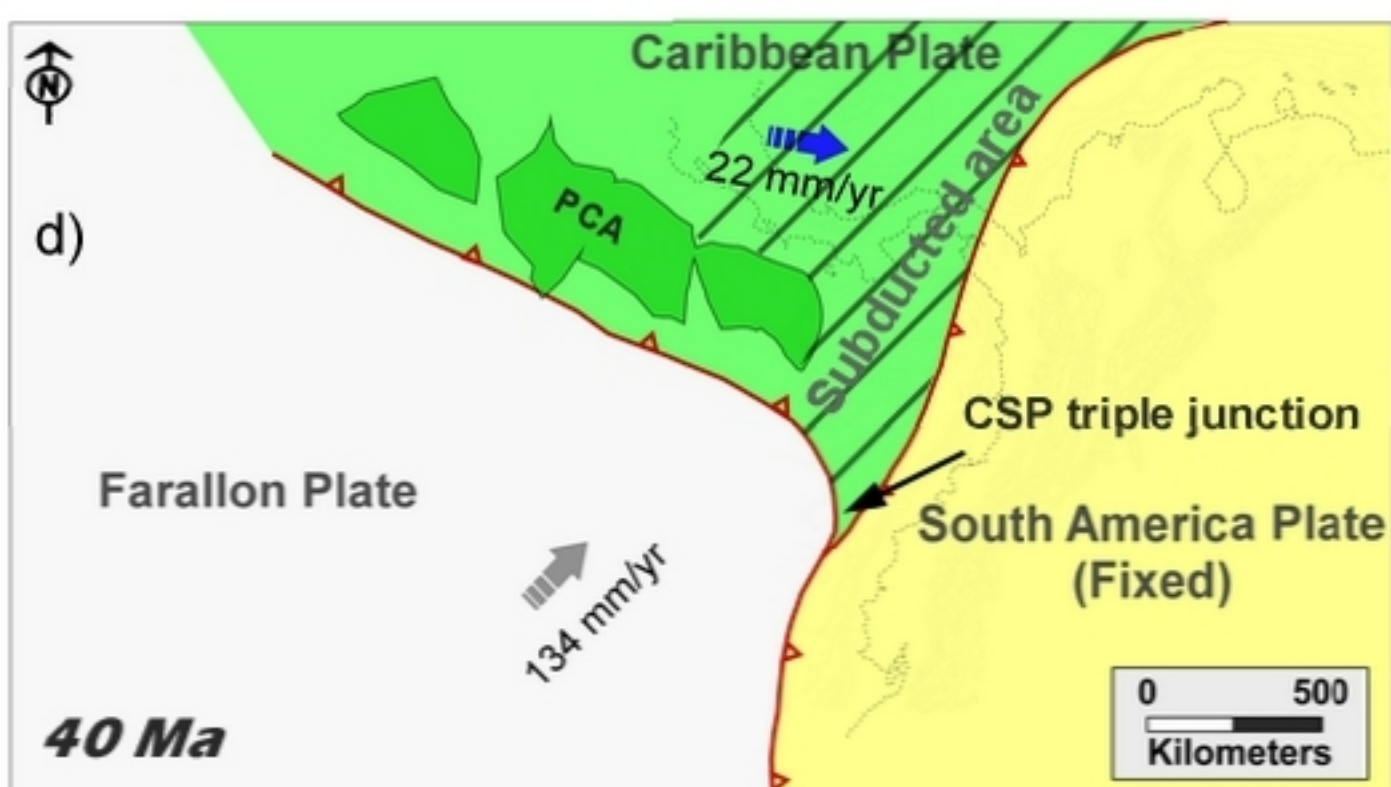
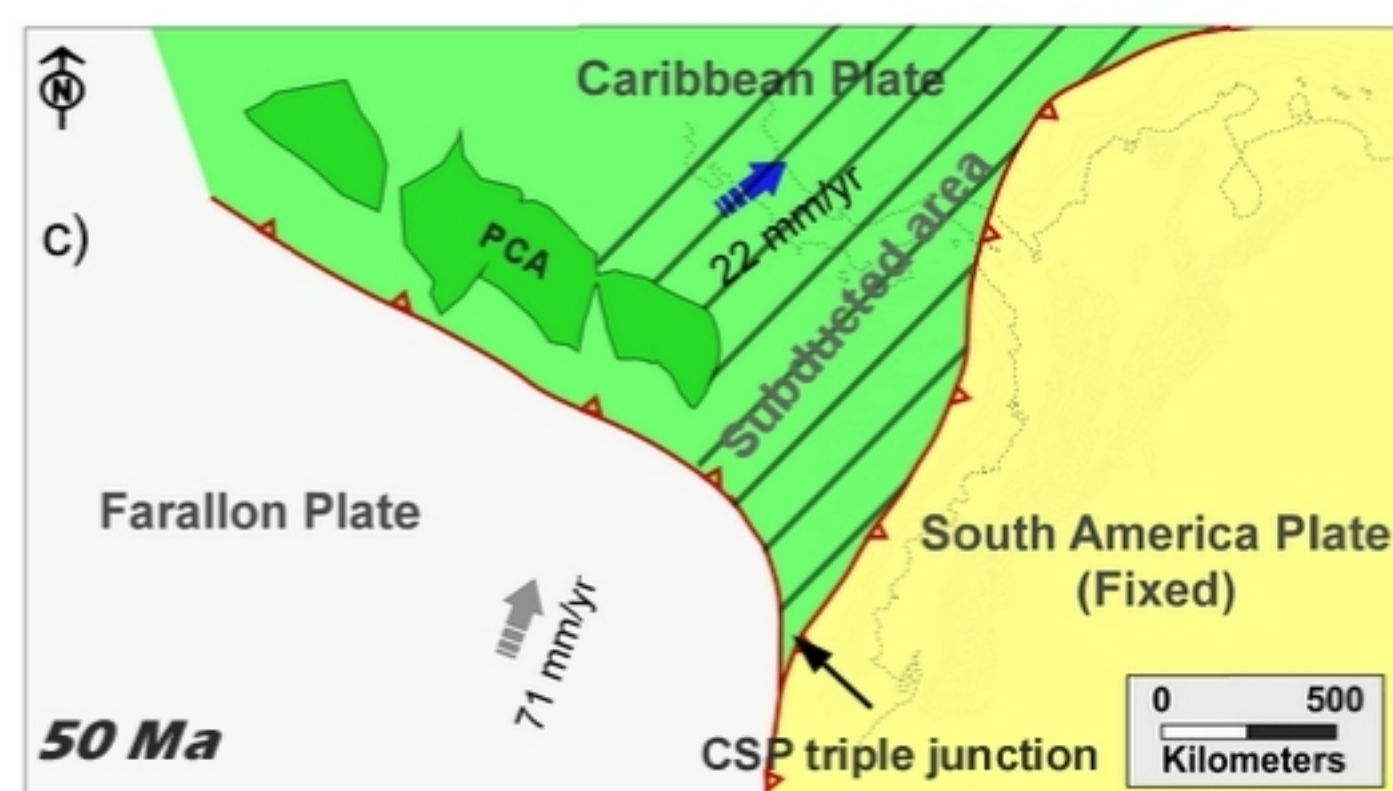
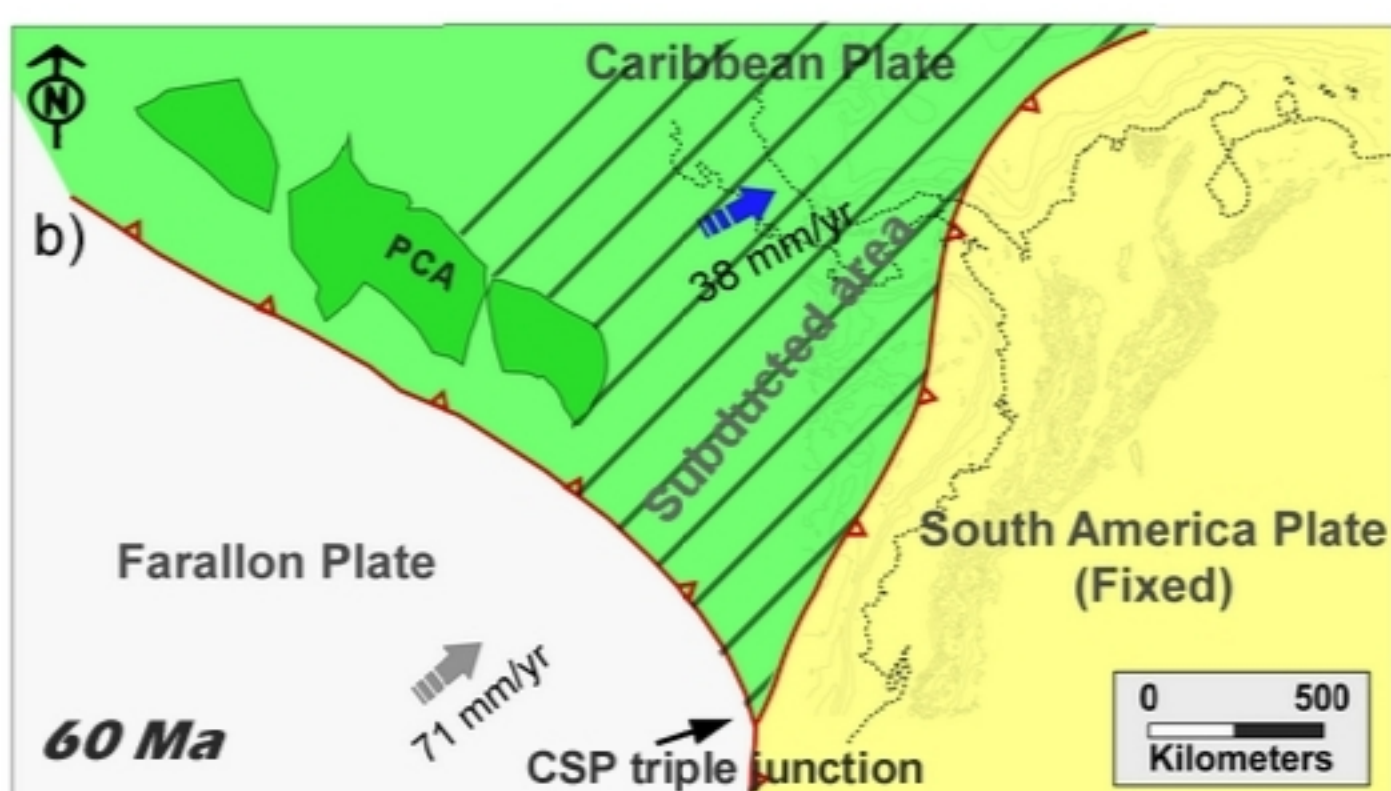
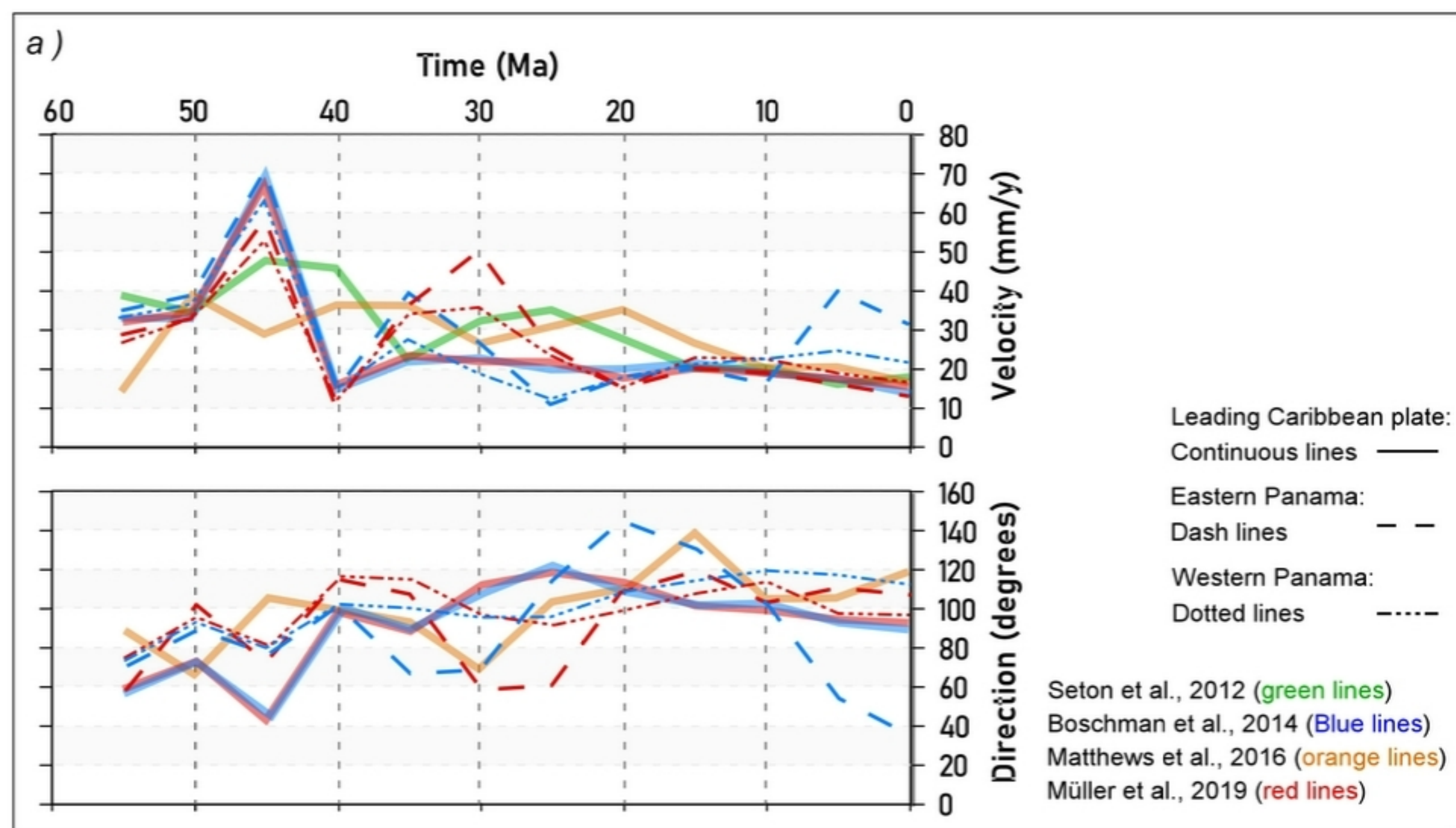
Previous models.



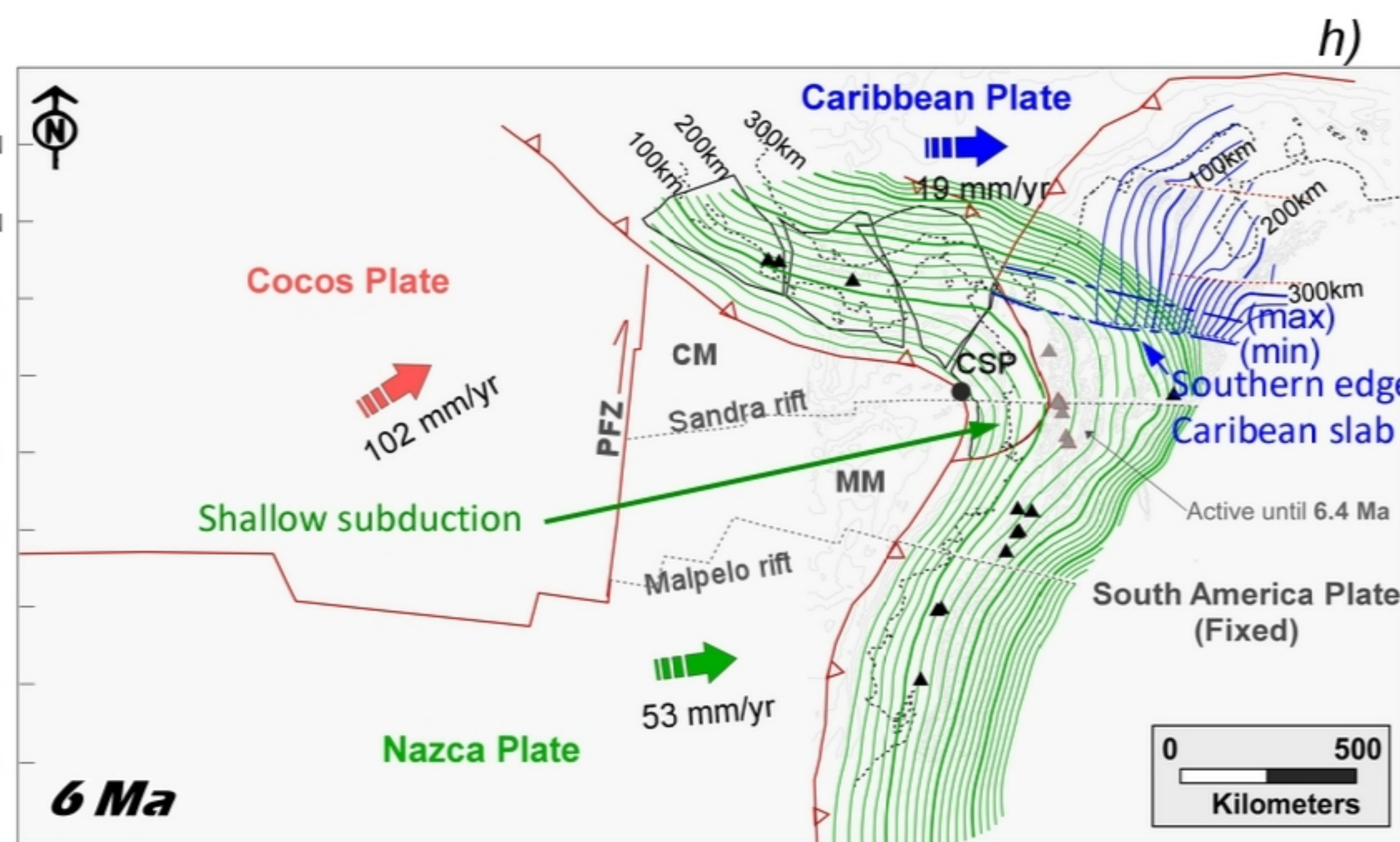
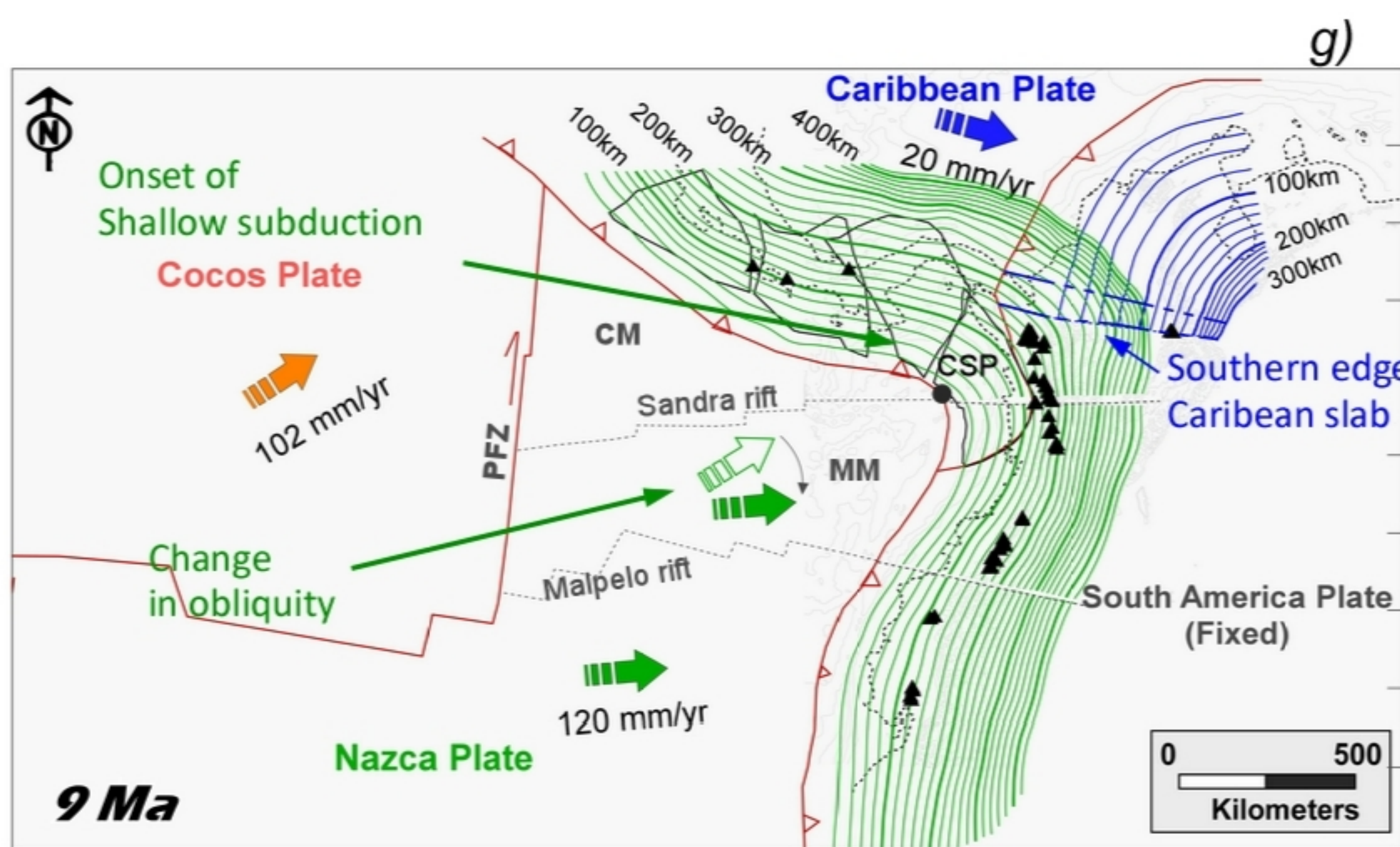
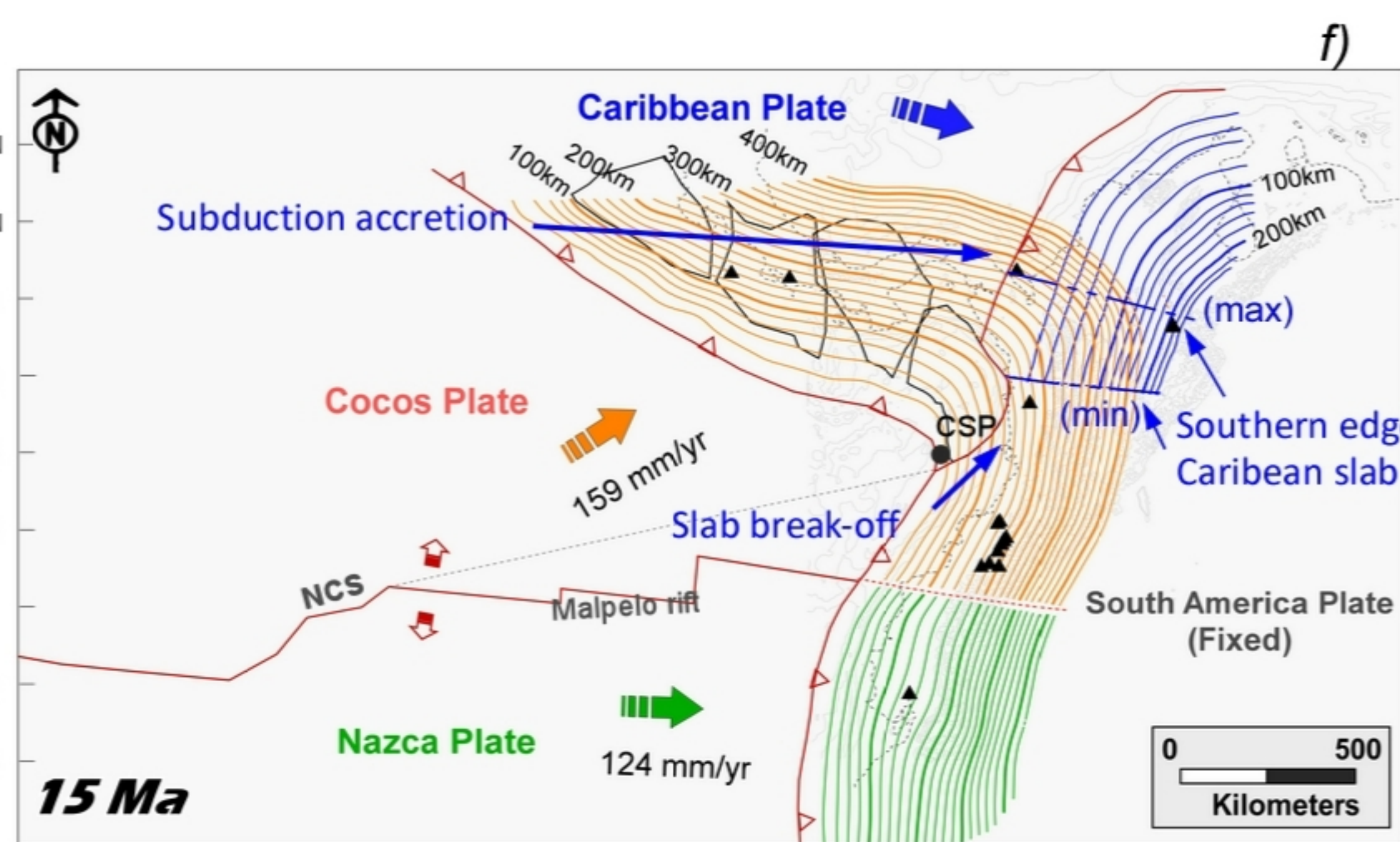
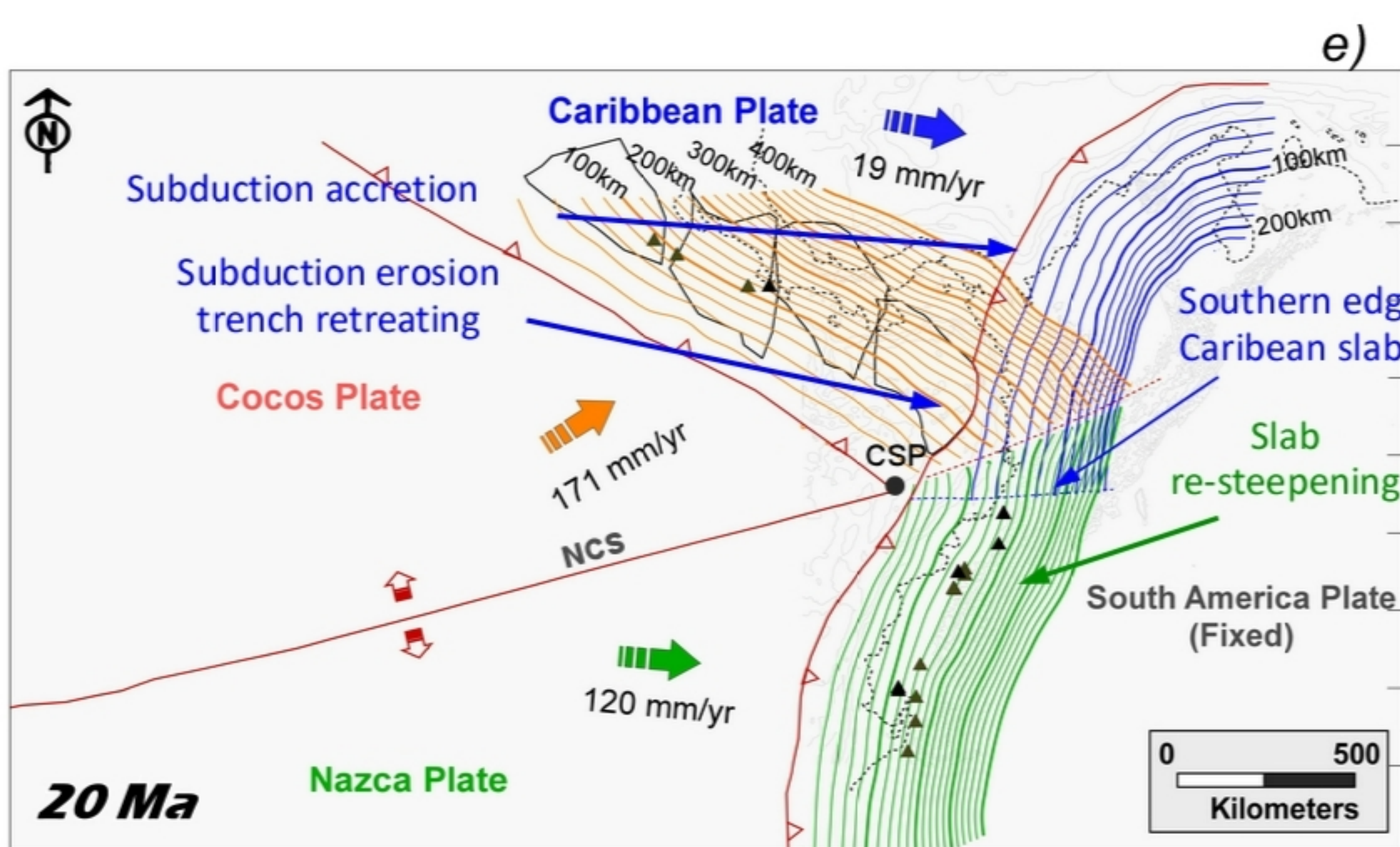
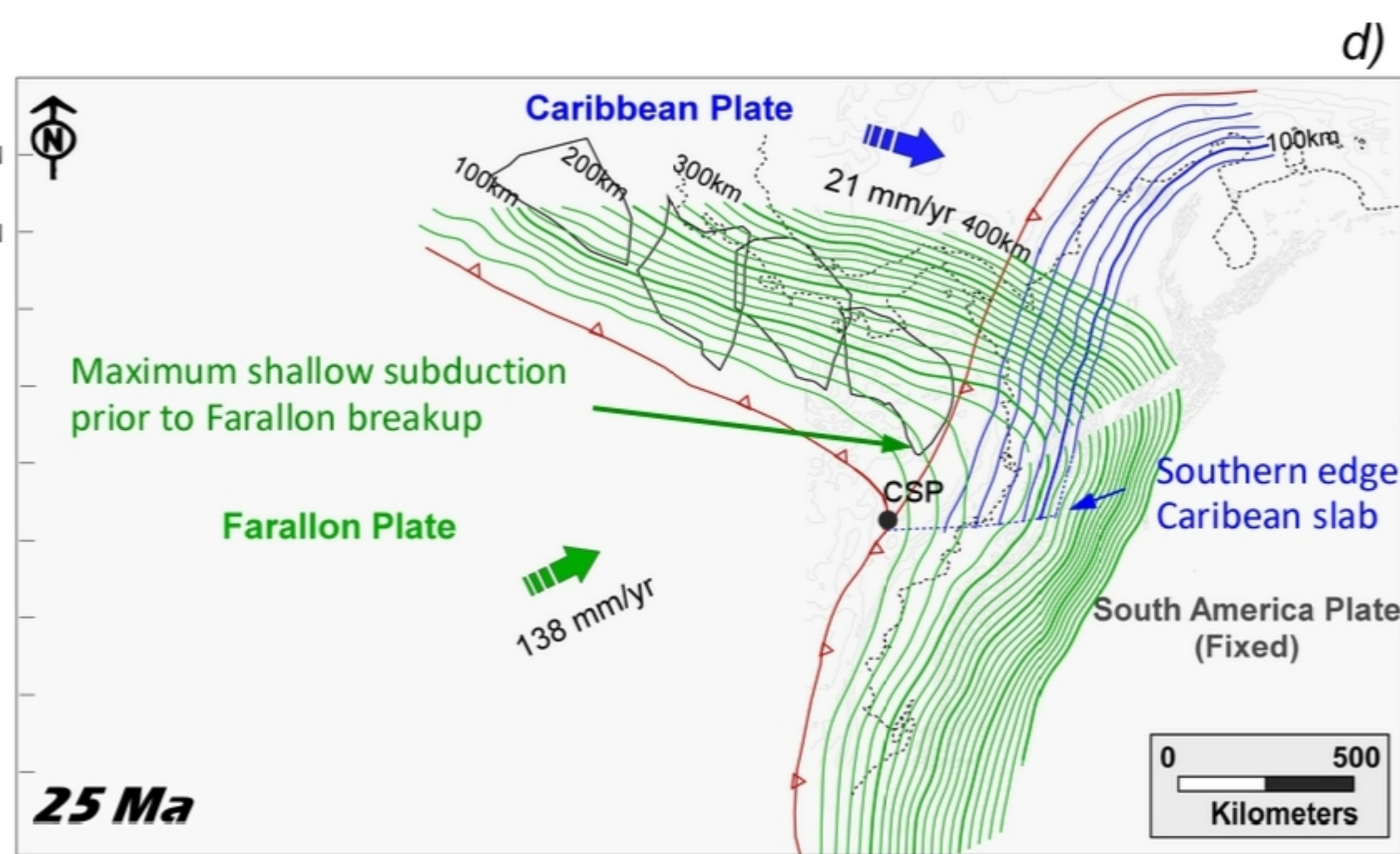
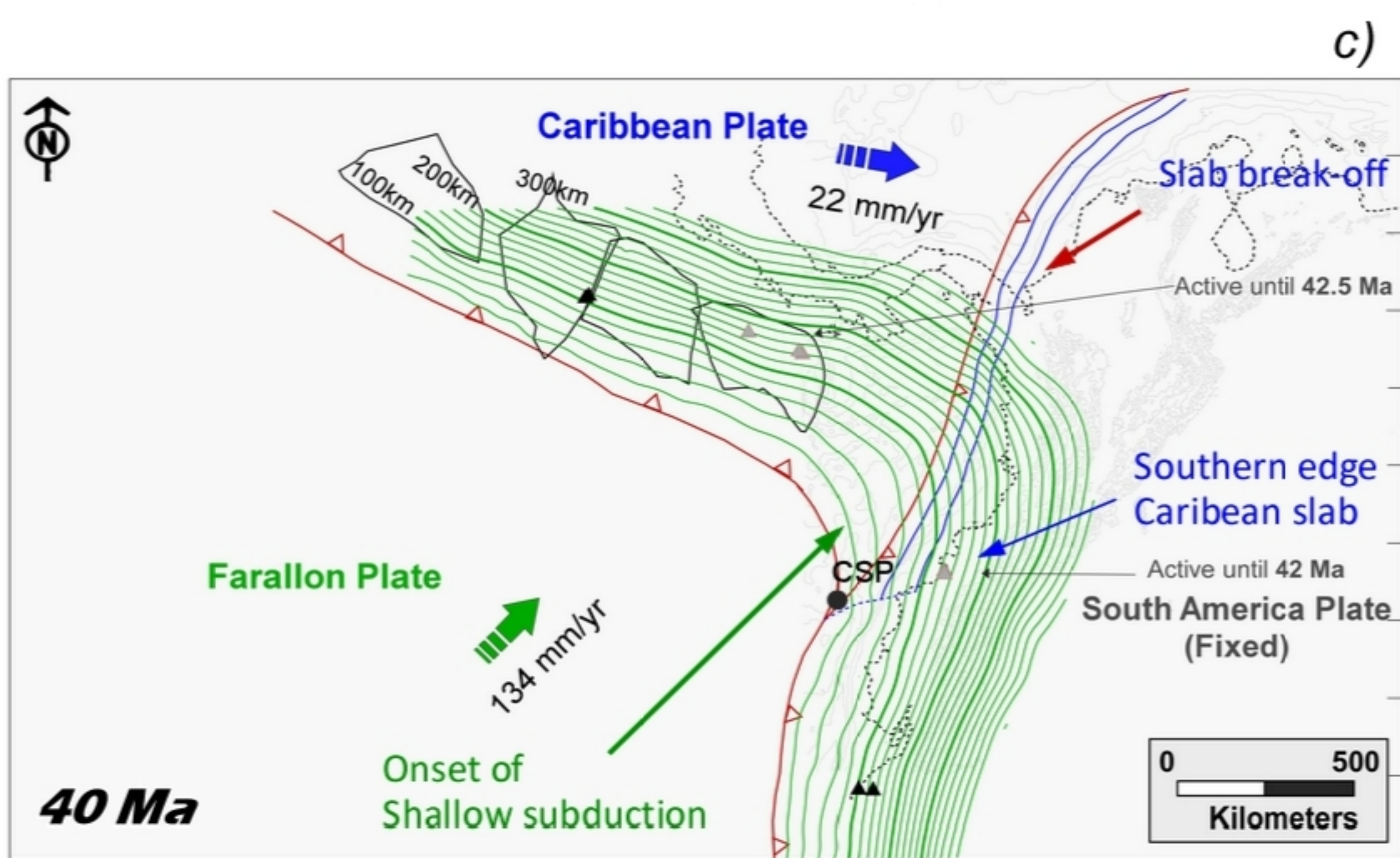
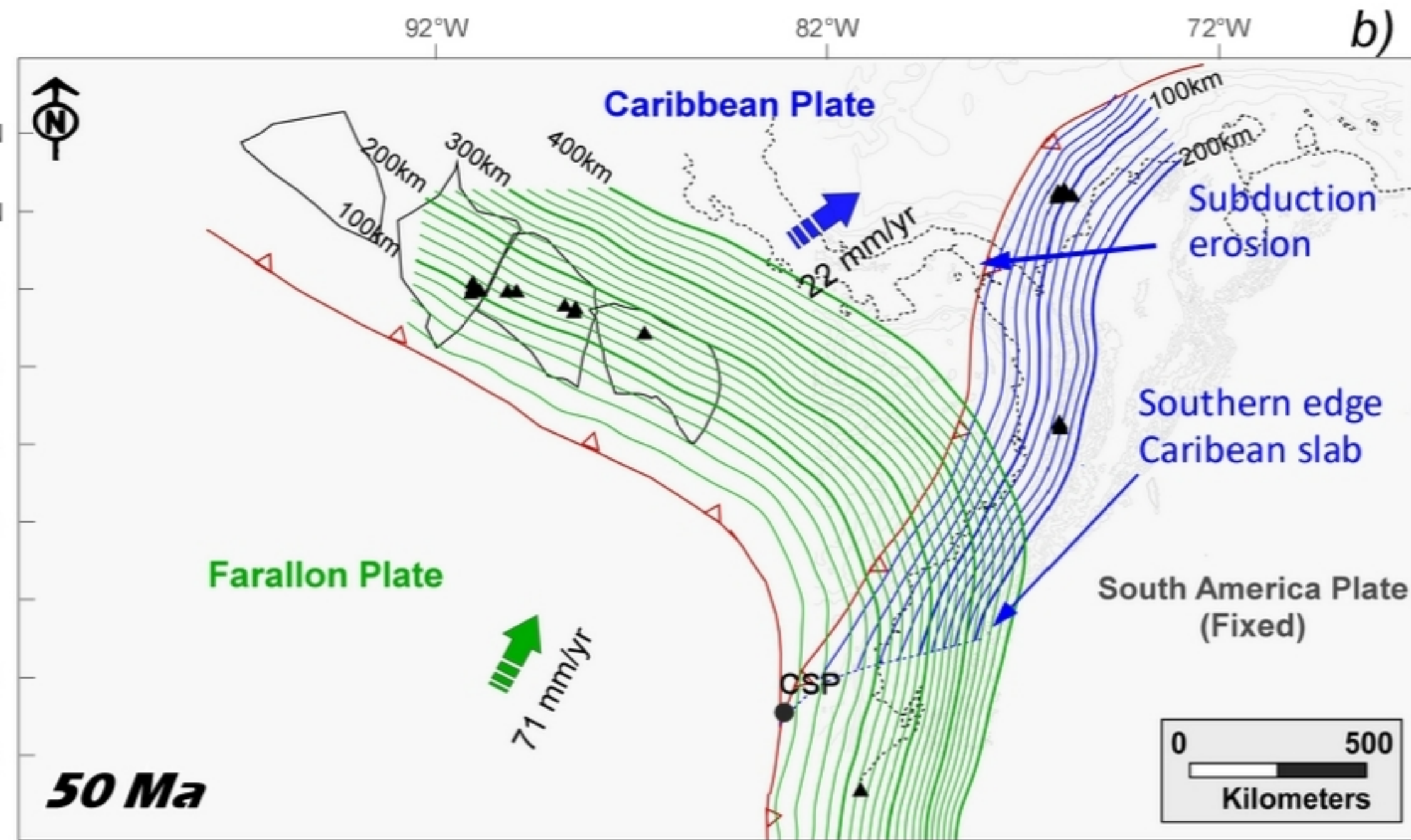
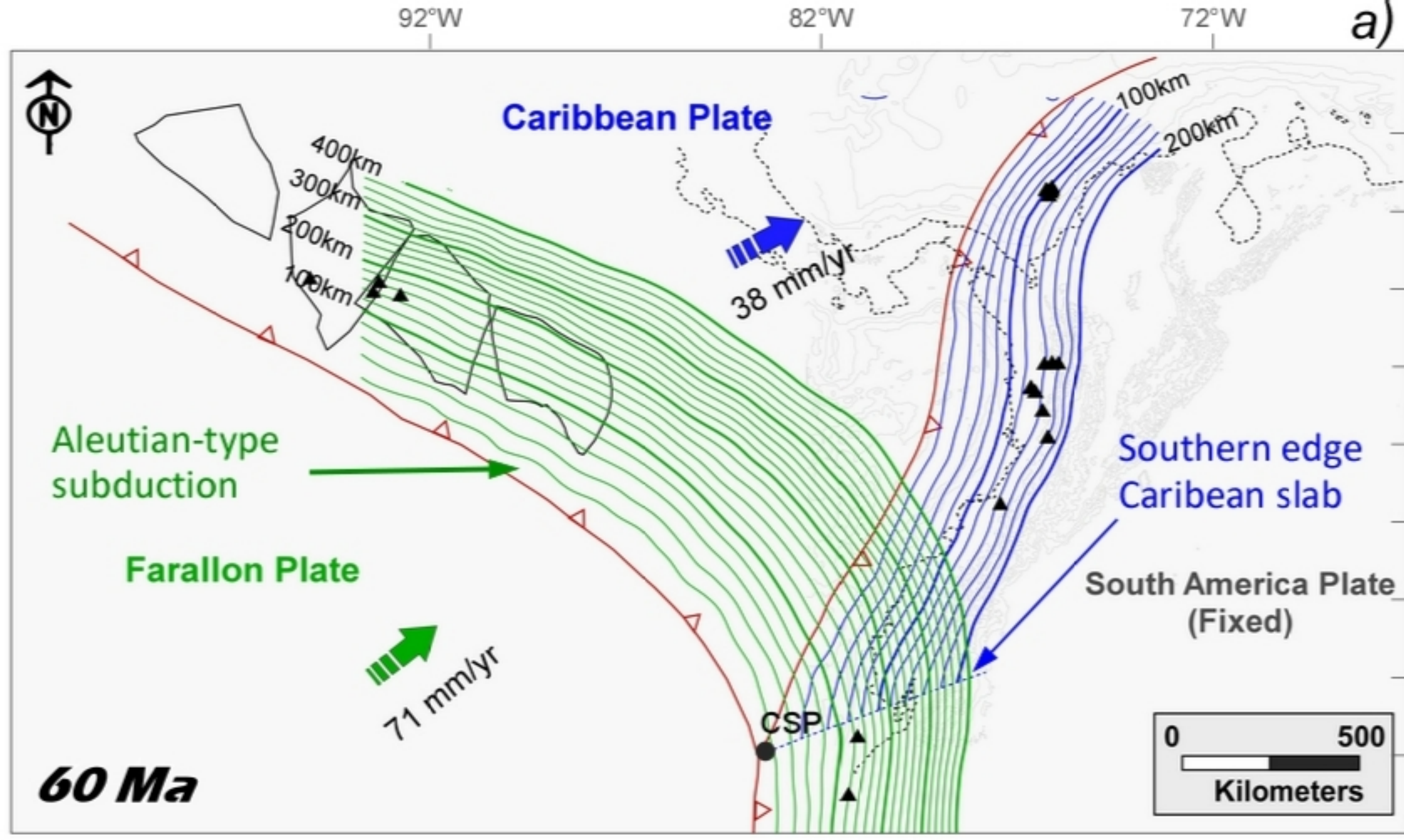
Paleotectonic reconstruction Nazca-Cocos plate boundary.



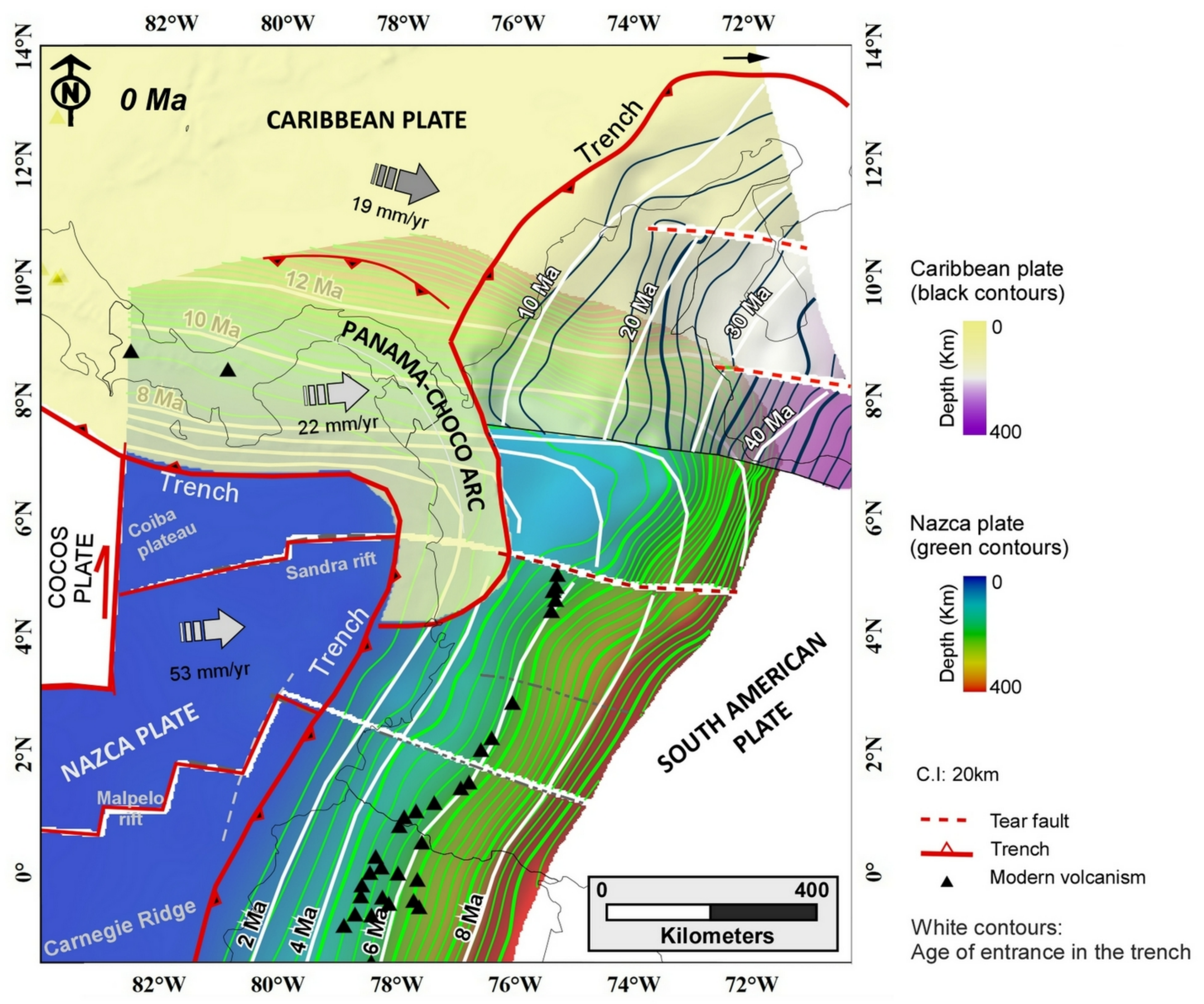
Paleotectonic reconstruction southwestern Caribbean plate.



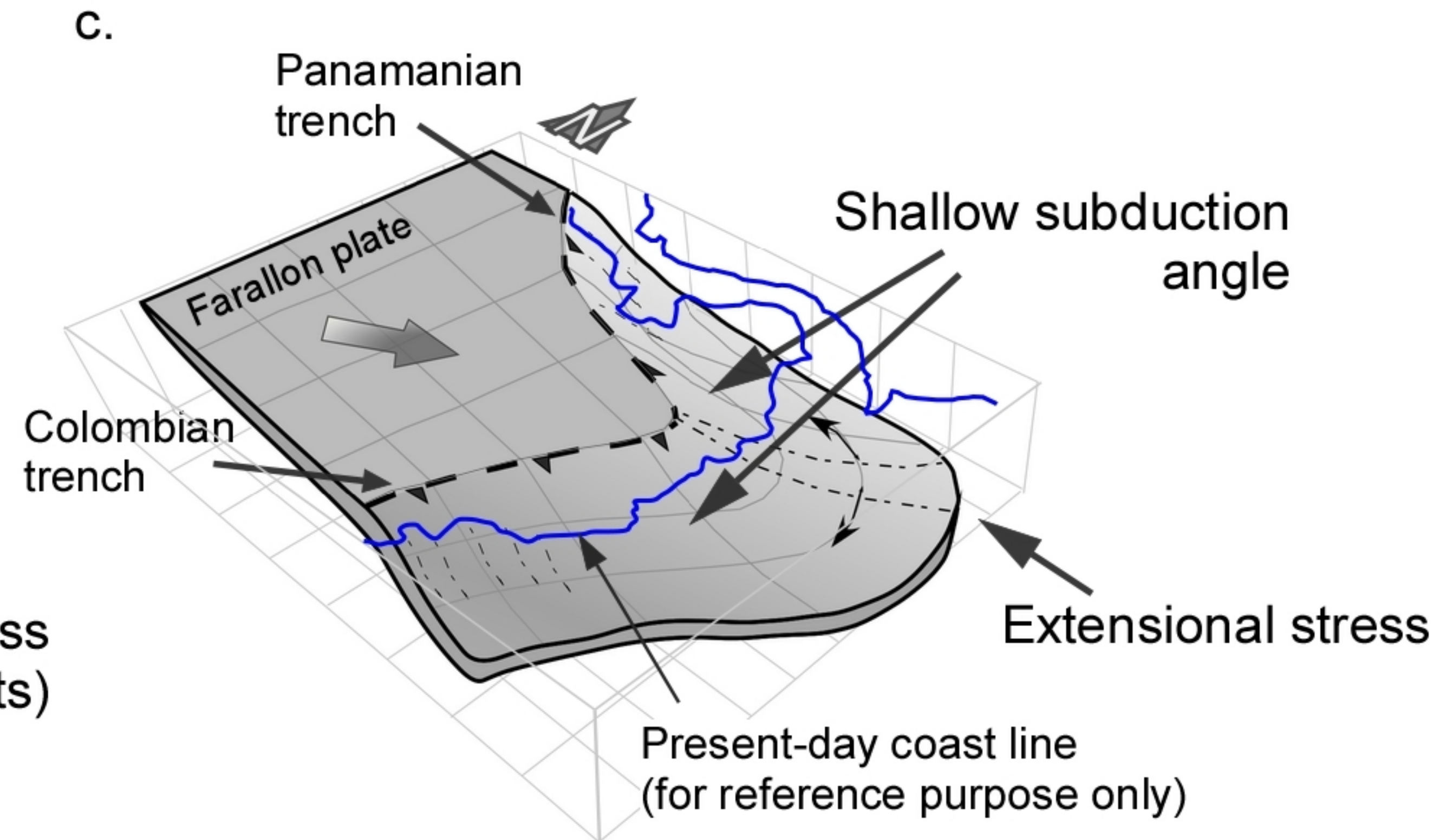
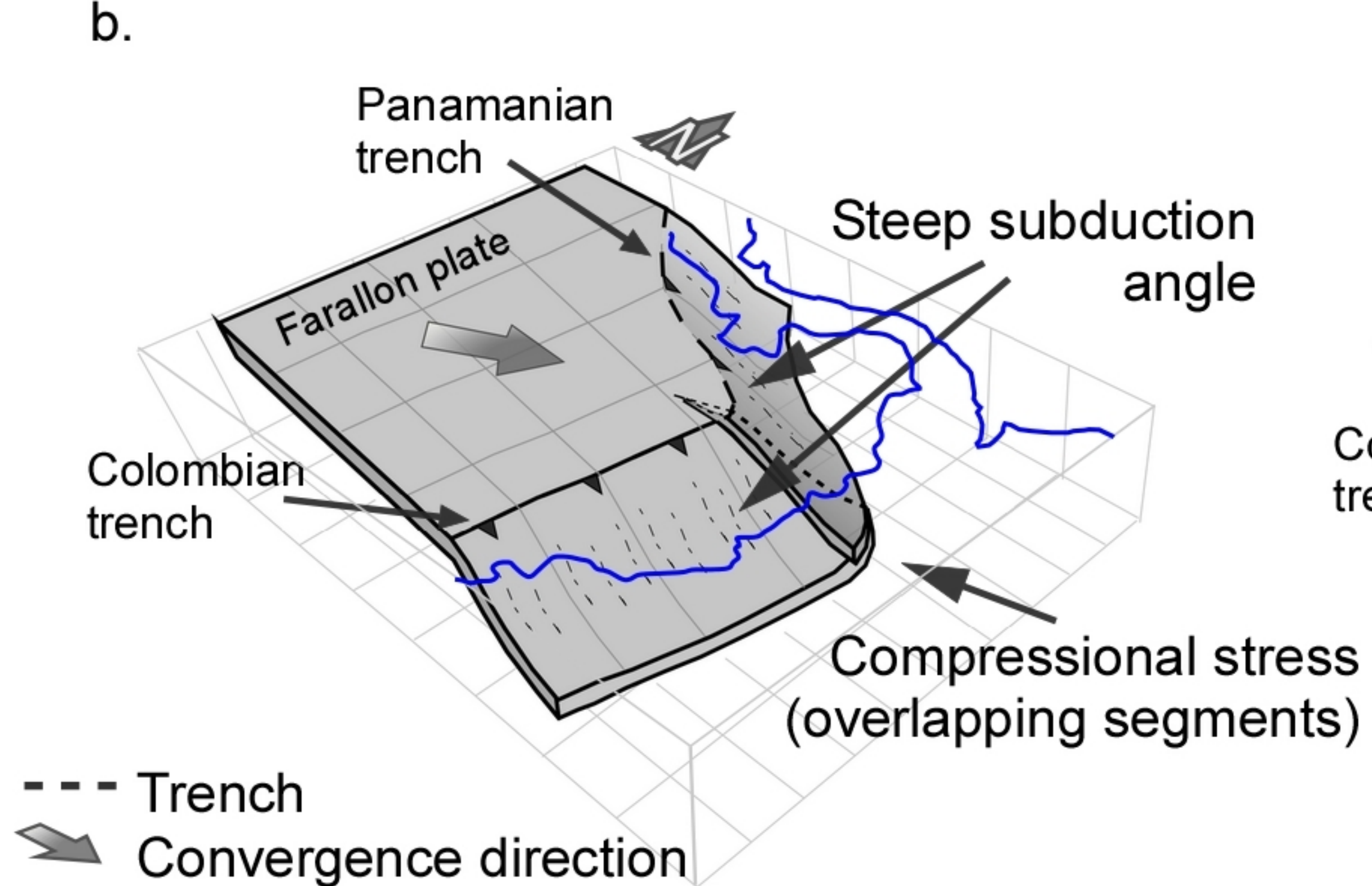
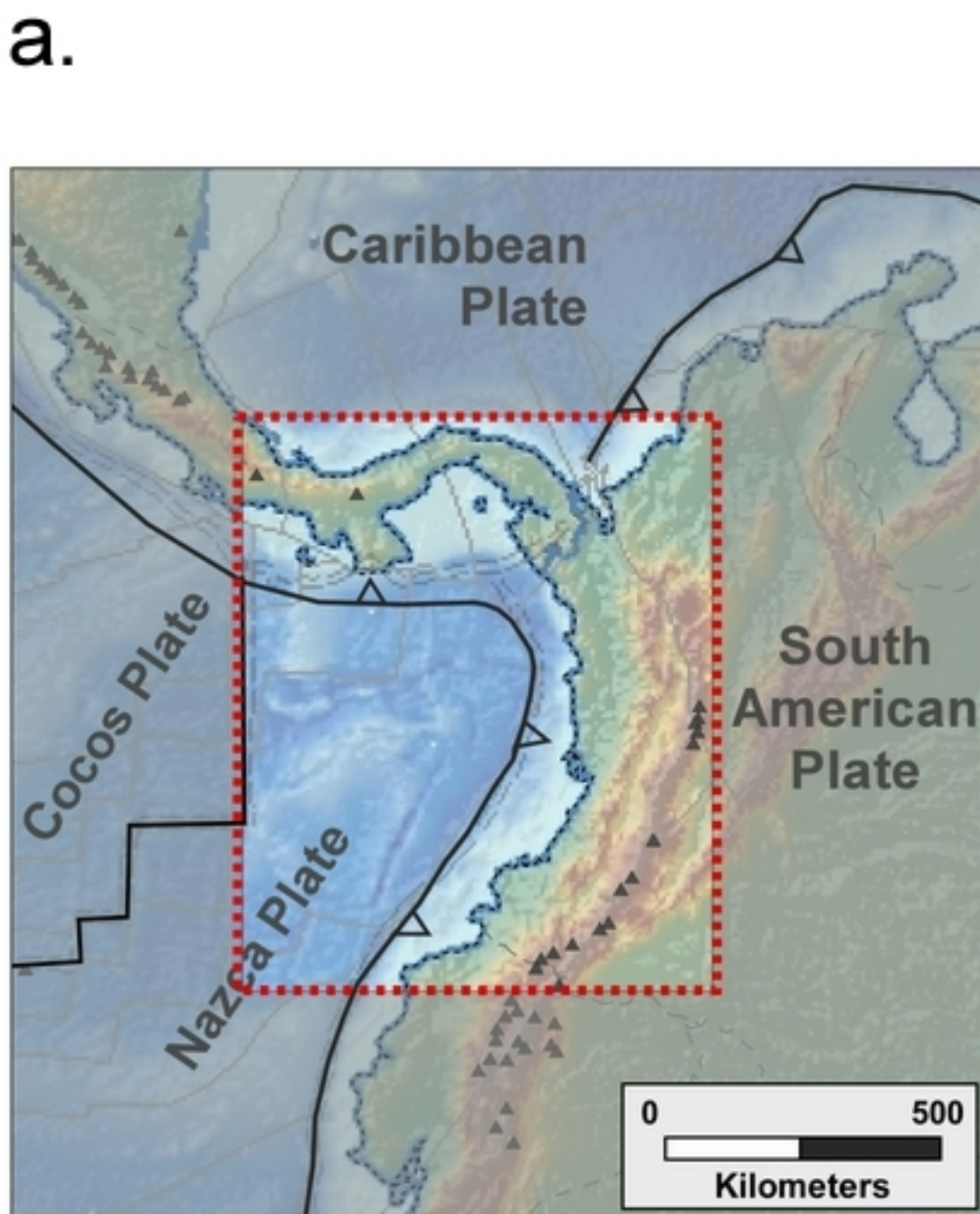
Reconstruction of the northwestern South America and Panama subduction systems.



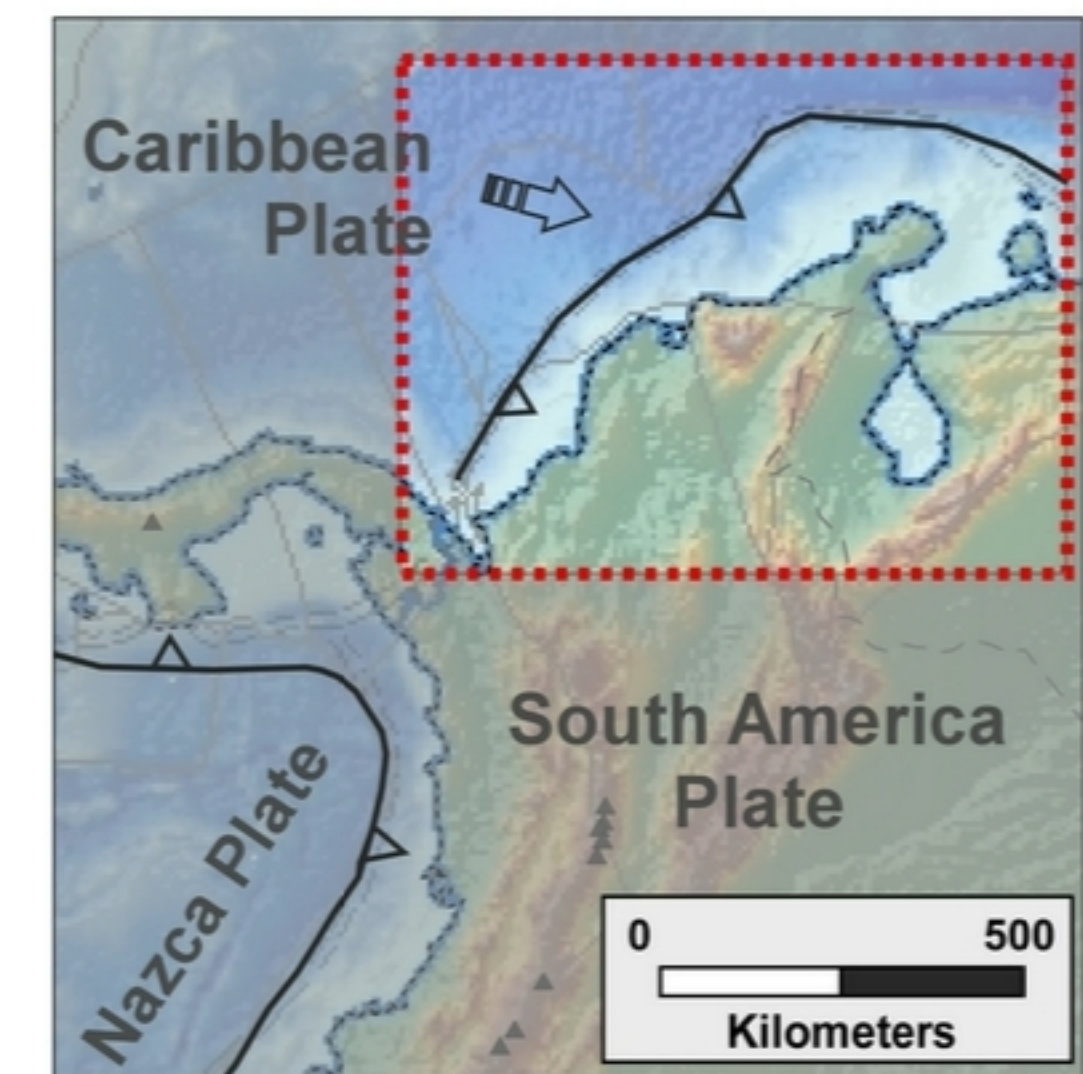
Present-day structural map of the Nazca and Caribbean slabs beneath NWSA.



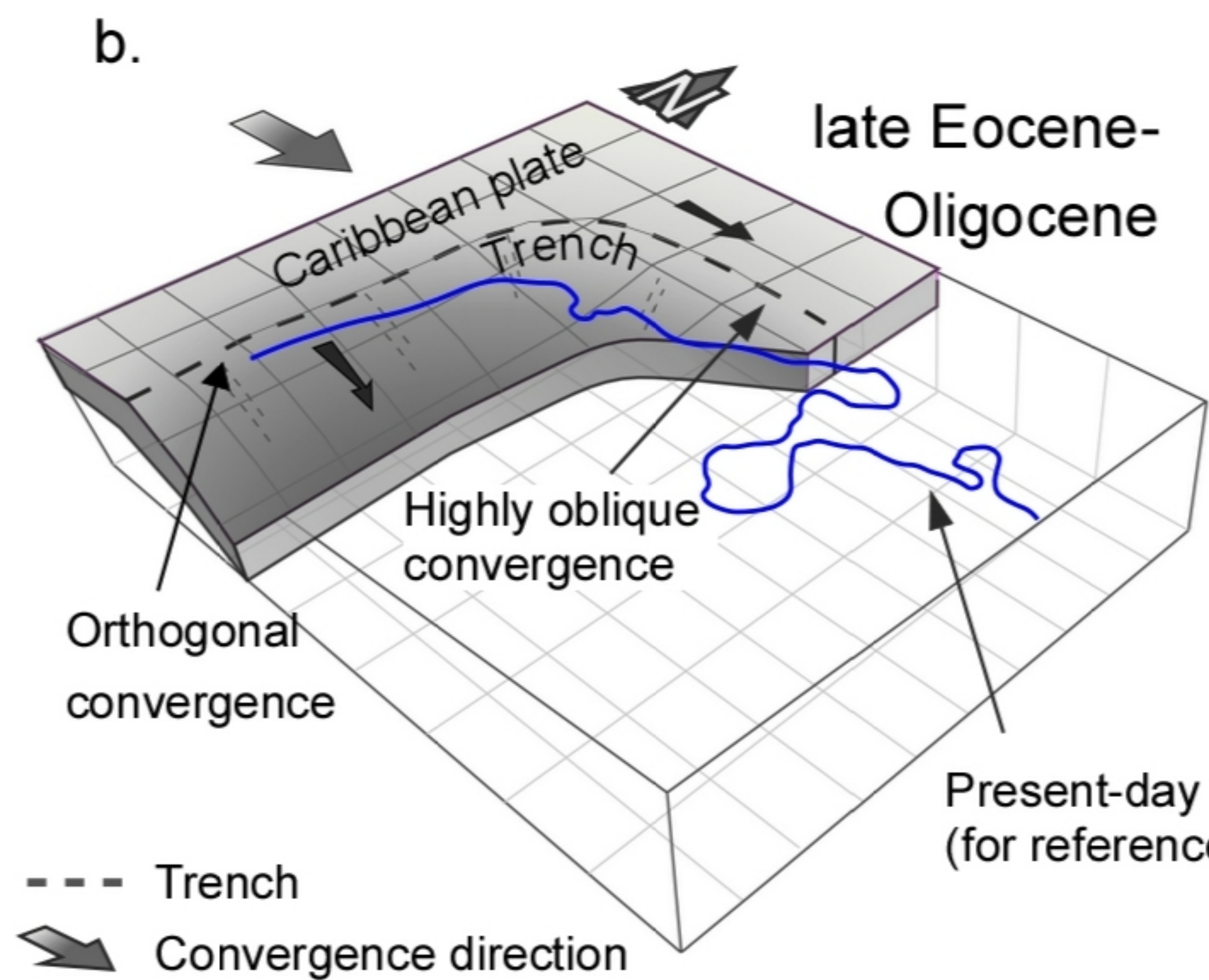
Subduction geometry of a single slab obliquely subducting under two orthogonal margins.



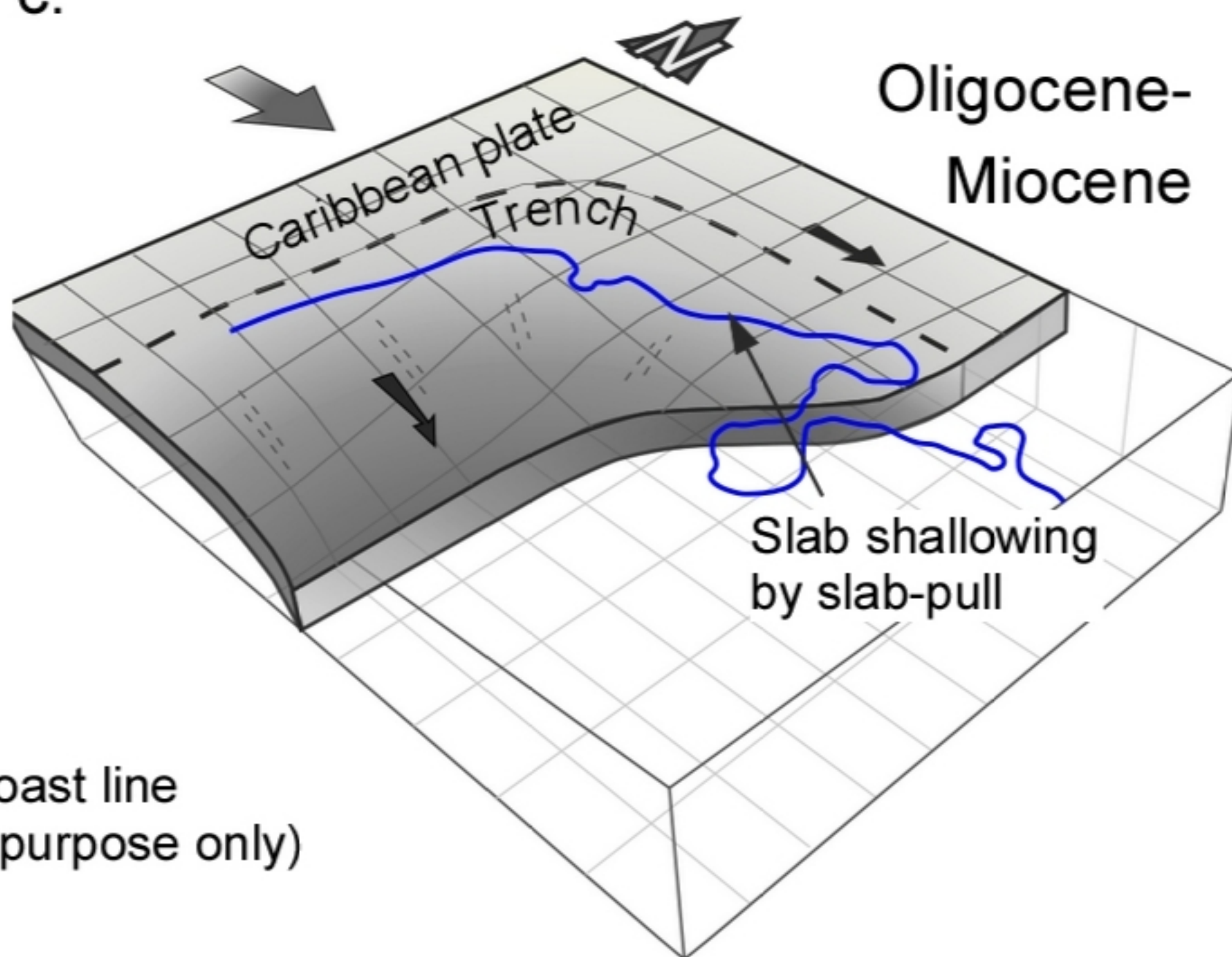
Sketch showing the convergence of the Caribbean plate against NWSA.



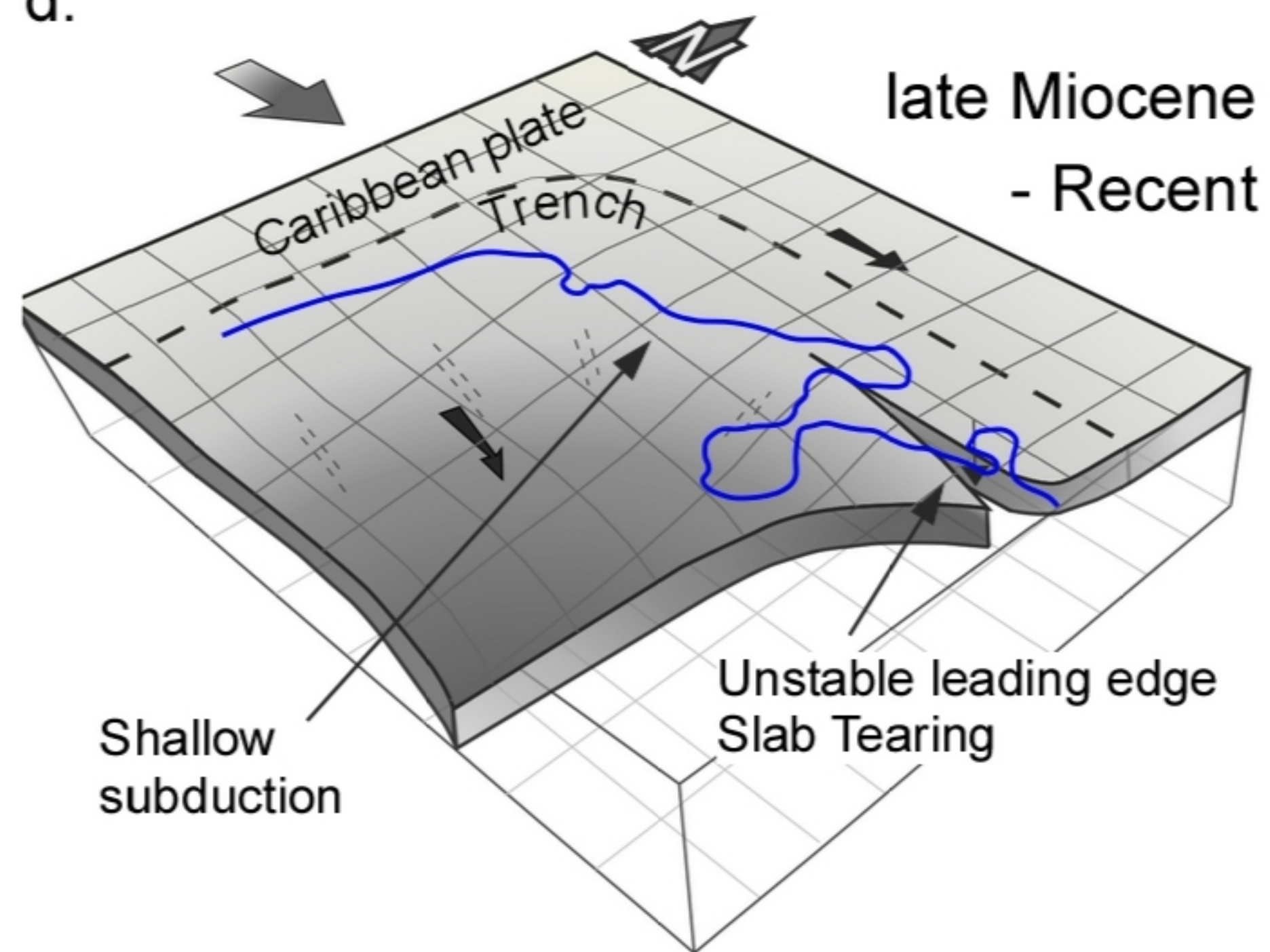
a.



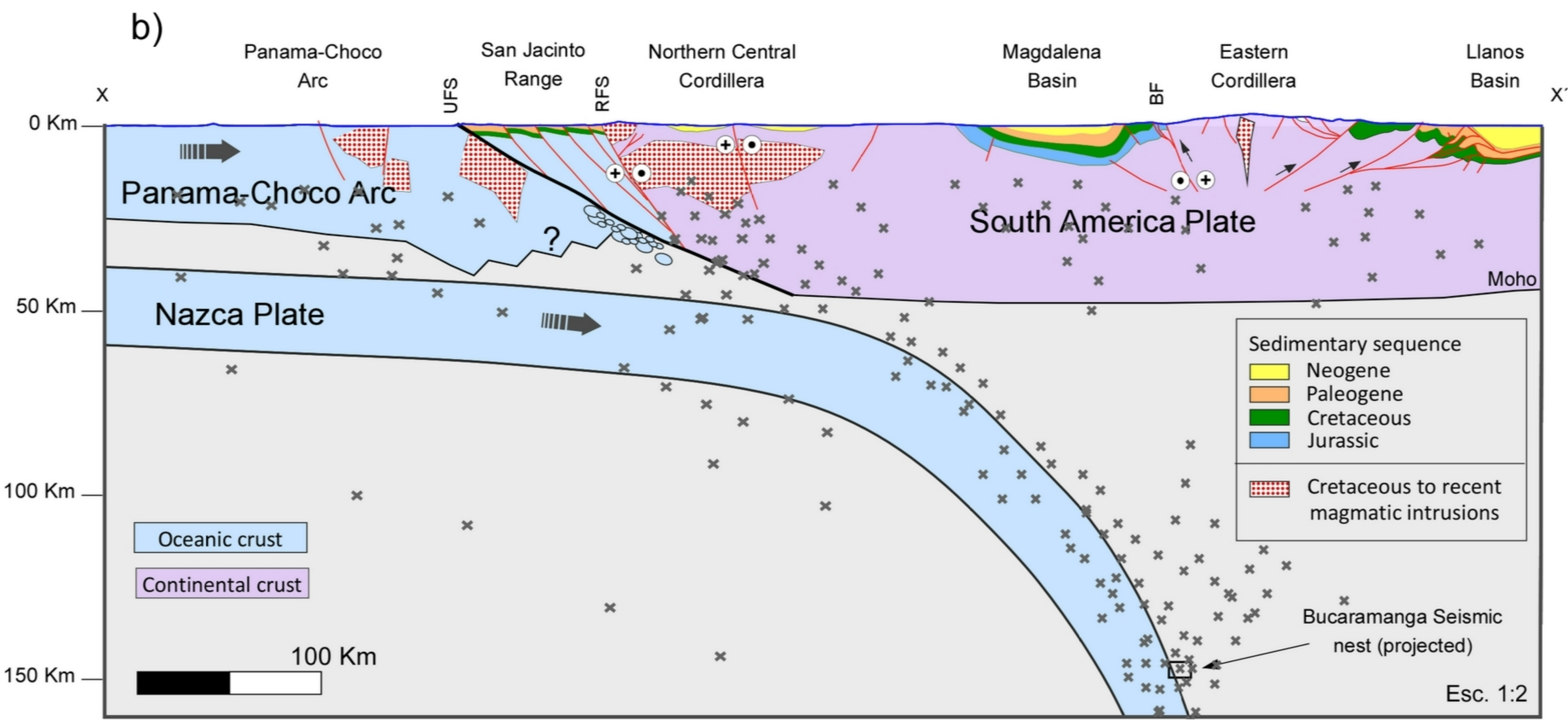
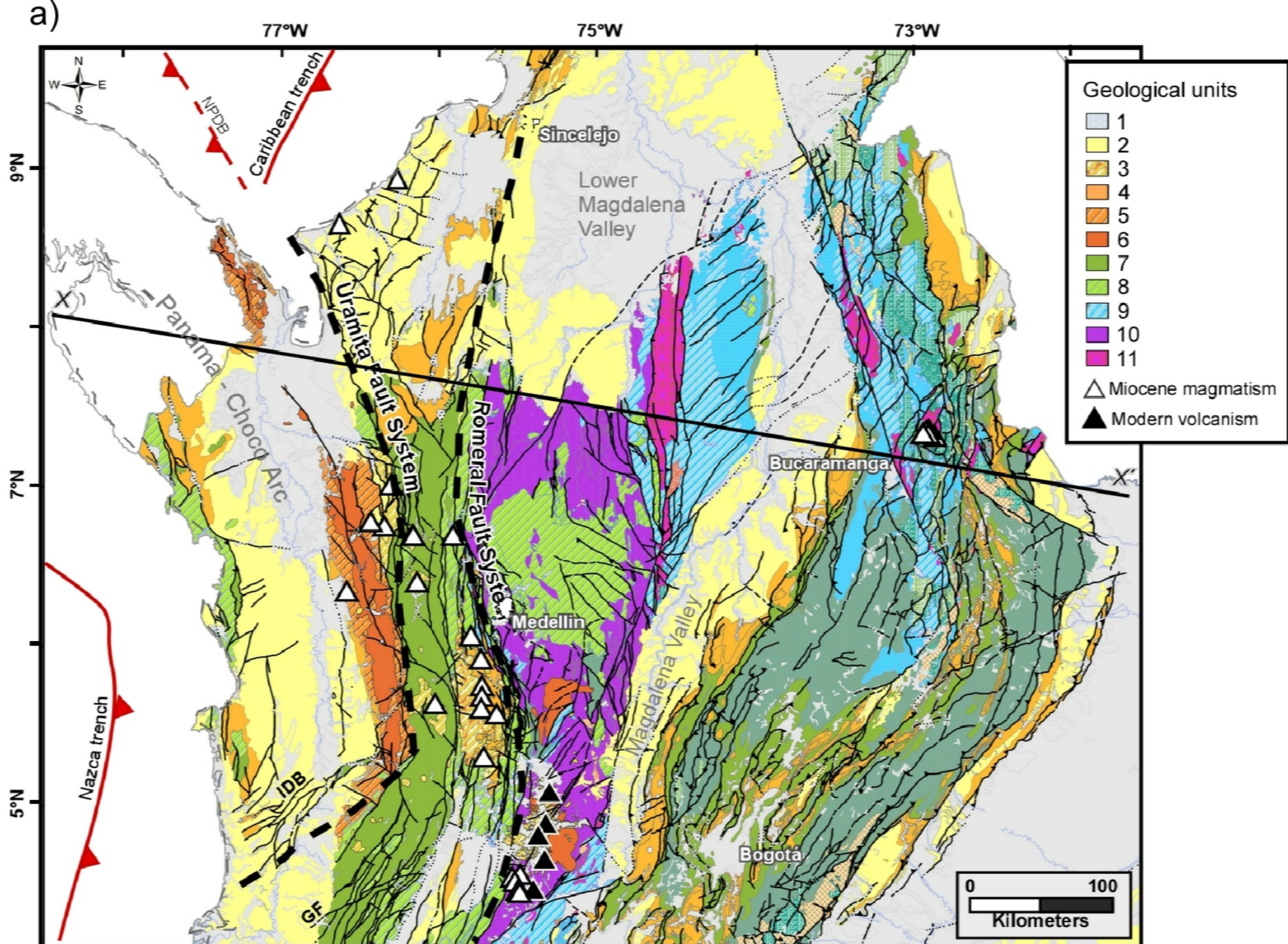
c.



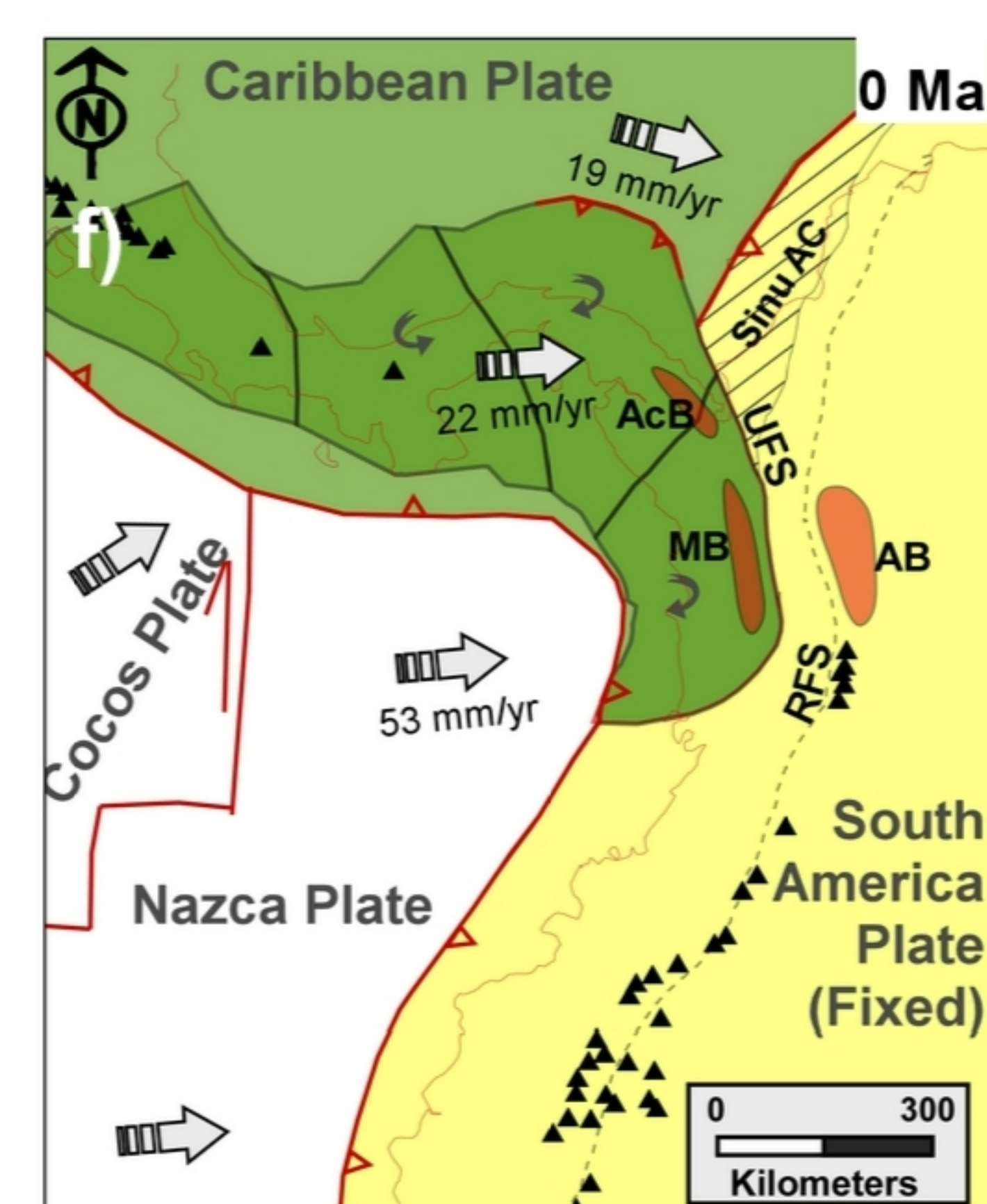
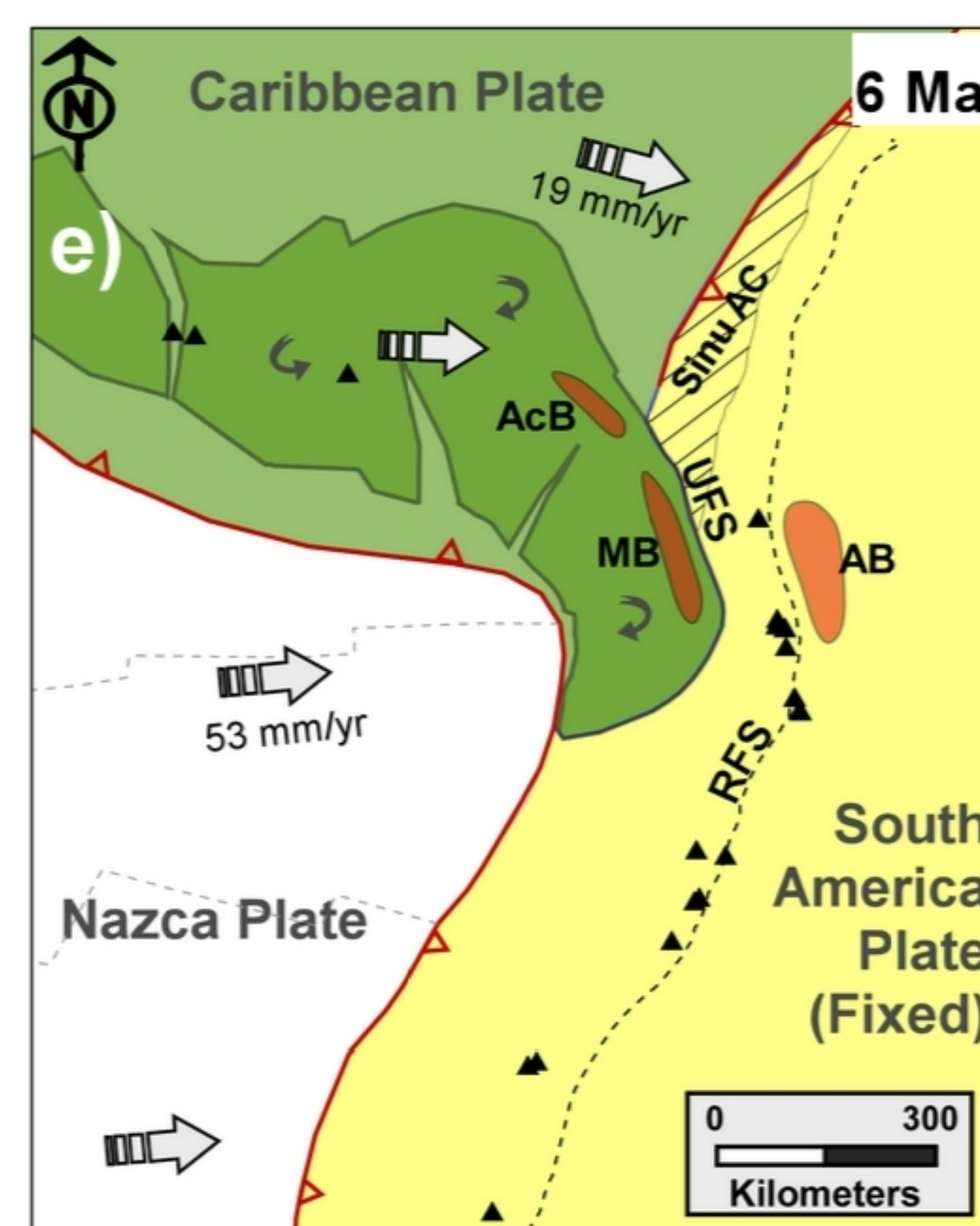
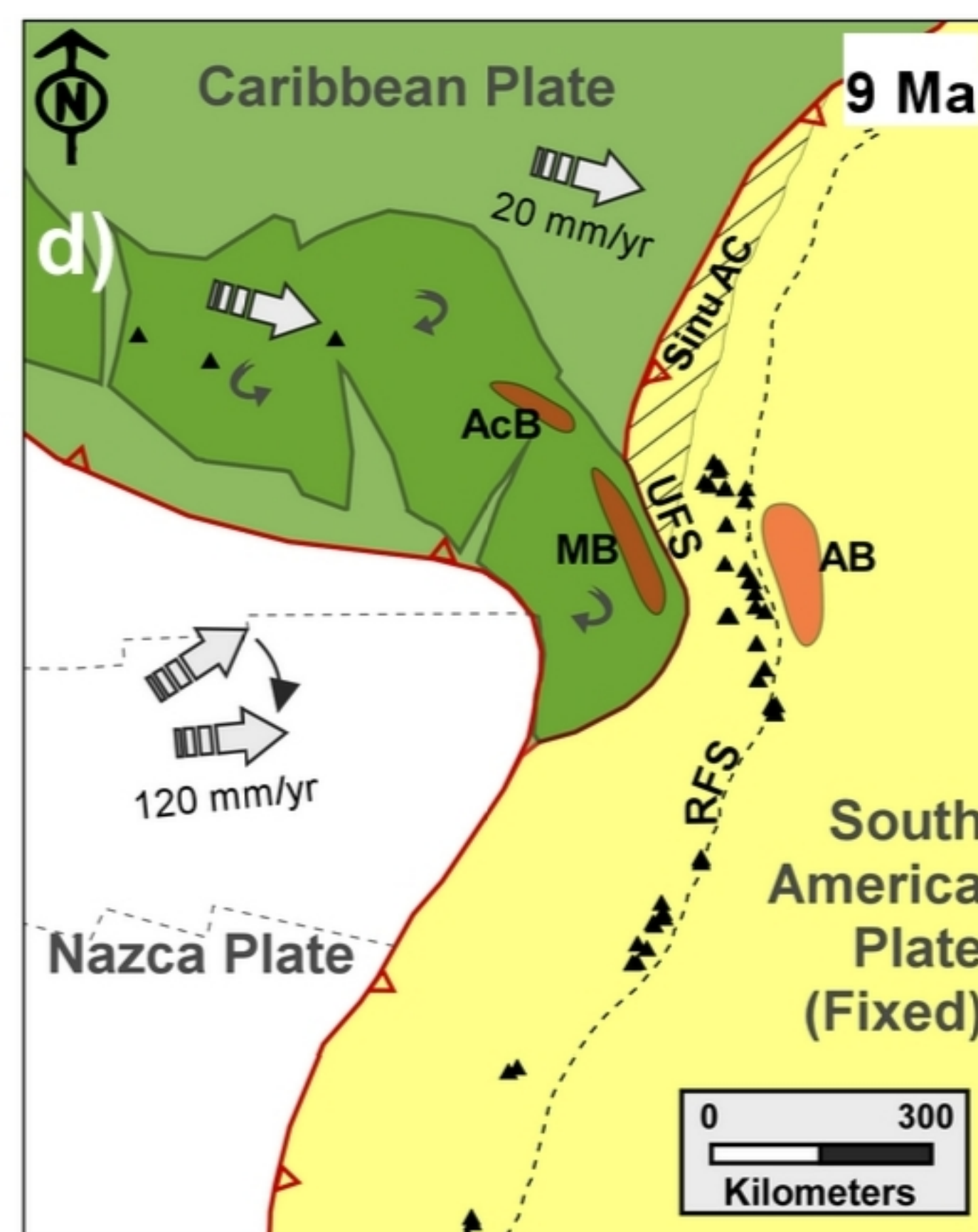
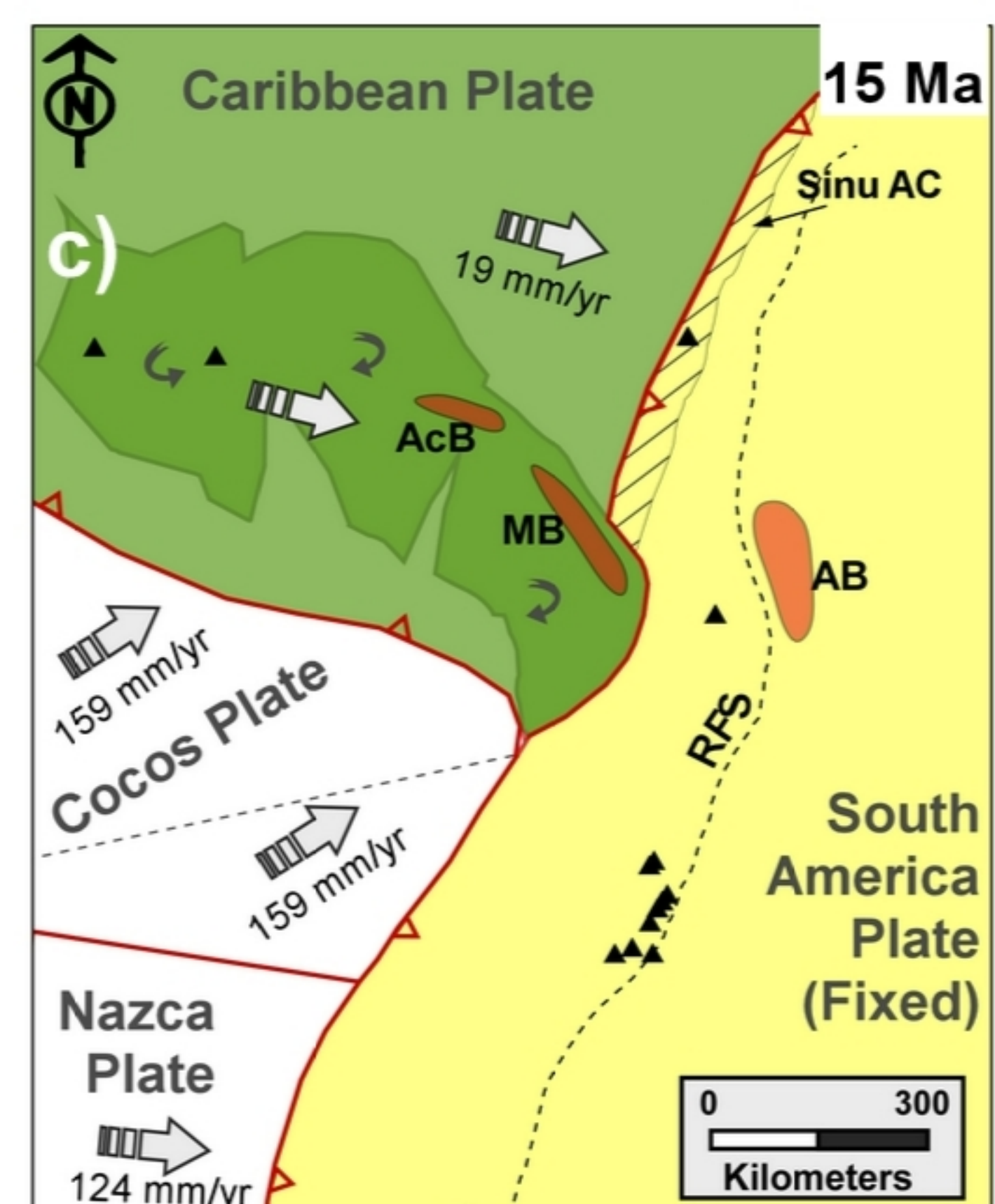
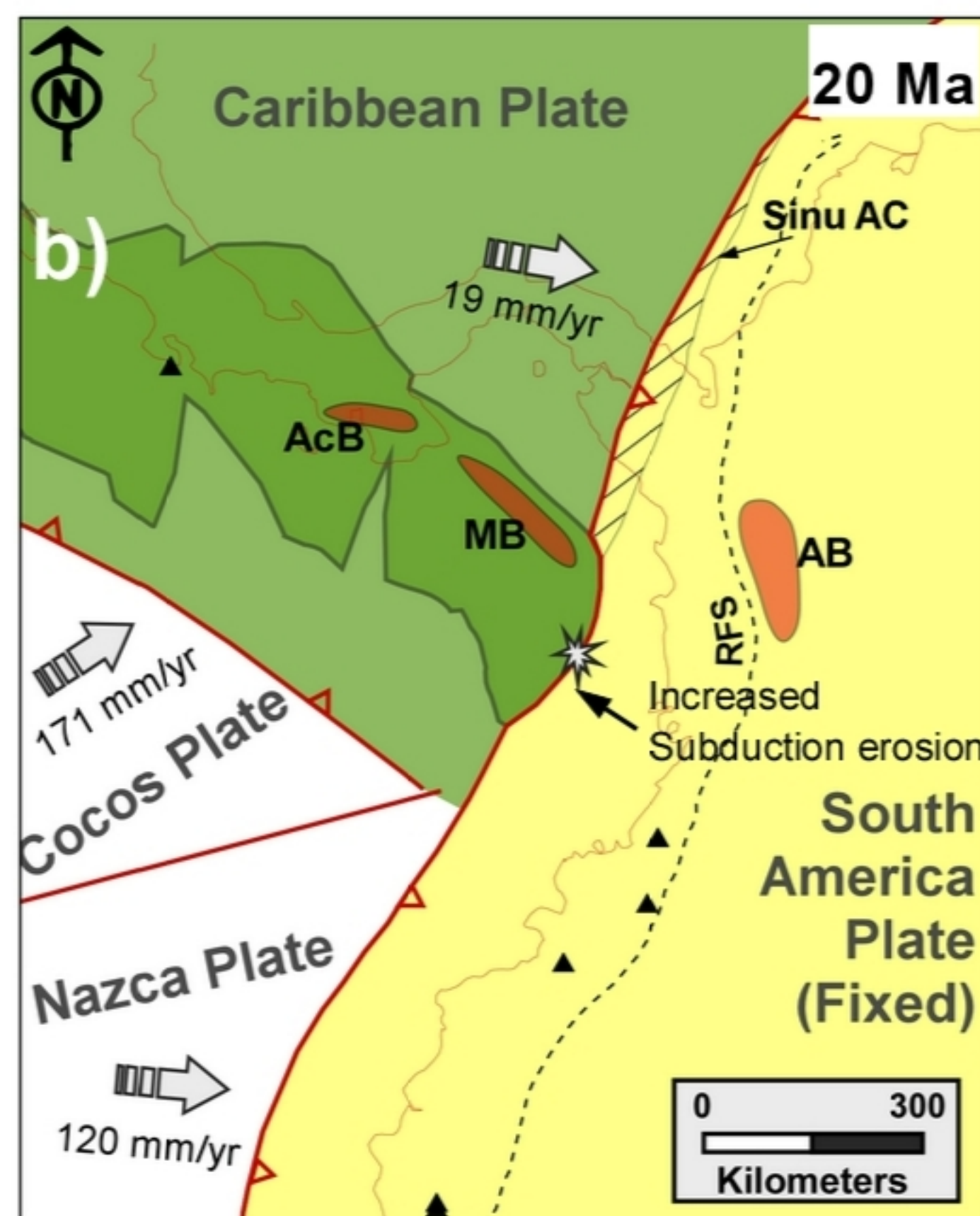
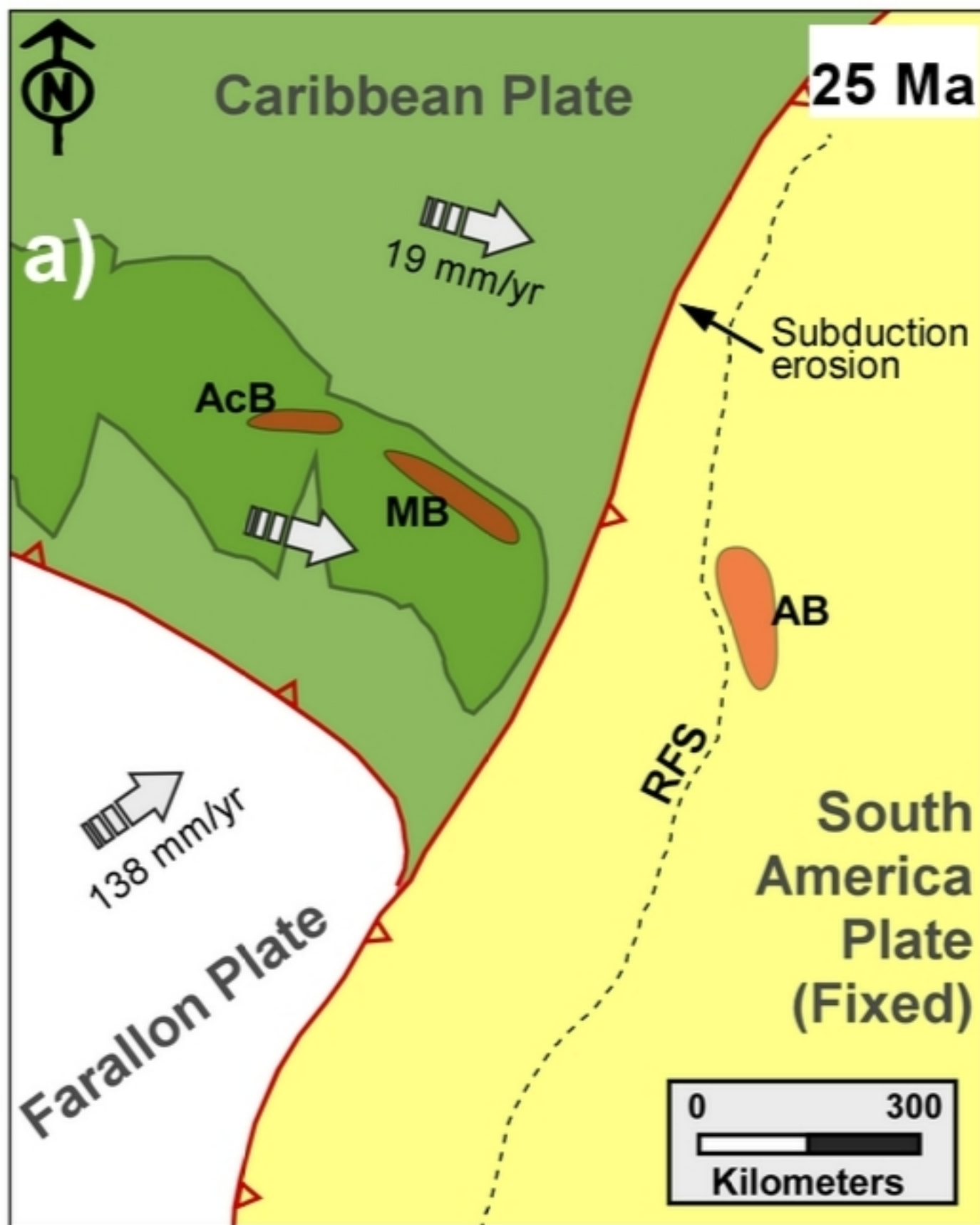
d.



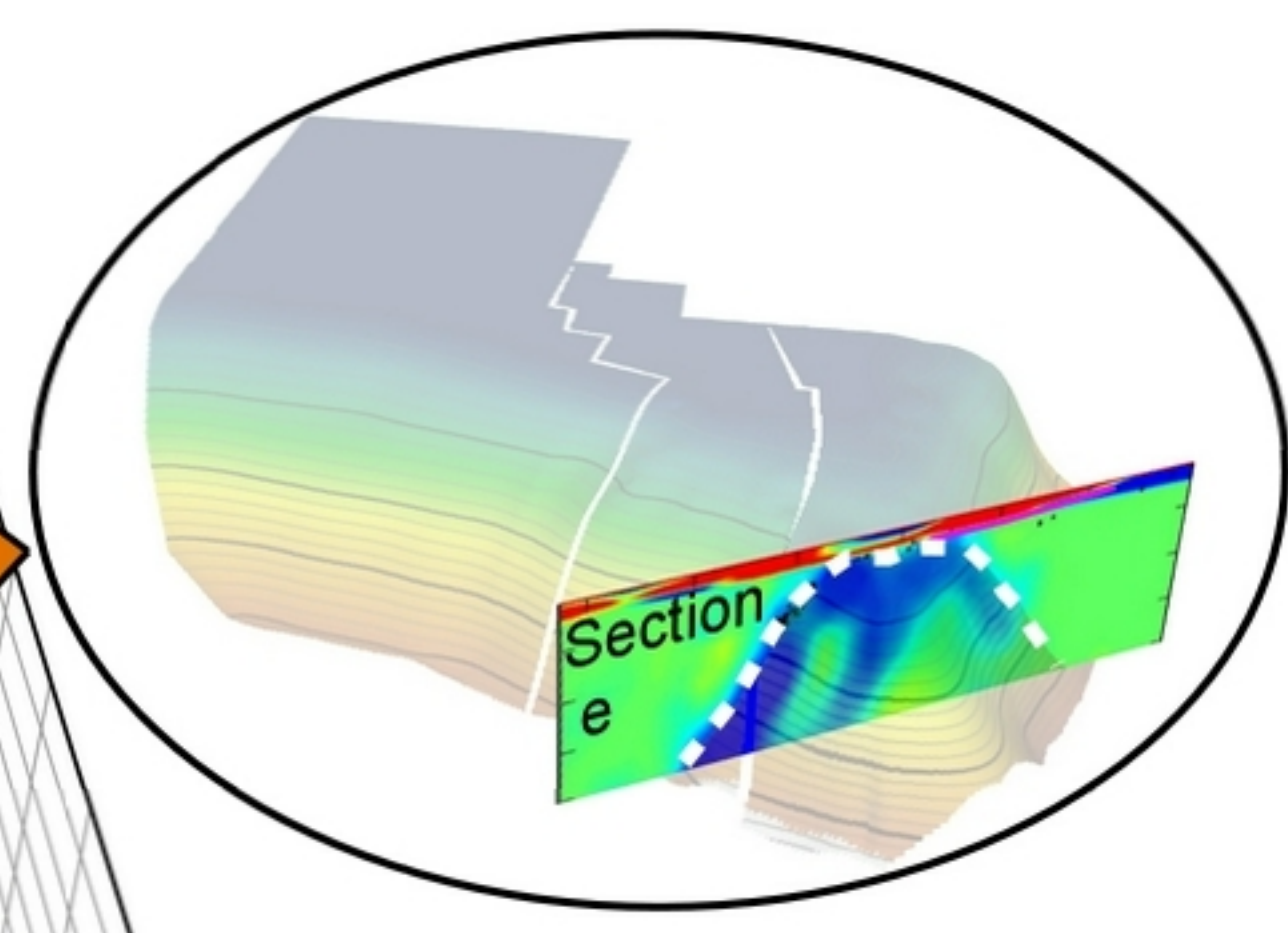
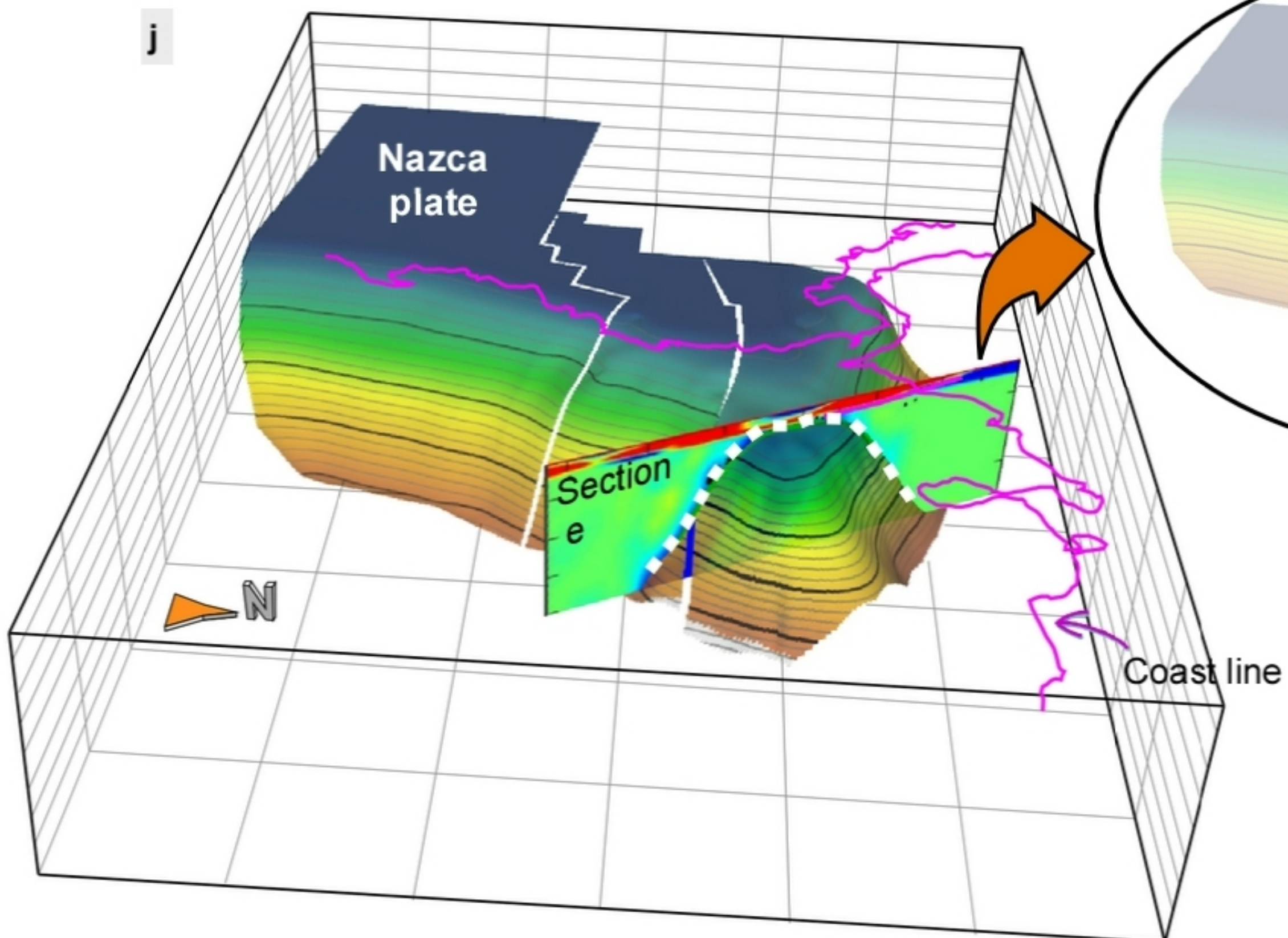
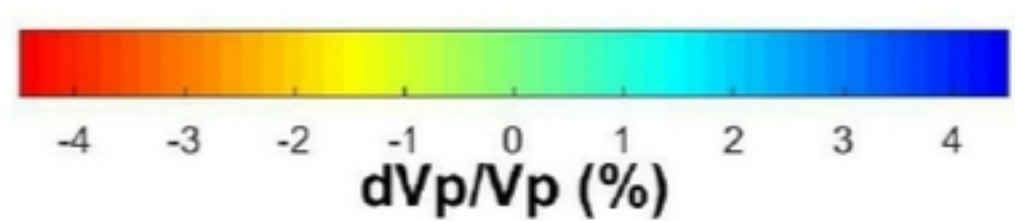
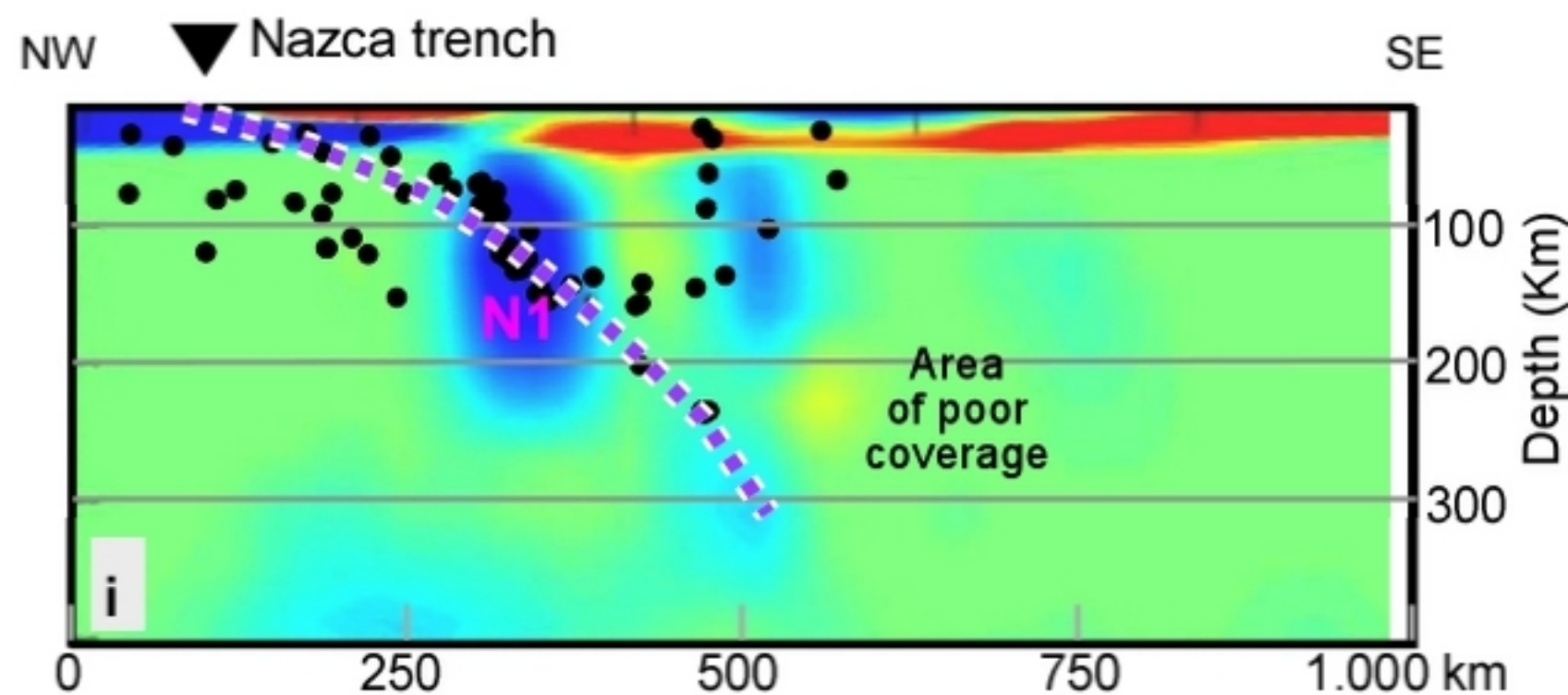
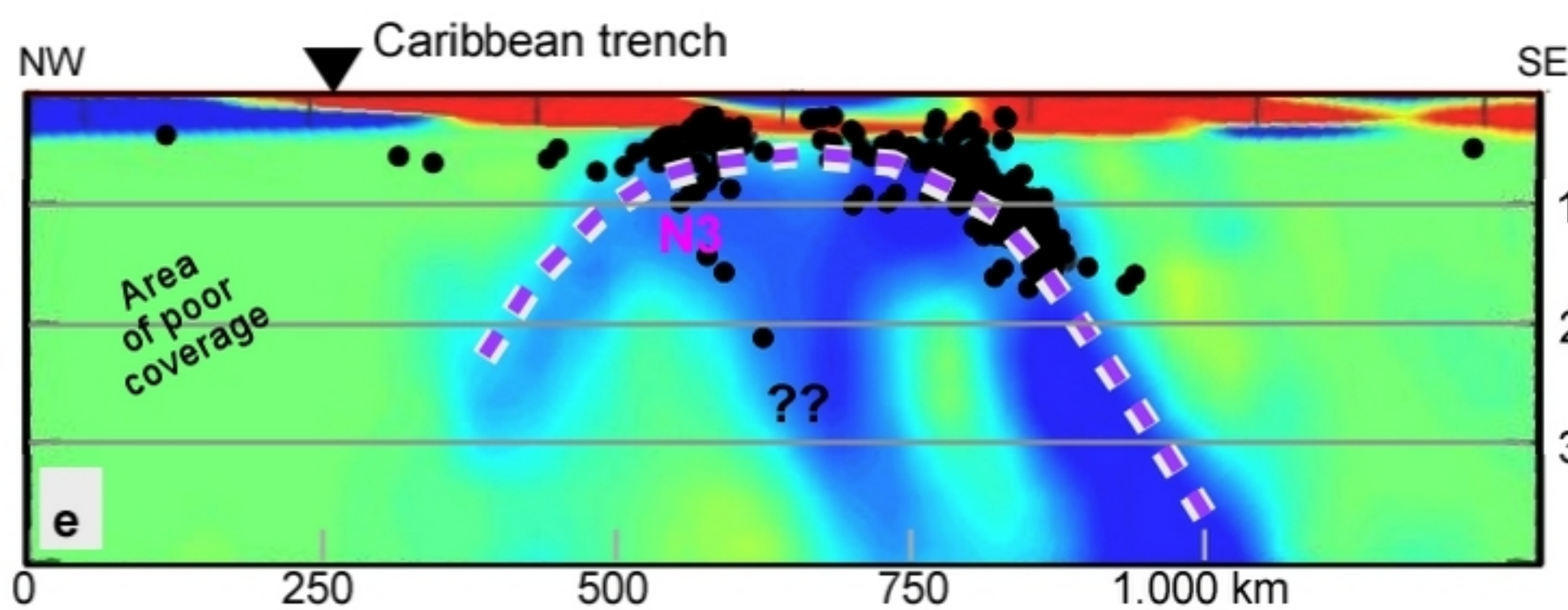
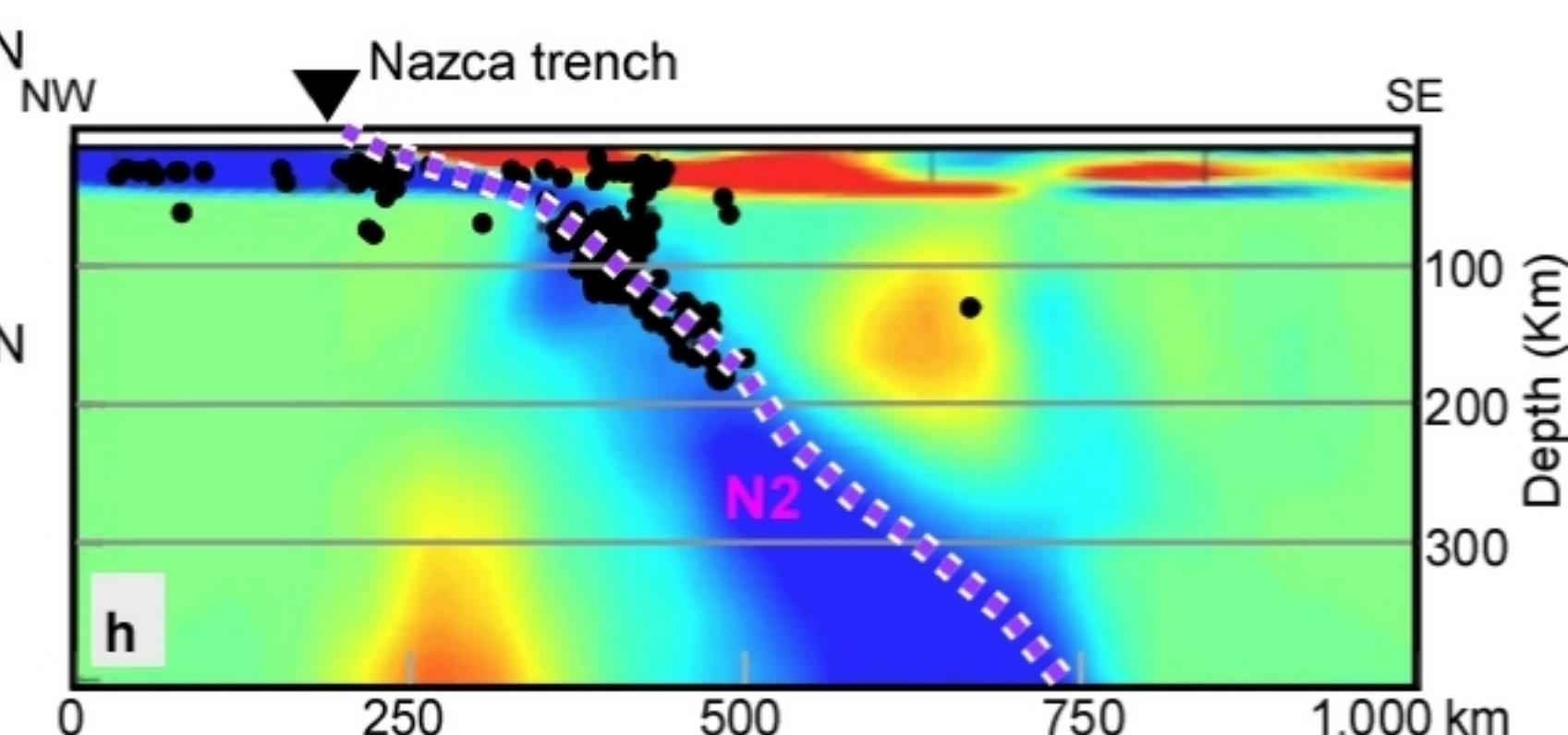
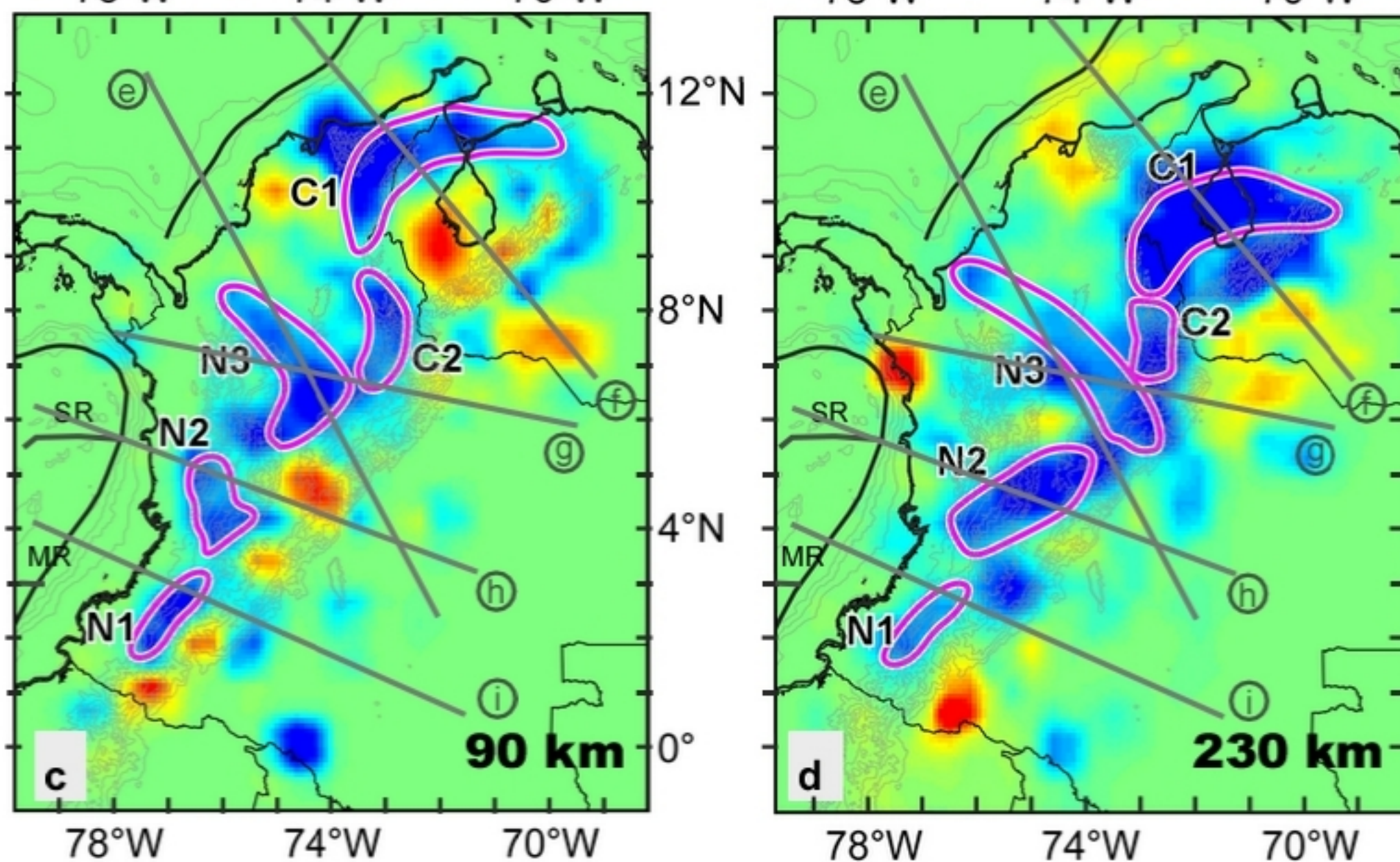
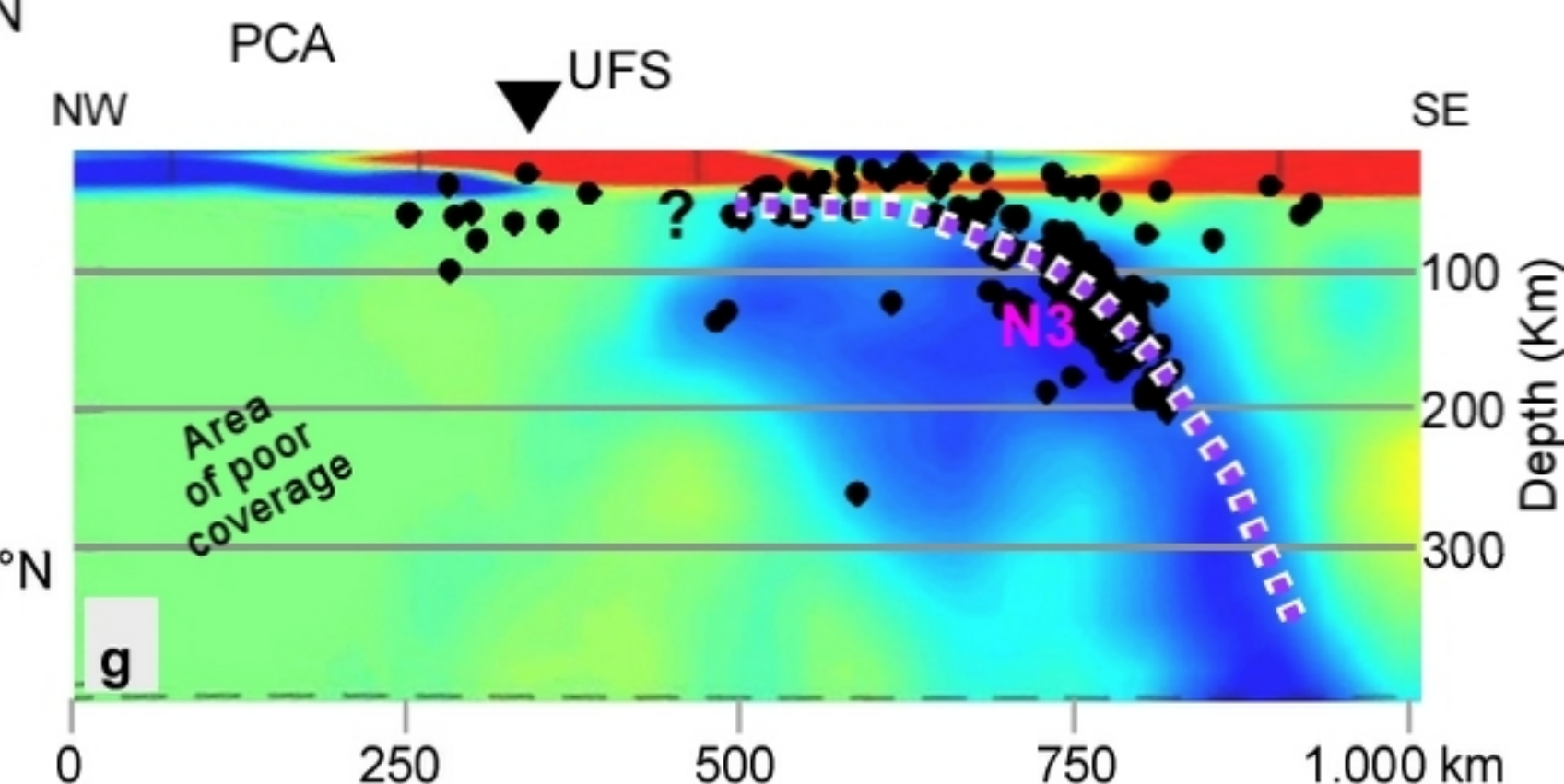
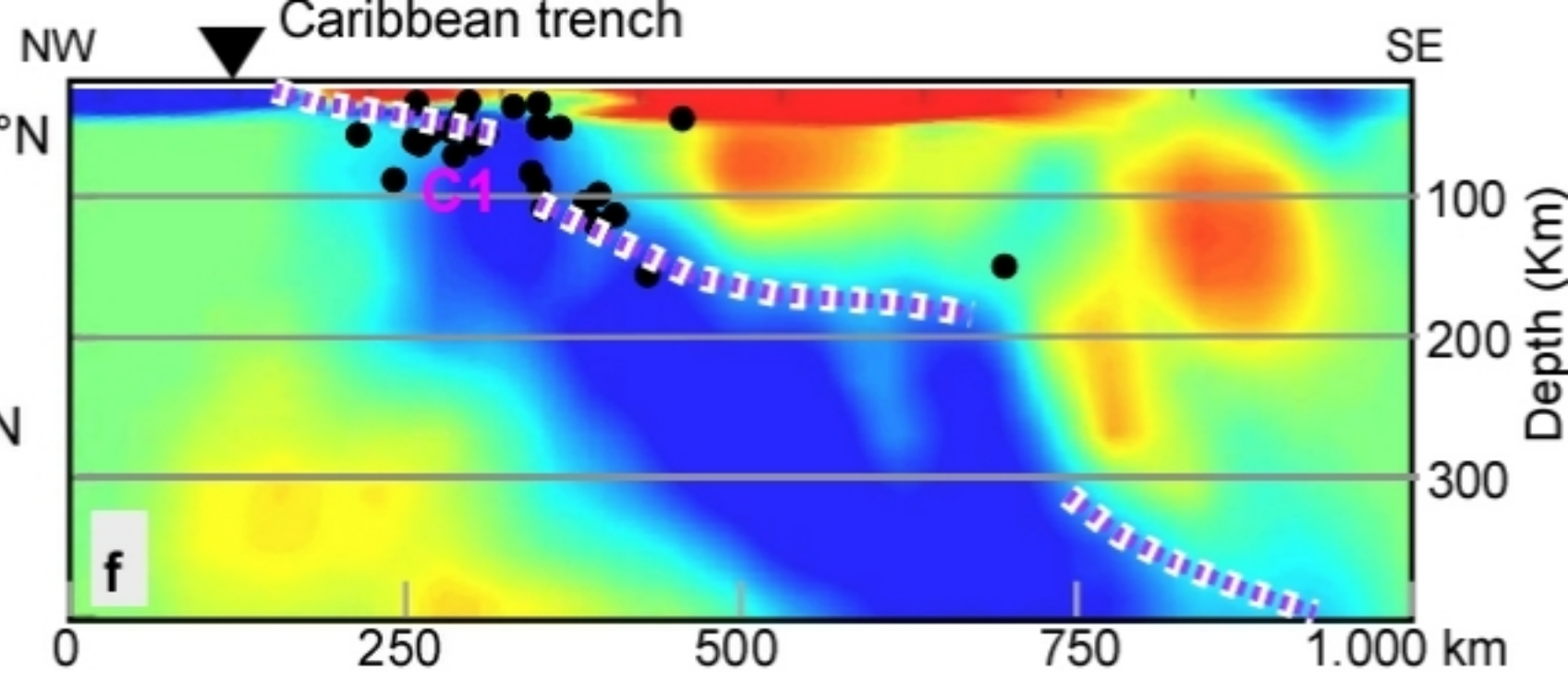
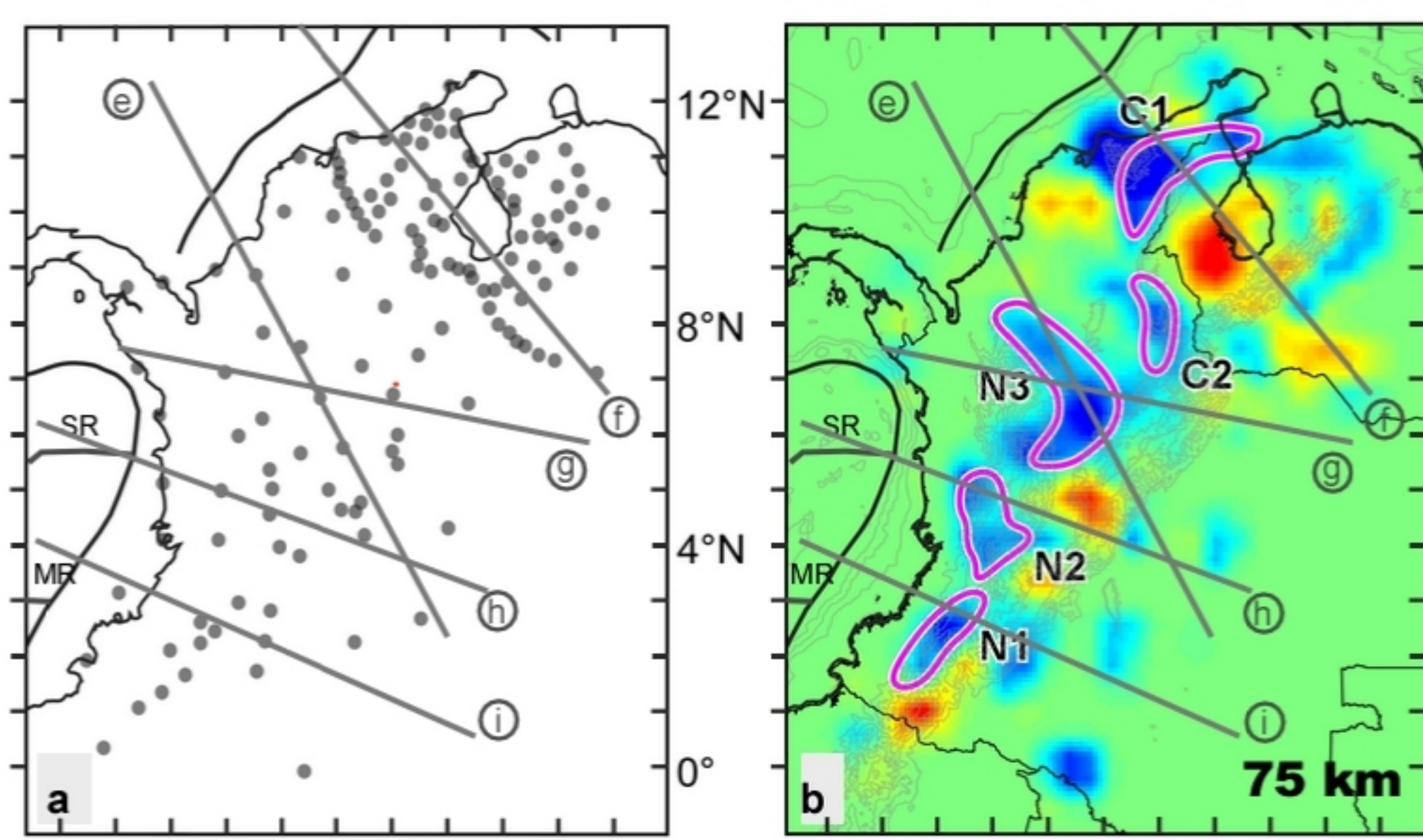
Geological map of NWSA and simplified cross section.



Paleogeographic reconstruction of the Panama-Choco Arc convergence and accretion to the South American margin.



Tomographic model.



Three-dimensional view of the tectonic configuration of the Nazca and Caribbean subduction zones.

0 Ma

